IMMUNOMODULATORY EFFECTS OF EXOSOMES: PROMISING CANDIDATES IN IMMUNOTHERAPY

A THESIS SUBMITTED TO

THE GRADUATE SCHOOL OF ENGINEERING AND SCIENCE

OF BILKENT UNIVERSITY

IN PARTIAL FULFILLMENT OF THE REQUIREMENTS

FOR THE DEGREE OF

MASTER OF SCIENCE

IN

MOLECULAR BIOLOGY AND GENETICS

By

Havva Özgen Kılgöz

August 2018

IMMUNOMODULATORY EFFECTS OF EXOSOMES: PROMISING CANDIDATES IN IMMUNOTHERAPY

By Havva Özgen Kılgöz

August 2018

We certify that we have read this thesis and that in our opinion it is fully adequate, in scope and in quality, as a thesis for the degree of Master of Science.

İhsan Gürsel (Advisor)

Şükrü Tüzmen (Co-Advisor)

Ali Osmay Güre

Kamil Can Akçalı

Approved for the Graduate School of Engineering and Science:

Ezhan Karaşan

Director of the Graduate School

ABSTRACT

IMMUNOMODULATORY EFFECTS OF EXOSOMES: PROMISING CANDIDATES IN IMMUNOTHERAPY

Havva Özgen Kılgöz

M.S. in Molecular Biology and Genetics

Advisor: Prof. Dr. İhsan Gürsel

August 2018

Exosomes are type of extracellular vesicles secreted from almost all cell types and carry numerous biological molecules such as nucleic acids, protein and lipids. They mediate many cellular processes including cellular communication and immune responses. Accumulating evidence suggests that these vesicles play a key role in the pathogenesis of inflammatory diseases, infectious diseases and many malignancies. The significant role of exosomes in cellular level also describe their intriguing potential in cancer therapeutics.

The primary aim of this thesis is to identify the immunomodulatory roles of distinct exosome species and extend the knowledge of exosome utilization in immunotherapy. The exosomes purified from i) RAW264.7 (murine macrophage-like), ii) EG7 (murine T cell lymphoma), and iii) HUH7 (human hepatocellular carcinoma) had distinct characteristics as well as immunomodulatory features upon murine splenocyte stimulation either alone or in combination with poly(I:C) (a TLR3 ligand), R848(a TLR7/8 ligand), and CpG ODN(a TLR9 ligand). Strikingly, these cell line-derived exosomes displayed changing internalization kinetics by immune cells.

Furthermore, the involvement of exosomes in the liver disease progression in the course of Hepatitis B virus (HBV) infection, cirrhosis and hepatocellular carcinoma (HCC) was investigated. As a result of patients' exosome stimulation assays with healthy peripheral blood mononuclear cells (PBMCs) and murine splenocytes, patient plasma-derived exosomes had inflammatory effects correlated with the severity of liver damage suggesting that these exosomes might have a pathological role in liver disease progression and/or pathogenesis.

In the final part, we used a dehydration-rehydration technique enabling external loading of desired Toll-like receptors (TLR) ligand within exosome and liposome. We developed a robust therapeutic vaccine delivery system in which injection of therapeutic vaccine to tumor burden animals enhanced anti-tumor activity and prolonged survival of HCC xenografts. In summary, this approach could broaden the immunotherapeutic utility of exosomes in the clinic.

Keywords: Exosomes, TLRs, HBV infection, Cirrhosis, HCC, Nanocarrier, Immunotherapy

ÖZET

EKSOZOMLARIN İMMÜNOMODÜLATOR ETKİLERİ: İMMÜN TEDAVİDE UMUT VERİCİ ADAYLAR

Havva Özgen Kılgöz

Moleküler Biyoloji ve Genetik Bölümü, Yüksek Lisans

Tez Danışmanı: Prof. Dr. İhsan Gürsel

Ağustos 2018

Eksozomlar, nükleik asit, protein ve lipid gibi biyolojik molekülleri taşıyan hücredışı keseciklerdir. Hemen hemen her hücre tipinden salınan eksozomlar, hücresel haberleşme ve immünite gibi birçok biyolojik olayı düzenlemektedir. Bilimsel çalışmalar eksozomların inflamatuvar, bulaşıcı ve malignant özellikteki birçok hastalığın patojenisitesinde kilit rol oynadığını göstermiştir. Dolayısıyla, eksozomlar, kanser tedavisi için büyük potansiyel taşımaktadır.

Bu tezin ana amacı, farklı eksozom türlerinin immünomodülatör özelliklerini ortaya çıkarabilmek ve bu bilgiler ışığı altında eksozomların immünoterapide kullanım alanlarını genişletebilmektir.

İlk etapta, i) RAW264.7 (makrofaj-benzeri fare hücre hattı), ii) EG7 (T hücre lenfoma hücre hattı) ve iii), HUH7 (insan hepatoselüler karsinoma) hücre hatlarından izole edilen eksozomların karakteristik özellikleri belirlenmiştir. Buna ek olarak, izole edilen bu eksozomların, fare splenositleri ile tek başına ya da CpG ODN (TLR9 ligandı), Poly (I:C) (TLR3 ligandı) ve R848 (TLR7-8 ligandı) gibi farklı TLR ligandları ile birlikte stimüle edildiklerinde, immünomodülasyon açısından farklı etkileri olduğu gösterilmiştir. Ayrıca, bu eksozomların, immün hücreleri tarafından değişen internalizasyon kinetikleri olduğu bulunmuştur.

Ayrıca, eksozomların karaciğer hastalıklarının (Hepatit B enfeksiyonu, siroz ve hepatosellüler karsinoma) gelişimindeki rolü araştırılmıştır. Eksozom stimülasyon deneylerinden edilen sonuçlara göre, hastalardan elde edilen eksozomların sağlıklı bireylerin periferal kan tek çekirdekli hücreleri ve fare dalak hücreleri üzerinde karaciğer hastalığının derecesi ile korele şekilde enflamatuvar etkileri olduğu

gösterilmiştir. Bu sonuçlar eksozomların karaciğer hastalığının seyri ve patojenitesinde önemli rol oynayabileceğini göstermektedir.

Tezin son bölümünde ise, Toll benzeri reseptör ligandlarının eksozom ve lipozom içerisinde dehidrasyon-rehidrasyon yöntemi tekniği ile eksternal yüklenmesine olanak tanıyan sistem kullanılmıştır. Bu yolla geliştirdiğimiz aşı ulaştırma sistemi fare deneylerinde anti-tümör aktivitesi göstermiş ve farelerin sağ kalımını arttırmıştır. Sonuç olarak, bu tezden elde edilen sonuçlar, eksozomların immünoterapötik amaçlı olarak klinikte kullanılabilmesinin önünü açabilecektir.

Anahtar kelimeler Eksozomlar, TLRs, HBV enfeksiyonu, Siroz, HCC, Nanotaşıyıcı, İmmünoterapi

Acknowledgements

At first, I would like to thank my supervisor Prof. Dr. İhsan Gürsel for his guidance, patience and support throughout my master's studies in ThorLab. I am grateful that he introduced me to the world of exosomes and for scientific inputs to do good science.
I would like to also thank my co-supervisor Assoc. Prof. Dr. Şükrü Tüzmen, who always believed in my ability to be successful in the academic arena. Your belief in me has made this journey possible.

I am also happy to know dear Prof. Dr. Mayda Gürsel and I appreciate her enthusiasm for science. I would like to thank her for sharing her academic knowledge with us.
I would like to offer my appreciations to this thesis committee members; Prof. Dr. Kamil Can Akçalı and Assoc. Prof. Dr. Ali Osmay Güre for accepting to be a part of my thesis jury.

I would love to thank all ThorLab members; Muzaffer Yıldırım, Tamer Kahraman, Fuat Cem Yağcı, Yasemin Özsürekçi, Fehime Eroğlu Kara, Volkan Yazar, Gökberk Göksu Kaya, İrem Evcili, Naz Bozbeyoğlu, Özlem Bulut for their friendship, support, encouragement during this two years and providing a great environment to work in. In particular, I would love to express my deepest feelings to my flatmate Gizem Kılıç for her precious friendship and support especially when I first came to Ankara and in my difficult times. I would like to thank my colleague, Seda Sabah Özcan, for her invaluable help and friendship throughout this two years. I will never forget all the memories we have shared together.

I would like to offer my special thanks to Mayda Gürsel group members, especially Asena and Naz for their great friendship.

I feel so lucky to know all our fabulous senior and intern students especially, Seda Kahraman, Başak Çorak and Ceren Perihan Gönül. I appreciate their helps whenever needed.

I want to thank MBG veterinarian Dr. Gamze Aykut for her endless help with guidance in the animal facility and Abdullah Amca for his motivational talks and positive energy.

To dear MBG family, you have all contributed to a supportive and collaborative work environment. I am truly grateful for all nice conversations over a cup of coffee. In particular, I want to thank Ünal, Sedef, Uğur, Ridho, Pelin, Özge and Said for their great friendship. I am also thankful to Oğuzhan and Onur for being more than a friend but a brother and sharing great times together. I also feel very lucky to meet again with Seniye in Bilkent, who always encouraged me and be my best friend. I will always miss weekend morning breakfasts with her.

I would love to thank my life-long friends in Cyprus and other countries; Elçim, Asya, Buse, Hasan, Hüseyin, Dilem, Mukaddes, Nazime, Luca and Funda abla for always being available to listen to me whenever I need them.

There is nothing in this world that is quite as strong and enduring as a family's love. Without the support and wisdom of my family, none of the important achievements of my life would have been possible. I would like to express my deepest gratefulness to my mother Feride, my father Yakup, my brother Kemal, my brother-in-law Salih, my sister-in-law Alev, my nephew Mehmet Melih, my nieces Ela and Beril Lena for their everlasting trust with love. They were the reason that I always believed "the sky is the limit". Thanks for your faith in me.

I believe everything is going on right when you least feel like it reminds yourself why you started this journey in the first place. My lovely thanks are to my sister Hatice, for being always behind me and cheering me up whenever I feel bad.

With my deepest love, I would like to thank my other half, fiance Erol for his continuous support, and endless love. Without him, my world would not be as beautiful as now.

'*Il successo non é mai casuale'*

'Success is not a coincidence'

Dedication

Dedicated to the loving memory of a monumental woman. I have the privilege to call her my aunt, Münüse Sadıkel who could not see this thesis completed…

Table of Contents

ABSTRACT ii

ÖZET iv

Acknowledgements vi

Dedication viii

Table of Contents ix

List of Figures xiv

List of Tables xvii

List of Schemes xviii

Abbreviations xviiii

1. CHAPTER 1 1

Introduction 1

1.1 The Immune System 1

1.1.1 Innate Immunity 3

1.1.1.2 TLRs: cell surface and endosomal receptors 3

1.2 Extracellular Vesicles (EV) 6

1.2.1 Exosomes: biogenesis, composition and characteristics 7

1.2.2 Modulation of immune responses by exosomes 10

1.2.3 Exosome in disease pathogenesis 11

1.2.4 Exosome in HBV transmission 12

1.2.5 Exosomes in cancer 13

1.3 Clinical Applications of EVs 14

1.3.1 Exosomes in tumor immunotherapy 14

1.3.2 Exosome as disease biomarkers 15

1.3.3 Exosomes as cargo-delivery vehicles 16

1.4 Hepatitis-B Virus (HBV), Cirrhosis, Hepatocellular Carcinoma (HCC) and Disease Pathogenesis 17

1.5 Subject and Outline of This Thesis 18

2. CHAPTER 2 20

Materials and Methods 20

2.1. Materials 20

2.1.1 Patients and Healthy Controls 20

2.1.2 Mouse Strains 20

2.1.3 General laboratory and cell culture reagents and materials 21

2.1.4 PRR Ligands 21

2.1.5 Lipids used in liposome preparation 22

2.1.6 ELISA Reagents 22

2.1.7 Flow Cytometry Reagents 25

2.1.8 Immunoblotting Antibodies and Reagents 27

2.2. Methods 29

2.2.1 Cell Line Maintenance 29

2.2.1.1 Cell Lines 29

2.2.1.2 Cryopreservation and cell thawing 30

2.2.1.3 Cell Counting 31

2.2.2 PBMC isolation from peripheral blood 32

2.2.3 Preparation of single cell suspension from mouse spleen 33

2.2.4 Preparation of peritoneal cavity cells (PECs) 33

2.2.5 Isolation of EVs and exosomes from cell culture supernatants 34

2.2.6 Isolation of exosomes from peripheral blood plasma 35

2.2.7 Protein isolation from cells and exosomes 36

2.2.8 Determination of protein concentration 36

2.2.9 Exosome characterization by flow cytometry 37
2.2.10 Surface marker staining by flow cytometry 38
2.2.11 Liposome preparation 38
2.2.12 Cargo loading into exosomes 39
2.2.13 Cytokine ELISA and SEAP reporter assay 40
2.2.14 Immunobloting 41
2.2.14.1 Preparation of protein samples 41
2.2.14.2 SDS-PAGE running 41
2.2.14.3 Transfer to the membrane 42
2.2.14.4 Blotting and development 42
2.2.15 Development of HCC xenograft in Athymic mice 422
2.2.16 Statistical Analysis 43
3. CHAPTER 3 44
Results 44
3.1. Immunomodulatory Effects of Cell Line-Derived Exosomes 44
3.1.1. Characterization of EG7, HUH7 and RAW exosomes 44
3.1.2. Stimulation of mouse splenocytes with EG7, HUH7 and RAW exosomes alone or in combination with TLR agonists 46
3.1.3. Internalization kinetics of cell line-derived exosomes by immune cells 51
3.1.4. Inflammatory potential of intraperitoneally administered exosomes from different cell sources 55
3.2. The Role of Exosomes in HBV infection, Liver Cirrhosis and Hepatocellular Carcinoma (HCC) 58
3.2.1. Plasma-derived exosome characterization 58
3.2.2. Circulating cytokine/chemokine profile of patients and healthy controls 65
3.2.3. Healthy control peripheral blood mononuclear cell (PBMC) stimulation with patient exosomes 70

3.2.4. *In vitro* stimulation of mouse strain specific immune cells with patient exosomes 72

3.3. Potential Therapeutic Cancer Vaccine Study: Ligand-Loaded Extracellular Vesicles (EVs) and Liposomes 74

3.3.1. Exosome and liposomes as therapeutic cancer vaccine delivery vehicles against established HCC model *in vivo* 74

3.3.1.1. Co-encapsulating CpG ODN and poly (I:C) within exosome and liposomes. 74

3.3.1.2. Encapsulating triple ligands: α-Galactosylceramide (α-GalCer), CpG ODN and poly(I:C) within exosome and liposomes……..…….79

4. CHAPTER 4 83

Discussion 83

Bibliography 88

Appendices 95

Appendix A 95

A1. Cell Culture Media, Buffers and Solutions 95

A1.1 Cell Culture Media 95

A1.1.1 RPMI-1640 and High Glucose DMEM: 95

A1.1.2 Exo-free FBS preparation: 95

A1.2 Buffers and Solutions 95

A1.2.1 PBS-BSA-Na azide Buffer (FACS Buffer) 95

A1.2.2 ELISA buffers 96

A1.2.2.1 Blocking buffer 96

A1.2.2.2 Wash buffer 96

A1.2.2.3 10X PBS (Phosphate Buffered Saline) 96

A1.2.3 Immunoblotting buffers 97

A1.2.3.1 RIPA buffer (Radio Immuno Precipitation Assay Buffer) 97

A.2.3.2 4x Laemmli buffer……..97

A1.2.3.3 30% Acrylamide mix……98

A1.2.3.4 10% SDS……...98

A1.2.3.5 1.5 M Tris (pH: 8.8)……98

A1.2.3.6 10.5 M Tris (pH: 6.8)…….……...98

A1.2.3.7 TBS 10X 98
A1.2.3.8 TBS-T 99
A1.2.3.9 10X Running buffer 99
A1.2.3.10 Transfer buffer 99
A1.2.3.11 Blocking and antibody incubation buffer 100
A1.2.3.12 5% Stacking gel 100
A1.2.3.13 10% Resolving gel 101
Appendix B 102
Supplementary Figures 102

List of Figures

Figure 1.1. Main types of EVs secreted from cells. 6
Figure 1.2. Biogenesis and uptake of exosomes. 8
Figure 1.3. Molecular composition and cargo of exosomes. *(Adapted from [43]).* 9
Figure 2.1. Representative counting chamber, hemocytometer. 31
Figure 3.1. Characterization of EG7, HUH7 and RAW exosomes by immunoblotting and flow cytometric bead method 45
Figure 3.2. Stimulation of mouse splenocytes with EG7 exosomes either alone or in combination with TLR ligands (K- and D-type CpG ODN, p(I:C), R848). 48
Figure 3.3. Stimulation of mouse splenocytes with HUH7 exosomes either alone or in combination with TLR ligands (K- and D-type CpG ODN, p(I:C), R848). 49
Figure 3.4. Stimulation of mouse splenocytes with RAW exosomes either alone or in combination with TLR ligands (K- and D-type CpG ODN, p(I:C), R848). 50
Figure 3.5. Exosome internalization by immune cell subsets in splenocytes. 52-54
Figure 3.6. Exosome internalization in peritoneal exudate cells (PEC). 56
Figure 3.7. Administration of SPDiOC stained exosomes to mice 57
Figure 3.8. Characterization of plasma-derived exosomes by flow cytometric bead method and immunoblotting. 59-61
Figure 3.9. The analyses of Alix and Grp94 protein expression on healthy and patient exosomes via immunoblotting. 62
Figure 3.10. Validation of PD-L1 expression 63-64
Figure 3.11. Screening of circulating Th1 and inflammatory cytokines/chemokines from patients' and healthy controls' plasmas by ELISA. 66-67
Figure 3.12. Screening of circulating Th2 and anti-inflammatory cytokines from patients' and healthy controls' plasmas by ELISA. 68-69
Figure 3.13. Stimulation of three different healthy controls' PBMCs with HBV carrier, Cirrhosis and HCC exosomes. 71
Figure 3.14. Stimulation of Balb/c and C57BL/6 splenocytes with HBV carrier, Cirrhosis and HCC exosomes. 73
Figure 3.15. Post-treatment HUH7 tumor growth curves over time. 76
Figure 3.16. Representative pictures of HUH7 tumor bearing mice at day=14 after, 4th injection of therapy. 77

Figure 3.17. Kaplan-Meier survival graphs of HUH7 tumor bearing mice. 78
Figure 3.18. Post-treatment HUH7 tumor growth curves over time..... 80
Figure 3.19. Representative pictures of Huh7 tumor bearing mice at day=14 after, 4th injection of therapy. 81
Figure 3.20. Kaplan-Meier survival graphs of HUH7 tumor bearing mice. 82

Figure S 1. Dot plots of cell-specific internalization of HUH7, EG7 and RAW exosomes by immune cell subsets in mouse splenocytes after 24 h incubation with SPDiOC labelled exosomes. 10302-103
Figure S 2. Dot plots of cell-specific internalization of HUH7, EG7 and RAW exosomes by immune cell subsets in mouse splenocytes after 24 h incubation with SPDiOC labelled exosomes. 104
Figure S 3. Fold change MFI of exosomal markers (CD9, CD63 and CD81) on ... 105
Figure S 4. Stimulation of Balb/c and C57BL/6 splenocytes with HBV carrier, Cirrhosis and HCC exosomes.. 106
Figure S 5. Tumor volumes of each animal received different exosome/liposome formulation and control group. 107
Figure S 6. Kaplan-Meier survival graphs of HUH7 tumor bearing mice..... 108

List of Tables

Table 1.1. List of TLRs and their ligands, adaptor proteins and produced cytokines (Adapted and modified from [24-29]). 5
Table 2.1. List of CpG ODNs 22
Table 2.2. List of antibodies and reagents used in ELISA..... 23-25
Table 2.3. List of purified and fluorochrome-conjugated antibodies used in flow cytometric analysis..... 26-27
Table 2.4. List of immunoblotting antibodies..... 27-27

List of Schemes

Scheme 3.1. Brief schema of scientific reasoning of *in vitro* experimental design...46
Scheme 3.2. Schematic illustration of the work-flow.....58

Abbreviations

APC	Antigen presenting cell
BSA	Bovine serum albumin
CD	Cluster of differentiation
CpG	Unmethylated cytosine-guanosine motifs
CTL	Cytotoxic T cells
DAMP	Danger-associated molecular pattern molecules
DC	Dendritic cell
DMEM	Dulbecco's Modified Eagle's Medium
DNA	Deoxyribonucleic acid
dsRNA	Double-stranded RNA
EDTA	Ethylenediamine tetra-acetic acid
ELISA	Enzyme linked-immunosorbent assay
HBV	Hepatitis B virus
HCC	Hepatocellular Carcinoma
IFN	Interferon
IL	Interleukin
i.p.	Intraperitoneal
IP-10	Interferon gamma-induced protein 10
IRAK	IL-1 receptor-associated kinase
IRF	Interferon-regulatory factor
MHC	Major Histocompatibility Complex
miRNA	MicroRNA

mRNA	messenger RNA
MV	Microvesicle
MVB	Multivesicular bodies
MyD88	Myeloid differentiation primary
NK	Natural killer
NKT	Natural killer T cell
ODN	Oligodeoxynucleotide
PAMP	Pathogen Associated Molecular Patterns
PBS	Phosphate buffered saline
PBMC	Peripheral blood mononuclear cells
PD-L1	programmed death-ligand 1
PEC	Peritoneal cavity cells
PEG	Polyethylene glycol
PGN	Peptidoglycan
poly(I:C)	Polyinosinic-polycytidylic acid
PNPP	p-nitrophenyl phosphate
PO-	Phosphodiester backbone
PRRs	Pattern recognition receptors
PS-	Phosphorothioate backbone
PNPP	p-nitrophenyl phosphate
RIG-I	Retinoic acid-inducible gene 1
RNA	Ribonucleic acid
RT	Room Temperature

SA-ALP	Streptavidin-alkaline phosphatases
s.c.	Subcutaneous
ssDNA	Single stranded DNA
ssRNA	Single-stranded RNA
STING	Stimulator of interferon genes
TGFβ	Transforming growth factor β
Th	T-helper
TIR	Toll/IL-1 receptor
TLR	Toll-like Receptor
TNFα	Tumor necrosis factor α
TRAF	TNF receptor associated factor
TRIF	TIR-domain-containing adapter-inducing IFN-β
Treg	Regulatory T cell
TSG101	Tumor susceptibility gene 101

CHAPTER 1

Introduction

1.1 The Immune System

The machinery that protects the organism from infection and foreign invaders is called the immune system. Although infectious microbes are considered to activate immune system, noninfectious foreign substances can also elicit immune response. When neutralizing pathogens enter the body such as bacteria, viruses, parasites, fungi, they are recognized by different immune cell subsets and removed from the body as a result of organized immune response. This defense does not only happen against foreign molecules, thereof, immune system cells are able to fight against the body's own cells, which have changed to be anomalous due to an illness, including cancerous cells [1]. This complex network consists of different cells, tissues and organs that can be classified into distinct responses such as innate and adaptive (acquired) immunity. Failure in any of these subclasses of the immunity, will most likely increase the susceptibility to an infection and result with a variety of pathological condition [2, 3]. The first-line barrier is the innate immune system which provide a rapid but short-lived response against pathogens to prevent microbial invasion. Innate immunity is an evolutionary ancient defense mechanism and it is present in all multicellular organisms. Although this first-line defense mechanism is based on a limited repertoire of receptors for the recognition of pathogens, it is able to target conserved features shared by numerous pathogens [3]. Besides, the components of innate immune system play a critical role in activating the following adaptive immune response.

In contradistinction to innate immune responses, the adaptive responses are highly antigen specific, providing long-lasting protection against recognized pathogens including bacteria, viruses, parasites and so forth [4]. Components involved in the adaptive immunity, are capable of distinguishing foreign- and self-molecules which is a fundamental ability of the adaptive immune system. Eventually, if the system fails and response destructively against the organism's own molecules, autoimmune diseases occur [5]. Remarkably, the adaptive immune system is able to orchestrate complex immune responses which then develops an immunological memory to provide faster immune response and eliminate the same pathogen more efficiently upon future exposures to same antigen [6, 7].

Adaptive immune system comprises two classes of responses; antibody response (humoral immunity), carried out by B lymphocytes (B cells) and cell-mediated immune response carried out by T lymphocytes (CD4+ T helper cells and cytotoxic T cells). In this context, generation of a specific antibody and T cell based adaptive responses take days, longer than an innate immune response [8]. B cells are the precursors of both antibody-producing cells which called plasma cells and long lasting memory B cells. In antibody responses, following B cell activation, they proliferate and differentiate into plasma cells which leads to antibody production. Secreted antibodies (also called immunoglobulins) circulate in the bloodstream and cross to other body fluids where they meet with foreign antigen. Binding of antibody to an antigen, inactivate pathogens also mark them for destruction by other cells by phagocytosis and neutralization [9]. In contrast, cell-mediated immunity does not rely on antibodies, but rather generate a response through the binding to peptides presented by major histocompatibility complex (MHC) on the surface of antigen-presenting cells (APCs). While cytotoxic T cells (CTLs) can recognize the antigens presented via MHC-I, CD4+ T helper cells can recognize the antigens presented via MHC-II on APCs [8, 10]. Remarkably, lymphocytes sense the presence of antigens by lymphocyte antigen receptors (TCR for T cells and BCR for B cells) which are generated by somatic rearrangements, making these receptors highly antigen-specific. Eventually, antigen-specific T cell activation is crucial for producing specific cytokines that further mediates the immune response, promote antibody production, as well as required for apoptosis of infected cells [11, 12].

1.1.1 Innate Immunity

The innate immune system is the earliest line of defense against infectious threats. Microbial determinants that are indicators of infection, are recognized by the innate immune cells- such as dendritic cells and macrophages- via germline encoded pattern recognition receptors (PRRs). Consequently, these microbial non-self molecular structures that are recognized by PRRs are called pathogen-associated molecular patterns (PAMPs). Bacterial cell wall components such as peptidoglycan (PGN), lipopolysaccharide (LPS), and unmethylated CpG motif containing synthetic oligodeoxynucleotides (ODNs) are some of the well-known PAMPs [13, 14].
Besides, damage-associated molecular pattern molecules (DAMPs) are released from the cells during the conditions such as cell lysis or tissue damage either in the absence or presence of pathogenic infections, alerting the innate immune system via PRRs [15, 16].

PRRs have been categorized as two distinct classes with respect to their localization within the cell, being either membrane-bound PRRs or cytoplasmic PRRs. Among these sensors; Toll-like receptors (TLRs), C-type lectin receptors (CLRs), retinoid acid-inducible gene I (RIG-I)-like receptors (RLRs), and nucleotide-binding and oligomerization domain (NOD)-like receptors (NLRs), AIM2-like receptors (ALRs) and intracellular DNA sensors such as cGAS, the family of TLRs have been studied most widely [14].

Within minutes of PAMP or DAMP engagement, PRRs trigger the generation of different pro-inflammatory cytokines by initiating intracellular signaling cascades ultimately, as well as orchestrate the activation of adaptive immune cells resulting in antigen-specific adaptive immune responses [17].

1.1.1.2 TLRs: cell surface and endosomal receptors

Mammals have a variety of PRRs as explained in previous part. Among these, TLRs are the best characterized and were the first to be identified by Medzhitov and Janeway

on 1997 (R. Medzhitov et al. Nature, 1997). From TLR family, 10 members (TLR1-TLR10) and 12 members (TLR1-TLR9, TLR11-13) are described to date in humans and mice respectively. TLRs are found in innate immune cells such as macrophages, DCs and non-immune cells including epithelial and fibroblast cells. Based on their localization, TLRs are divided into two subfamilies. Among all, TLR1, TLR2, TLR4, TLR5, TLR6, TLR10 are located on the plasma membrane and called cell surface TLRs, whereas the rest of the members include TLR3, TLR7, TLR8, TLR9, TLR11, TLR12 and TLR13 are located on the endosomal compartment, called intracellular TLRs [18]. Up to the present, several TLR agonists have been identified. These ligands are summarized in **Table 1.1**.

Each TLR have a part with leucine-rich repeats (LLRs) displaying a horseshoe-like structure, acquired for PAMPs/DAMPs recognition, a transmembrane domain and a Toll/IL-1 receptor (TIR) domain containing adaptor proteins where located in the cytoplasm, mediates downstream signal transduction. Mentioned ectodomain having a horseshoe-like structure interact with specific PAMP or DAMP as homo- or heterodimer along with a co-receptor. Upon PAMPs/DAMPs recognition, the adaptor molecules containing TIR domains such as differentiation primary response gene 88 (MyD88) and TIR-domain-containing adaptor-inducing interferon-β (TRIF) initiates signal transduction cascades that result in the activation of NF-kB, IRFs or MAP kinases to maintain the expression of fundamental pro-inflammatory cytokines, type I IFNs and chemokines which contribute to host defense responses [18] [19].

The TLRs not only facilitate the eradication of pathogens, but they also play a central role in the development of several disorders such as cardiovascular disease and metabolic syndrome. Thus, there are several studies investigating the TLR status in distinct classes of disorder, trying to identify the possible sequelae of TLR-induced long-term inflammation on these diseases pathogenesis [20]. On the other hand, some studies are defining the significant role of TLRs in the autoimmunity, calling TLRs as attractive targets for therapeutic intervention, to ameliorate autoimmune diseases [21],[22]. In summary, these findings show that TLRs are indispensable in the early phase of infection as well as in linking innate and adaptive immunity, thus,

maintaining the integrity of the host defense response. In this respect, they are considered to be adjuvant receptors [23].

Table 1.1. List of TLRs and their ligands, adaptor proteins and produced cytokines (Adapted and modified from [24-29]).

TLR	Ligand (s)	Signal Adaptor	Cytokine Production
TLR1/2	Lipoprotein, LTA, PGN, PAM3CSK4	MyD88, TIRAP/Mal	Pro-inflammatory cytokines
TLR2	Glycolipids, Mannan, Mutin	MyD88, TIRAP/Mal	Pro-inflammatory cytokines
TLR3	dsRNA, Poly (I:C), PolyU	TRIF	Type I Interferon, Pro-inflammatory cytokines
TLR4	LPS, Fibronectin, S100A	MyD88, TIRAP/Mal, TRAM, TRIF,	Type I Interferon, Pro-inflammatory cytokines
TLR5	Flagellin	MyD88	Pro-inflammatory cytokines
TLR 2/6	Zymosan, PAM2CSK4, Diacylated lipopeptides, β-glucan	MyD88, TIRAP/Mal	Pro-inflammatory cytokines
TLR7/8	ssRNA, Imiquimod, Resiquimod	MyD88	Type I Interferon, Pro-inflammatory cytokines
TLR9	Unmethylated CpG DNA	MyD88	Type I Interferon, Pro-inflammatory cytokines
TLR10	-	MyD88	Anti-inflammatory
TLR11	Profilin	MyD88	Pro-inflammatory cytokines
TLR13	Bacterial 23S RibosomalRNA	MyD88, TAK-1	Type I Interferon, Pro-inflammatory cytokines

1.2 Extracellular Vesicles (EV)

Extracellular Vesicles (EVs) are membrane surrounded heterogeneous population of vesicles that are actively released from the cells and are important components of intercellular communication. Based on their biogenesis, size, and biophysical properties, EVs are divided into subgroups which mainly comprise exosomes, microvesicles (MVs) and apoptotic bodies. Regardless of their origin, all EVs carry a variety of biomolecules such as RNA, lipids, possibly DNA and proteins (**Figure 1.1**) [30, 31]. Accumulated studies are showing the significance of these vesicles in a broad range of physiological and pathological processes [32]. Even though all EV subtypes are important in many biological processes, exosome is the focal point of interest throughout this thesis.

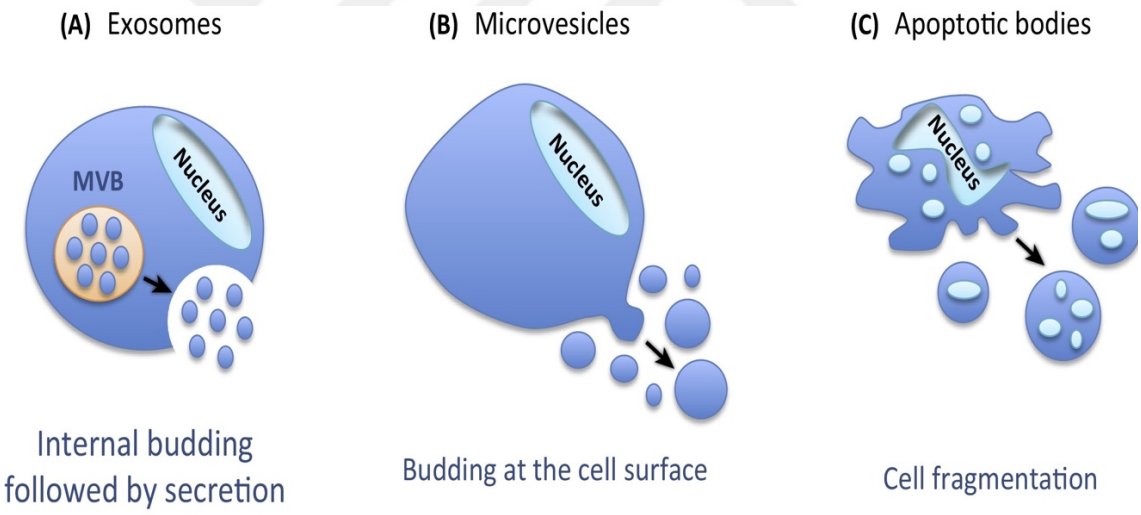


Figure 1.1. Main types of EVs secreted from cells.

(A) *Exosomes, formed by internal budding* ***(B)*** *Microvesicles (MVs), formed by budding from the plasma membrane* ***(C)*** *Apoptotic bodies, released from apoptotic cells, undergoing programmed cell death (Adapted from [33]).*

1.2.1 Exosomes: biogenesis, composition and characteristics

Since the discovery of exosomes 35 years ago, it has become obvious that exosomes are of great importance to mediate cell-to-cell communication, instead of being considered as cellular waste disposal in the early 80's [34].
Virtually all cell types release exosomes, which are a class of extracellular vesicles (EVs), with a size range of 30-150 nm. This lipid bilayer surrounded nanovesicles can be purified from various body fluids such as saliva, serum, plasma, urine and from cell line supernatants [35]. Although various techniques have been developed to isolate exosomes from biological fluids, contamination of isolated exosomes with other nanoparticles remains to be main challenge and should be avoided. The most frequently used method for isolating exosomes is differential ultracentrifugation and its considered to be the gold standard [36, 37].

Exosomes are generated within the endosomal system; initiated by the plasma membrane invagination to form vesicles in the early endosomes. This process requires endosomal sorting complex responsible for transport (ESCRT) machinery. This is followed by the maturation of early endosomes to late endosome, also called multi-vesicular bodies (MVBs). During MVB process, intraluminal vesicles (ILVs) are generated by inward budding of endosomal membrane and intracellular molecules accumulates into ILVs. Eventually, generated MVBs fuse with either lysosomes for degradation or the plasma membrane results in the release of exosomes into the extracellular milieu (**Figure 1.2**) [38-40].

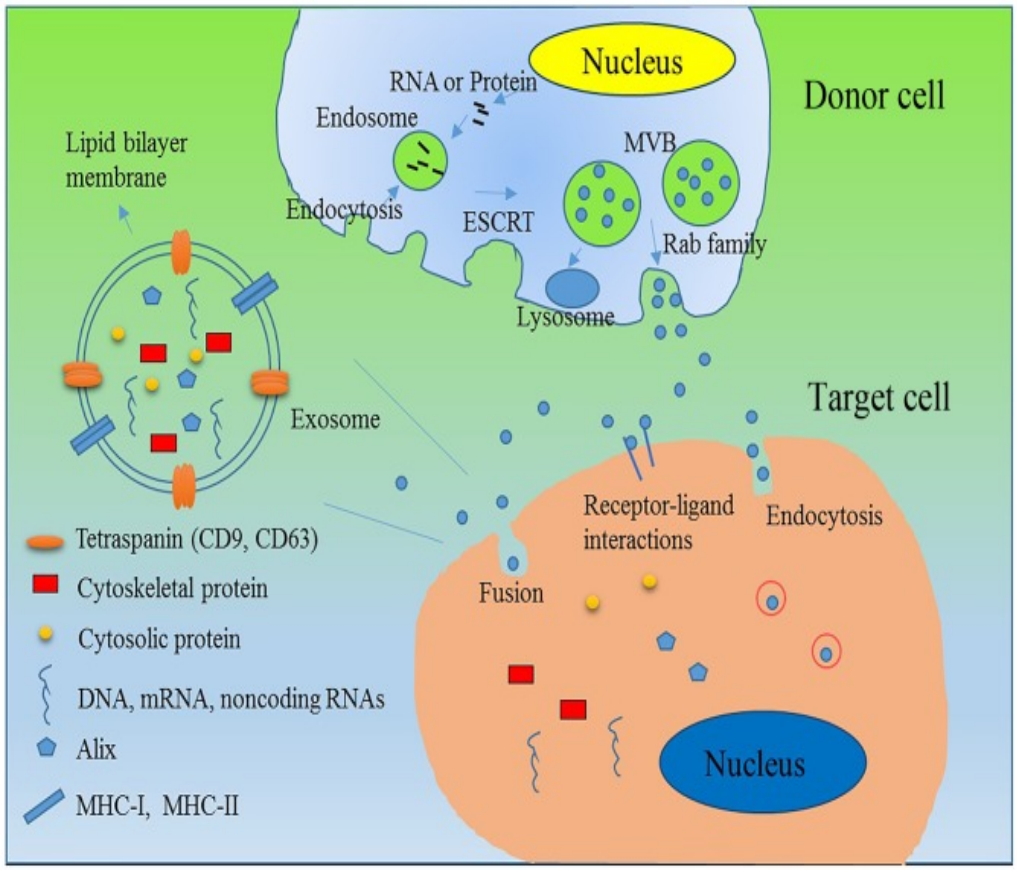


Figure 1.2. Biogenesis and uptake of exosomes.

Exosomes are formed by ESCRT-dependent pathway. After secretion of exosomes, they may be up taken by other cells via direct fusion with the plasma membrane, endocytosis or a receptor-ligand interaction. ESCRT: Endosomal sorting complex responsible for transport, MVB: Multi-vesicular bodies (Adapted from [41]).

Exosomes cover diverse cellular components including transmembrane proteins (e.g., PGRL, CD13), nucleic acids (e.g., DNA, mRNA, miRNA) lipids (e.g., cholesterol), metabolic enzymes (e.g., GAPDH, ATPase), heat shock proteins (e.g., Hsp70, Hsp90), membrane trafficking proteins (e.g., annexins and RABs proteins), tetraspanins (e.g., CD9, CD63), adhesion molecules (e.g., ICAM-I, integrins), cytoskeletal proteins (e.g., tublin, actin), proteins associated with multivesicular body (MVB) formation (e.g., TSG101, ALIX), as well as various tissue-specific molecules involved in immunoregulation (e.g., CD80, CD86, MHC-I/II, PD-L1) (**Figure 1.3**). Notably, other than aforementioned biological molecules, it has been shown that, lipid ceramide allows internal vesicle formation, therefore required for exosome secretion [35, 42].

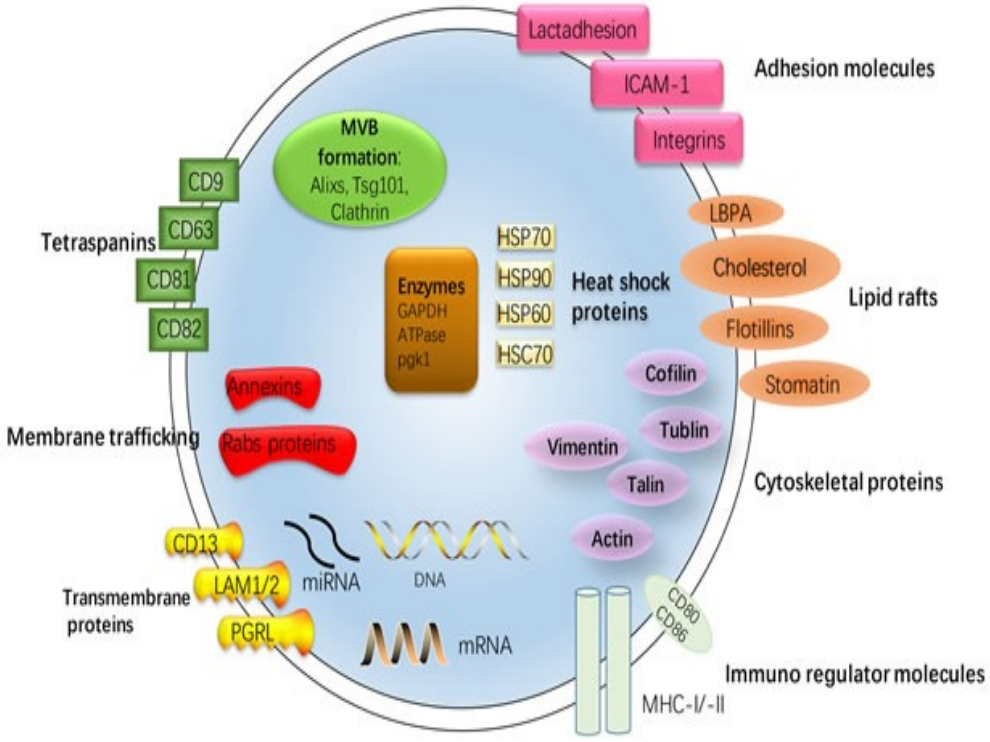


Figure 1.3. Molecular composition and cargo of exosomes *(Adapted from [43]).*

1.2.2 Modulation of immune responses by exosomes

Exosomes are highly heterogeneous and mimic the phenotypic state of the cell of origin. Hence, under health and disease conditions, exosomes are known to act as a modifier of physiological state of the host. Among many, these effects include activation or suppression of the immune system. Therefore, in different physiological and pathological conditions, exosomes are known to act as immune system activators or suppressors [43, 44].

There are various studies, trying to underline the immunomodulatory ability of mesenchymal stromal cells (MSCs). Although the mechanism for MSCs' immunomodulatory effects is still not well understood, accumulating evidence indicates that MSC-derived exosome play a significant role in the communication between MSCs and target tissue therefore, exert their therapeutic effects in several disorders [41, 45]. In one article, they stated that MSCs-derived exosomes isolated from healthy controls' bone marrow, promoted anti-inflammatory cytokine TGF-β secretion but suppressed pro-inflammatory factor TNF-α and IL-1β secretion in *in vitro* stimulation assays. Moreover, they found that, the level of regulatory T cells (Treg) and cytotoxic T lymphocyte-associated protein 4 (CTLA-4) were promoted after exosome administration [46]. Overall, MSC-derived exosomes showed immunomodulatory properties by also inducing the conversion of T helper type 1 (Th1) into T helper type 2 (Th2) cells [47]. Notably, placenta-derived exosomes are shown to be involved in suppressive immunity and have a role in normal placental development as well as in maternal immunotolerance during normal pregnancy [48].

Since Dendritic cell-derived exosomes (Dex) harbor functional MHC–peptide complexes together with other immune-stimulating molecules, they have been proposed to be promising candidates for immune-cell dependent tumor rejection [49]. In addition, antigen presenting cell (APC)- derived exosomes are enriched in MHC class I and II complexes and costimulatory molecules that present tumor antigens that to target cells, resulting with the eradication of established tumors by CD8(+) T cell as well as by NK cell activation [50, 51].

1.2.3 Exosome in disease pathogenesis

Accumulating evidence indicate that exosome play a very important role in immune modulation therefore, associated with the pathogenesis of a variety of diseases [52]. Recently, exosomes have been shown to be involved in autoimmune diseases' pathogenesis including rheumatoid arthritis (RA), Sjogren's syndrome (SS) and systemic lupus erythematosus (SLE). For instance, salivary gland-derived exosomes were found to be enriched in E3 ubiquitin–protein ligase TRIM21, Ro(SS-A), Lupus La protein (SS-B) and the Smith antigen (Sm), autoantigens majorly involved in Sjogren's syndrome (SS) and systemic lupus erythematosus (SLE) [51].

In addition, it has been pointed out that human breast milk-derived exosomes might contribute to the development of newborn immunity including tolerance induction and protect infants from allergy development [53, 54]. It has also been demonstrated that exosomes isolated from breast milk inhibited anti-CD3-induced IL-2 and IFN-γ production *in vitro* and augmented the number of $Foxp3^{+}CD4^{+}CD25^{+}$T regulatory cells, indicating that human breast milk-derived exosomes have immunomodulatory features that might shed light on the link between breast milk and infant's immunity [53].

Moreover, exosomes isolated from immature DC, stimulated with immunomodulatory cytokines including IL-4, IL-10 were effectively inhibited inflammation in delayed-type hypersensitivity (DTH) and attenuated the severity of collagen-induced arthritis (CIA) *in vivo* [51, 55].

Since exosomes modulate immune response via transfer of their cargo, their function following injury have investigated in peripheral nerve regeneration. In that study, they showed that group of cells in the central nervous system (CNS), as well as Schwann cells in the peripheral nervous system (PNS) are able to release exosomes. These exosomes have found to provoke the switch of a Schwann cell phenotype from mature to non-myelinating that provide support to axons, following the injury, thus indicating the role of exosomes in nerve regeneration [56].

1.2.4 Exosome in HBV transmission

The innate immune system is crucial for controlling viral infections and several PRRs are involved in recognition and degradation of the viral nucleic acids. During HBV infection, RIG-I senses the 5'- ε region of HBV pregenomic RNA (pgRNA) promoting robust production of type III IFNs in a RNA-binding dependent manner [57]. Besides, cGAS recognizes dsDNA from HBV and activates the downstream STING pathway that triggers type I IFN production and exhibiting antiviral activities [57, 58]. Thus, RIG-I have a dual role acting as an HBV sensor to activate innate immune response and fight against infection in human hepatocytes.

Recently, exosomes have been brought to focus in the field of viral transmission and new insights into exosome-mediated innate immune response during HBV infection have been provided [59, 60]. Exosomes are known to transfer different biological cargo between the cells. During HBV infection, they have been reported to mediate transmission of HBV-derived nucleic acids and proteins to healthy hepatocytes. NK cells were detected to internalize HBV+ exosomes, thus exosomes were transmitted HBV to uninfected hepatoma cells. This viral transmission through exosomes were also enhanced by transforming growth (TGF)-β treatment, by increasing the uptake capacity of NK cells, indicating that this process can be regulated via cytokines associated with disrupted NK-cell activity [61]. Moreover, exposure of chronic hepatitis B (CHB) patients' exosomes to healthy donor cells, have led to impaired NK cell activity including IFNγ production, cytolytic activity and dysfunctional NK-cell proliferation in healthy hepatocytes, thus, contribute to viral persistence [62]. It is also reported that, retroviruses can escape from immune cells, eventually bud inside microvesicular bodies (MVBs) and secrete within exosomes [63].

On the other hand, exosomal cargo was modified with HBV infection in hepatocytes, underlying various important immunosuppressive miRNA profile within exosomes. For instance, it has been shown that HBV infection of hepatocytes upregulated miR-21 and miR-29 expressions, of which these immunosuppressive miRNAs eventually transmitted to macrophages, thus suppressing IL-12 expression that is a well-known cytokine to activate NK-cells [61, 64]. In another study, HBV derived double stranded DNA was found to be transmitted via ceramide-triggered EVs to naïve hepatocytes.

The same study also demonstrated that transmission of HBV DNA by these EVs was also resistant to antibody neutralization [65]. Although, the role of exosome in hepatitis C virus (HBC) transmission between cells have been demonstrated recently, the effects of exosome in mediating HBV infection has begun to be identified [66].

1.2.5 Exosomes in cancer

Exosomes serve significant roles within the tumor microenvironment, especially in cell to cell communication between tumor cell and stromal cell. Immune cell-derived exosomes carry tumor antigens, which results with the eradication of tumor cells by triggering anti-tumor response via CD8+ T cells, CD4+ T cells and NK cells. [67] However, tumor derived-exosomes (called TEXs) are emerging regulators of tumorigenesis [68]. These exosomes also regulate many processes including invasion, coagulation, angiogenesis, metastasis and immunoregulation [69]. Tumor cells are able to secrete more exosomes than healthy cells with distinct characteristics [70]. These exosomes are putative mediators of metastatic colonization in secondary organs [71].

On the other hand, numerous studies have been linked tumor progression with chronic inflammatory processes and diminished immune cell activity. For instance, breast cancer cell line-derived exosomes have been shown to promote pro-inflammatory cytokine production including IL-6 and TNFα through Toll-like receptor 2-dependent activation of NF-κB following the internalization of tumor derived-exosomes by macrophages. Although both cancer- and non-cancerous cell line derived-exosome were found to target macrophages, only breast cancer-derived exosomes was able to induce pro-inflammatory activity of distant macrophages during cancer progression [72].

The intercellular communication in the metastatic niche is critical for facilitating cancer metastasis. In a very recent study, high metastatic hepatocellular carcinoma (HCC) cells were found to secrete exosomal miR1247-3p, promoting cancer progression by secreting pro-inflammatory cytokines such as IL-6, IL-8 through NF-κB signaling in fibroblasts [73].

Another exosome study has revealed that, lung cancer-derived exosomes can elicit suppressive effect on innate immunity by the delivery of exosomal cargo with activated epidermal growth factor receptor (EGFR) to host macrophages. This was further demonstrated by the suppression of interferon regulatory transcription factor 3 (IRF3) and type I interferon (IFN) expression. Unlike the previous studies that mentioned tumor derived-exosome mediated inflammation, this work provided an understanding for different mechanism of action for the roles of exosomes in the modulation of immune responses to cancer [71].

1.3 Clinical Applications of EVs

1.3.1 Exosomes in tumor immunotherapy

Exosomes' intriguing roles in the context of cancer, made them as novel anticancer therapeutics. The potency of dendritic cell (DC) derived-exosomes (also called Dex) are promising in tumor immunotherapy. Several phase I and II clinical trials have been conducted in different cancer types, demonstrating the use of Dex in tumor immunotherapy. Based on the propensity of Dex to carry tumor associated molecules as well as co-stimulatory molecules, they have been proposed to be a bright tool to mediate T and NK cell-based immune responses to facilitate immune cell-dependent tumor eradication in cancer patients [74, 75].

Beyond the scope of cargo delivery, exosomes are good candidates for therapeutic cell-free vaccine development against malignancies, which is a rapidly growing field in drug development against cancer. Although APC-derived exosomes are able to present tumor antigens and orchestrate the generation of cancer-specific adaptive immune responses, exosomes derived from other sources including cancer cells may act as immune suppressive that favors tumor progress and escape from the immune system. Tumor cell-derived exosomes (TEXs) carry tumor antigens that can presented to DCs and further trigger tumor-specific cytotoxic T lymphocyte (CTL) activation [76]. However, TEX promoted anti-tumor response is limited and is susceptible to induce tolerance. Therefore, TEXs are being modified to develop exosome-based

tumor vaccines artificially, as well as to augment immunogenicity of exosomes. For instance, in one study, exosomes were isolated from tumor cells and genetically engineered to encode cytokine genes IL-2 and IL-18. Eventually, these exosomes were shown to promote CTL response with DC maturation and NK cytotoxicity. Other important methodology to induce tumor-specific T cell responses was the combinational therapy where direct fusion of TEXs with antigens [77].

Programmed death-ligand 1 (PD-L1) is a co-inhibitory molecule, commonly up-regulated on cancer cells and suppress the activation of T cells [78] pathway inhibition is one of the major breakthroughs in tumor immunotherapy research. Most of tumor-derived exosomes are also enriched in these suppressive molecules such as PD-L1, or PD-L2, also mimic the phenotypic state of cellular origin [79].

1.3.2 Exosome as disease biomarkers

Recent advances in the research of exosomes, provided abundant exosomal molecules including mRNA, miRNA and proteins, as potential disease biomarkers revealing the diagnostic power of exosomes in many disorders [80]. Several exosomal miRNAs have been characterized as novel biomarkers, in many diseases including Alzheimer's disease, Rheumatoid arthritis (RA) and cancer. For instance, serum-derived exosomes highly enriched in miR-355 expression was found to be associated with shorter survival time in patients diagnosed with malignant gliomas [81]. Preeclampsia is a pregnancy complication that is associated with ineffective diagnostic and treatment strategies, as a result of unaddressed etiology of the disorder. Meanwhile, placenta-derived exosomes have been established as potential biomarkers in preeclampsia [82].

Moreover, proteomics analyses result indicated an accumulation of human leucine rich alpha-2-glycoprotein 1 (LRG1) expression in urinary exosomes of non-small cell lung cancer (NSCLC) patients compared to healthy individuals, making it a potential biomarker for diagnosis of NSCLC [83].

Among several lipidomics research that brought to focus recently, there were several lipids identified in urinary exosomes that underlined the potential use of lipids in urinary exosomes as prostate cancer biomarkers [84, 85].

1.3.3 Exosomes as cargo-delivery vehicles

Since exosomes play an important role in intercellular communication, they have been proposed to be potent candidates for immunotherapy, and as a "natural nanocarrier" for cargo delivery against several immunological diseases and cancer. Exosomes naturally contain biological molecules such as proteins and nucleic acids, therefore, other biological materials could also be loaded into exosomes. Beyond other advantages, exosomes provide increased efficiency when weaponized in exosomes, by protecting encapsulated cargo from endonuclease degradation [86] as well as reduce drug accumulation in non-target organs. For instance, it has been showed that, administration of exosome encapsulated chemotherapy drug, Doxorubicin (ExoDOX) resulted in less drug accumulation in cardiac tissue and other non-target organs, with also reduced drug toxicity [14]. In another study, they have been demonstrated that, macrophage-derived exosome loaded chemotherapy drug paclitaxel (ExoPTX), decreased tumor growth in mouse metastatic model of Lewis lung carcinoma more efficiently than did paclitaxel alone [13, 15]. Notably, bioengineered exosomes are established to deliver different siRNAs and chemotherapeutic molecules against cancer cells, which resulted with a generation of exosome-based cancer vaccines. This work is in progress with early-phase clinical trials [75, 87].

On the other hand, efficient delivery of macromolecular therapeutic agents to across blood-brain barrier (BBB) is the main obstacle in the treatment of neurological disease. Nevertheless, exosome has been shown to be a novel natural shuttle for biological molecule (specially siRNA) systemic delivery to the brain [88].

1.4 Hepatitis-B Virus (HBV), Cirrhosis, Hepatocellular Carcinoma (HCC) and Disease Pathogenesis

Hepatitis B virus (HBV) is a double stranded DNA virus that primarily infects human hepatocytes and often develops into chronic liver disease such as acute or chronic hepatitis, Cirrhosis and liver cancer [89]. Although many individuals infected with HBV recover, around 10% are incapable of clearing the virus, thus become chronically infected. Chronic infection might give rise to mild liver disease or in some cases develop active disease which then turn into cirrhosis and liver cancer [90]. Major risk factors for Cirrhosis are chronic infection with hepatitis B virus (HBV), hepatitis C virus (HCV), alcoholic liver disease, and nonalcoholic steatohepatitis (NASH). Hepatocellular carcinoma (HCC) is the malignant tumor of hepatocytes and is the fifth most common cancer in men and seventh most common in women. It is also the most common type of liver cancer which accounts for 75% of all liver cancers. Most HCC patients that accounts for almost 90% of all cases, have a background of chronic liver disease and cirrhosis. Other risk factors for HCC development include intake of aflatoxin-contaminated food, obesity, diabetes, genetic conditions such as hemochromatosis (iron overload), and some metabolic disorders [91].

1.5 Subject and Outline of This Thesis

Exosomes mimic the phenotypic state of the cell of origin. Hence, under health and disease conditions, exosomes are known to act as a modifier of the physiological state of the host. Among many, these effects include activation or suppression of the immune system. Only recently exosomes have been brought to focus in the field of viral diseases and as drug/vaccine nanocarriers, thus their role remains to be fully elucidated. It is aimed to understand the biological fates and effects of these distinct exosomes derived from cell culture supernatants and patient plasmas, on the immune system both *in vitro* and *in vivo* conditions. Moreover, inclusion of proper immunostimulatory endosomal TLR specific ligands within exosomes and harnessing them as a potent therapeutic cancer vaccine against hepatocellular carcinoma is another aim of this study. Therefore, in this study, exosomes were investigated in three distinct subsections.

In the first part, the exosomes purified from i) RAW264.7 (murine macrophage-like), ii) EG7 (murine T cell lymphoma), and iii) HUH7 (human hepatocellular carcinoma) and were analyzed to assess their distinct characteristics, as well as immunomodulatory roles on immune cells either *in vitro* or *in vivo* conditions. Here, the contribution of exosomes to the immune response in the presence of various immunostimulatory TLR ligands including CpG ODN, poly(I:C) and R848 was also studied.

In the second part, the involvement of exosomes to the course of liver disease progression during HBV infection, cirrhosis and HCC was investigated. From patients' plasmas, several cytokines and chemokine levels were analyzed aiming to define the immunological background of these diseases. After exosome characterization, healthy PBMCs were stimulated with patients' exosomes to demonstrate the effects of exosomes on the immune cells as well as its involvement in the course of the disease progression. Moreover, these exosomes isolated from three distinct patient populations were incubated with naive murine splenocyte aiming to compare the pathological potential in the mouse immune system.

The last part of this thesis is dedicated to the analyses of HCC cell line (i.e. from HUH7) derived exosomes as a "therapeutic cancer vaccine". As these nanovesicles

have the capacity to transfer different biological molecules from donor to recipient cells and are robust targets for immunotherapeutic interventions, we sought to use the exosomes as nanocarriers. To this end, multiple immune stimulants (nucleic acid sensing TLR ligands and iNKT ligands) were loaded into HUH7 exosomes to determine whether cargo-loaded exosomes could enhance the anti-tumor response in established HCC model. Consequently, to compare the performance of this exosome-based therapeutic vaccine delivery system, a well-established lipidic nanocarrier -neutral liposomes- were also employed as the reference "conventional" cancer vaccine delivery platform together with our exosome groups, thus tumor regression profiles as well as survival rates of animals were investigated *in vivo*.

CHAPTER 2

Materials and Methods

2.1. Materials

2.1.1 Patients and Healthy Controls

All patient samples investigated in this study were obtained from Bozok University, Faculty of Medicine, Gastroenterology Polyclinic as well as from Ankara Yuksek Ihtisas Hospital, Gastroenterology Polyclinic. In this study, peripheral blood of 10±2 HBV positive (HBV DNA level ≥ 2000 IU/mL), 10±2 Cirrhosis (chronic HBV-related), 10±2 HCC (chronic HBV-related) patients and 5±2 healthy control individuals were included.

The study was approved by the Institutional Review Board. Individuals were informed about all aspects of the study and informed consents provided (Human Ethical committee approval #2017-08/01).

2.1.2 Mouse Strains

Adult *Nude* (male, 6–10 weeks old) mice used for establishment of HCC model, *BALB/c* (male, 6–8 weeks old) and *C57BL/6* (male, 6–8 weeks old) used for ex vivo experiments were maintained in laboratory animal research facility unit of the Department of Molecular Biology and Genetics in Bilkent University. All mice strains were sustained under controlled conditions; at 22°C with having unlimited access of

food and water. All experimental procedures were approved by the animal ethical committee of Bilkent University (Bil-AEC/Protocol# 2016/2).

2.1.3 General laboratory and cell culture reagents and materials

DMEM High Glucose, RPMI-1640 mediums used all along cell culture together with 1x PBS, FBS, L-glutamine, 2-mercaptoethanol and DNase/RNase free water were purchased from Gibco (Maryland, USA). Other supplementary reagents including Na-Pyruvate, HEPES, NEAA, Pen-Strep and Trypsin-EDTA were purchased from Lonza (Basel, Switzerland). Zap-OGLOBIN® II Lytic reagent and Isoton II diluent buffer were purchased from Beckman Coulter (California, USA). Trypan Blue alongside Hypure Molecular Biology Grade Water which was used for cell counting, obtained from Hyclone (Cramlington, UK). Lymphocyte Separation Medium (Cat# C4754.0100) that was used in PBMC isolation process, purchased from Genaxxon Bioscience (Ulm, Germany). BCA Protein Assay kit (Cat# 23225) used for protein quantification was obtained from Thermo Fisher Scientific (Massachusetts, USA).

From donor plasmas, exosome purification was performed by using plasma/serum exosome purification kit (Cat #58300) purchased from Norgen (Ontario, Canada).

During the cell freezing process, Mr. Frosty, isopropanol filled container was used and was purchased from Thermo Fisher Scientific.

2.1.4 PRR Ligands

Different agonists were used in *in vitro* stimulations and *in vivo* studies. Lipopolysaccharide (LPS; TLR4 ligand) was purchased from Sigma (Missouri, USA), poly (inosinic acid: cytidylic acid) (poly(I:C); TLR3 ligand) was purchased from Amersham (Buckinghamshire, UK). R848 (TLR7/8 ligand) was purchased from Invivogen (Toulouse, France). *α-Galactosylceramide* (KRN7000, *α*-GalCer) used in triple reagent encapsulation into exosomes and liposomes, were purchased from Avanti Polar Lipids (Alabama, USA).

CpG ODNs (TLR9 ligands) used throughout the study listed below (**Table 2.1**) were synthesized by Alpha DNA (Montreal, Canada) or supplied from NIH, USA. All ODNs were endotoxin free.

Table 2.1. List of CpG ODNs.

ODN	Brand	Length	Sequence (5'-3')
K23	Alpha DNA	12 mer	TCGAGCGTTCTC (PS*)
D35-3CG	Alpha DNA	20 mer	GGTCGATCGATCGAGGGGGG (MB**)
1555-3CG	NIH	20 mer	GACGTTGACGTTGACGTTGG (PS)

**PS: Phosphorothioate linkages **MB: Mix (PS and PO) linkages between bases.*

2.1.5 Lipids used in liposome preparation

Cholesterol (Chol) and L-α-phosphatidylcholine (PC) used for neutral liposome preparation were purchased from Avanti Polar Lipids.

2.1.6 ELISA Reagents

Monoclonal unlabeled coating and biotinylated reporter antibody pairs and recombinant proteins (**Table 2.2**), used in cytokine ELISA were purchased from Biolegend (California, USA), MabTech (Nacka, Sweden), BD (New Jersey, USA) and Thermo Fisher Scientific.

B16-Blue IFNα/β reporter cells were obtained from Invivogen.

2HB 96-well plates used in ELISA were purchased from Thermo Fisher Scientific and SPL Life Sciences (Gangwon, Korea).

Table 2.2. List of antibodies and reagents used in ELISA.

Reagent Name	Catalog #	Brand Name	Working Concentration
Anti-human IL-4	3410-1A-20	MabTech	1 µg/ml
Biotin anti-human IL-4	3410-1A-20	MabTech	1:1000 dilution
Human recombinant IL-4	3410-1A-6	MabTech	12.5 ng/ml
Anti-human IL-5	33-91-1A-6	MabTech	2 µg/ml
Biotin anti-human IL-5	33-91-1A-6	MabTech	1:1000 dilution
Human recombinant IL-5	34-90-1A-6	MabTech	12.5 ng/ml
Anti-human IL-6	501102	Biolegend	2 µg/ml
Biotin anti-human IL-6	501202	Biolegend	1:1000 dilution
Human recombinant IL-6	3460-1A-20	MabTech	20 ng/ml
Anti-human IL-8	3560-1H-6	MabTech	2 µg/ml
Biotin anti-human IL-8	3560-1H-6	MabTech	1:1000 dilution
Human recombinant IL-8	3560-1A-6	MabTech	25 ng/ml
Anti-human IL-10	3430-1A-6	MabTech	2 µg/ml
Biotin anti-human IL-10	3430-1A-6	MabTech	1:1000 dilution
Human recombinant IL-10	3430-1A-6	MabTech	8 ng/ml
Anti-human IL-12	511002	Biolegend	5 µg/ml
Biotin anti-human IL-12	508802	Biolegend	1:1000 dilution
Human recombinant IL-12	554633	BD	250 ng/ml

Anti-human IL-13	3471-1A-6	MabTech	2 µg/ml
Biotin anti-human IL-13	3471-1A-6	MabTech	1:1000 dilution
Human recombinant IL-13	3470-1A-6	MabTech	4 ng/ml
Anti-human IFNγ	507502	Biolegend	5 µg/ml
Biotin anti-human IFNγ	502504	Biolegend	1:1000 dilution
Human recombinant IFNγ	RIFNG50	Thermo	50 ng/ml
Anti-human IP-10	555046	BD	2 µg/ml
Biotin anti-human IP-10	555048	BD	1:500 dilution
Human recombinant IP-10	551130	BD	100 ng/ml
Anti-human IL-1β	3416-1A-6	MabTech	2 µg/ml
Biotin anti-human IL-1β	3416-1A-6	MabTech	1:1000 dilution
Human recombinant IL-1β	3416-1A-6	MabTech	25 ng/ml
Anti-human TGF-β	3550-1A-6	MabTech	2 µg/ml
Biotin anti-human TGF-β	3550-1A-6	MabTech	1:1000 dilution
Human recombinant TGF-β	3550-1A-6	MabTech	1.25 nM
Anti-human TNF-α	3510-1A-6	MabTech	2 µg/ml
Biotin anti-human TNF-α	3510-1A-6	MabTech	1:1000 dilution
Human recombinant TNF-α	3510-1A-6	MabTech	12.5 ng/ml
Anti-mouse IL-6	504502	Biolegend	2 µg/ml
Biotin anti-mouse IL-6	504602	Biolegend	1:1000 dilution

Mouse recombinant IL-6	575702	Biolegend	100 ng/ml
Anti-mouse IL-10	504902	Biolegend	4 µg/ml
Biotin anti-mouse IL-10	505004	Biolegend	1:1000 dilution
Mouse recombinant IL-10	575804	Biolegend	1.25 µg/ml
Anti-mouse IL-12	505202	Biolegend	4 µg/ml
Biotin anti-mouse IL-12	505302	Biolegend	1:1000 dilution
Mouse recombinant IL-12	573102	Biolegend	100 ng/ml
Anti-mouse IFNγ	AN18	MabTech	1 µg/ml
Biotin anti-mouse IFNγ	R4-6A2	MabTech	1:1000 dilution
Mouse recombinant IFNγ	3321-1A-20	MabTech	40 ng/ml
SA-ALP	3310-8	MabTech	1:1000 dilution
PNPP	34047	Thermo	1 tablet + 1 ml buffer + 4 ml ddH_2O/ plate

2.1.7 Flow Cytometry Reagents

All fluorochrome-labeled antibodies (**Table 2.3**) used for cell surface staining and exosome staining were obtained either from Biolegend or BD. Fixation Medium A used for cell fixation was obtained from Invitrogen (Massachusetts, USA). 3.5 µM 4% w/v Carboxyl latex beads used in conjugation of exosomes for flow cytometry analysis were obtained from Life Technologies (USA). Flow cytometric analyzes were performed via NovoCyte Flow Cytometer (ACEA Biosciences, California, USA).

Table 2.3. List of purified and fluorochrome-conjugated antibodies used in flow cytometric analysis.

Antibody Name	Catalog #	Brand Name
Purified anti-human CD9	312102	Biolegend
Purified anti-human CD63	353014	Biolegend
Purified anti-human CD81	349502	Biolegend
Anti-human CD9-PE	312106	Biolegend
Anti-human CD63-PE	353004	Biolegend
Anti-human CD81-PE	359506	Biolegend
Anti-human CD274-PE	329706	Biolegend
Anti-mouse CD3-PE	100206	Biolegend
Anti-mouse CD4-APC	100516	Biolegend
Anti-mouse CD8-Pe/Cy5	107110	Biolegend
Anti-mouse CD11c-PE	553802	BD
Anti-mouse CD19-FITC	115506	Biolegend
Anti-mouse B220- Pe/Cy5	103210	Biolegend
Anti-mouse F4/80- Pe/Cy7	123114	Biolegend
Purified anti-mouse CD9	124802	Biolegend
Purified anti-mouse CD63	143902	Biolegend
Purified anti-mouse CD81	104902	Biolegend
Anti-mouse CD9-PE	124806	Biolegend

Anti-mouse CD63-PE	143904	Biolegend
Anti-mouse/rat CD81-PE	104906	Biolegend
Mouse IgG1-PE	400114	Biolegend
Mouse IgG2b-PE	401208	Biolegend
Rat IgG2a-PE	400507	Biolegend
Armenian Hamster IgG-PE	4000907	Biolegend

2.1.8 Immunoblotting Antibodies and Reagents

Detailed specificities of primary and secondary immunoblotting antibodies were listed in **Table 2.4**.

Table 2.4. List of immunoblotting antibodies.

Antibody Name	Catalog #	Brand Name	Working Concentration
β-actin	8H10D10	Cell Signaling	1:2000 dilution in 5% milk
STING	D2P2F	Cell Signaling	1:2000 dilution in 5% BSA
PD-L1	E1L3N	Cell Signaling	1:500 dilution in 5% milk
Anti-rabbit IgG-HRP linked	7074P2	Cell Signaling	1:5000 dilution in 5% milk
Anti-mouse IgG-	7076P2	Cell Signaling	1:5000 dilution in 5%

HRP linked			milk
Anti-rat IgG HRP linked	N/A	N/A	1:5000 dilution in 5% milk
Anti-goat IgG	sc-2033	Santa Cruz	1:5000 dilution in 5% milk
ALIX	sc-49268	Santa Cruz	1:500 dilution in 5% milk
TSG101	ab83	Abcam	1:500 dilution in 5% milk
Grp-94	sc-32249	Santa Cruz	1:500 dilution in 5% milk

Pre-stained protein ladder (10-250 kDa, cat #26619), 0.45 μm PVDF transfer membranes and chemiluminescent substrate (ECL) for detection of horseradish peroxidase (HRP) activity from antibodies, were obtained from Thermo Scientific. At the end of immunoblotting process, membrane visualization was carried out by Amersham Imager 600. See *Appendix A* for immunoblotting buffer and solution recipes.

2.2. Methods

2.2.1 Cell Line Maintenance

See *Appendix A* for cell culture media recipes.

2.2.1.1 Cell Lines

HUH7 (or Huh7)

Huh7 human hepatocellular carcinoma cell line was cultured in 10% DMEM, high glucose complete medium. For sub-culturing, cells were trypsinized with 2x trypsin-EDTA and media was changed every 2-3 days. For supernatant collection, cells were maintained in exo-free FBS supplemented 5% DMEM, high glucose complete medium.

EG7-OVA

EG7-OVA is derived from EL4 (mouse lymphoma cell line). Cells were cultured in 10% RPMI 2-mercaptoethanol (Gibco, USA) and 1 mg/ml Geneticin (Hyclone, USA) supplemented medium. When cells were reached around 80% confluency, they were passaged as 1:5 ratio. For supernatant collection, cells were maintained in exo-free FBS supplemented 5% RPMI, 2-mercaptoethanol supplemented complete medium.

RAW 264.7

Raw 264.7 mouse macrophage-like cells were cultured in 10% RPMI medium. When cells were reached around 80% confluency, they were gently scraped and subcultured as 1:5 ratio. For supernatant collection, cells were maintained in exo-free FBS supplemented 5% RPMI complete medium.

2.2.1.2 Cryopreservation and cell thawing

Cells within the cryotube that was taken from liquid nitrogen, thawed by using water bath at 37 °C. Hereafter, the DMSO containing liquid cell suspension were transferred to 15 ml falcon and diluted by adding pre-warmed 2% FBS supplemented RPMI-1640 complete medium (2% RPMI, hereafter) until the volume reaches 13 ml. Later, cells were centrifuged at 300 X g for 10 mins and resuspended in 1 ml 10% FBS supplemented RPMI-1640 complete medium (10% RPMI, hereafter).

For selecting the seeding density and flask size to be used, number and type of cell is important. T-25 or T-75 flasks were selected accordingly. The volume of the flasks was completed to 5 ml and 15 ml respectively and put into cell culture incubator which was adjusted to 37°C with 5% CO_2.

Cryopreservation is crucial process to long-term maintenance of *cells*.
Before this process, the confluency and the viability of cells were checked. If they were almost 80% viable and confluent, cells were trypsinized/scraped (for adherent cells) or directly collected into a falcon (for suspension cells) and centrifuged at 300 X g for 5 mins.

According to the number of cells to be freeze, the cell pellet was resuspended in different volumes of ice-cold FBS. In general, the pellet was resuspended as $5x10^6$ cells in 500 µl and transferred to cryotubes with equal volume of 20% DMSO so that the cryotubes had final 10% DMSO concentration. Hereafter, the cryo tubes were placed into Mr. Frosty, isopropanol filled cell freezing container and stored at -80^oC. For longer preservation, they should be kept in liquid nitrogen. Therefore, after one-to-three-day storage at -80°C, cryo tubes were placed into liquid nitrogen tank.

2.2.1.3 Cell Counting

For mouse splenocyte, PEC and human PBMC studies, cell counting was performed either by BD Accuri C6 or NovoCyte flow cytometers. In short, after centrifugation cell pellet was resuspended in 1 ml complete RPMI-1640 medium than 20 µl single cell suspension was added into 5 ml of Isoton II diluent buffer. 2-3 drops of Zap-Oglobin II lytic reagent was added to get rid of the red blood cells. 100 µl from this solution was assessed by flow cytometer. The appropriate gate for live cells was taken in order to eliminate dead and apoptotic cells from the population. Total live cell number was calculated by multiplying the counted events with the dilution factors.

Other used cell lines described in Section 2.2.1 were counted by hemocytometer. After centrifugation of the cells at 300 X g for a total 5-10 minutes, cell pellet was resuspended in 1 ml respective medium, then 10 µl from 1 ml single cell suspension was 10 times diluted with fresh media in an eppendorf and then mixed with Trypan blue at 1:1 ratio, to identify dead cells during counting via the hemocytometer. 10 µl from this 20-fold diluted suspension was transferred onto hemocytometer and observed under the light microscope. The microscope was adjusted to hemocytometer grids (1 mm^3/each) where represented in red square frames in **Figure 2.1**.

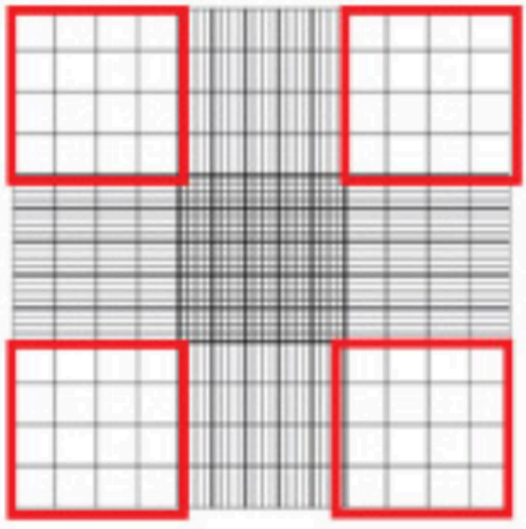


Figure 2.1. Representative counting chamber, hemocytometer.

From the counted viable cells, total cell number was calculated according to the formula below.

$$\text{Total Cell \#: } \left(\frac{\text{Counted cell \# in red frames}}{4}\right) \times 10^4 \times 20 \text{ (dilution factor)} \times 1 \text{ (ml)}$$

2.2.2 PBMC isolation from peripheral blood

Peripheral blood was collected from each patient and healthy control as 10-20 ml in K_3EDTA anticoagulant containing blood collection tubes.

As the first step of PBMC isolation, 1.5 volumes of peripheral blood were layered drop by drop on top of 1 volumes of lymphocyte separation medium (LSM) in 15 or 50 ml falcons. While layering, the tube should be tilted slightly and immobilized to avoid mixing two layers. Following the density gradient centrifugation at 600 X g for 30 mins in break 'off' setting, the top phase, plasma was collected into a new falcon tube and centrifuged at 1500 X g for 10 mins to get rid of any remaining cells and cellular debris. After this step, plasma was either snap-frozen and preserved or used in EV and/or exosome isolation immediately.

The remaining interface having a cloudy appearance, consists of PBMCs. Therefore, this layer was carefully collected and transferred to a new falcon by a sterile pasteur pipette. Two times washing step were performed by using 2% RPMI to complete the tube and centrifuged at 600 X g for 10 mins at each washing step and supernatants were discarded. At last, PBMC pellet was resuspended in 1 ml 5% FBS supplemented RPMI-1640 (5% RPMI, hereafter) and counted by flow cytometer.

2.2.3 Preparation of single cell suspension from mouse spleen

Cervical dislocation was the method used throughout animal experiments when sacrificing the mice to collect different organs and tissues.

After cervical dislocation, BALB/c or C57Bl/6 mice spleens were taken into 2-3 ml ice-cold complete 2% RPMI containing 6-well plate or 60x15 mm petri dish. Then, in cell culture hood, spleens were crushed with the back of syringe plunger to make tissue as single cell suspension. Cell suspension was transferred to 15 ml falcon and completed up to 14 ml with warm 2% RPMI and centrifuged at 300 X g for 5-7 mins. The supernatant was discarded, and pellet was resuspended in 1 ml 5% RPMI. Cell counting was done by flow cytometer. Prepared splenocytes were used either in cell culture stimulation assays or were fixed for flow cytometric analysis.

2.2.4 Preparation of peritoneal cavity cells (PECs)

To evaluate the internalization of the exosomes by peritoneal immune cells, SPDiOC stained exosomes were administrated to BALB/c mice intraperitoneally (IP) as 50 µg exosome/mouse. After 18 and 36 hrs, PECs were collected by injecting and recollecting of 10 ml of sterile ice-cold 1x PBS into euthanized mice. Collected PBS was centrifuged for 2 times with warm 2% RPMI at 300 X g for 7 mins. Then, cell pellet was resuspended with 5% RPMI and counted with flow cytometry. At last, cells were fixed and stored at +4^{o}C until they were analyzed for SPDiOC positivity by flow cytometry.

2.2.5 Isolation of EVs and exosomes from cell culture supernatants

Isolation of EVs and exosomes from cell culture supernatants was based on differential centrifugation method [92]. Briefly, following the centrifugation of collected supernatants at 1500 X g for 10 mins to get rid of any remaining cells or debris, they were either snap-frozen in liquid nitrogen and conserved at -80^{o}C, or directly allocated for EV / exosome isolation. If the isolation would be from snap-frozen supernatants, they were slowly thawed by overnight incubation at +4^{o}C and vortexed mightily before starting the isolation process in order to separate any vesicle or protein aggregation to EVs / exosomes during the storage at -80^{o}C.

Supernatants gone through aforementioned steps, were transferred to sterile ultracentrifuge tubes (Beckmann Coulter) to be centrifuged at 10000 X g (8700 rpm for SW28 rotor) for 10 mins at +4^{o}C to eliminate larger particles.

For exosome isolation, there was an additional step where the supernatant was collected and passed through 0.2 μm filter to ensure that all particles larger than 220 nm were eliminated. It should be noted, if the purpose was to isolate EVs not exosomes; this filtering step was omitted.

Hereafter, the supernatants were transferred to other ultracentrifuge tubes. If necessary, the tube volume was completed up to 35 ml with sterile 1x PBS. Following the next centrifugation step at 100000 X g (27500 rpm for SW28 rotor) for 90 mins at 4^{o}C, EVs were adhered to the bottom surface of the tubes. Therefore, the supernatants were aspired and the remaining ~ 2 ml EV containing solution was resuspended gently by pipetting and completed into 35 ml with sterile 1x PBS. As the final washing step, ultracentrifugation at 100000 X g (27500 rpm for SW28 rotor) for 90 mins at 4^{o}C was performed. Supernatant was discarded and EV pellet was collected by resuspending in desired amount of sterile 1x PBS. EVs were kept at +4^{o}C for further use or snap-frozen to be stored at -80^{o}C for a longer time.

2.2.6 Isolation of exosomes from peripheral blood plasma

Exosome purification kit was used for isolating exosomes from peripheral blood plasma. Kit protocol was optimized and modified from original manufacturer's instructions. All steps were carried out at room temperature (RT).

As the first step, plasma was centrifuged at 10000 X g for 5 mins to get rid of any remaining contaminants. For each plasma sample, 15 ml falcon tubes were labelled properly, and 1 ml nuclease free H_2O was mixed with 100 µl Exo C buffer from the kit then, 1 ml plasma was added. The solution mixed well by vortexing about 10 secs. To the mixture from previous step, 200 µl Slurry E was added and vortexed for about 10 secs followed by 10 mins incubation. Importantly, kit reagent Slurry E was mixed thoroughly prior to use to ensure that resin was completely resuspended. After incubation, the solution was vortexed and centrifuged at 4000 rpm for 2 mins. The supernatant was discarded, and slurry pellet was resuspended in 200 µl ExoR Buffer and homogenized by vortex. This was followed by 10 mins incubation. Then, the solution was mixed well by vortex and centrifuged at 2000 rpm for 2 mins. At the end, supernatant was transferred to a Mini Filter Spin column assembled in an elution tube and centrifuged at 6000 rpm for 1 min to eliminate any remaining resin from the purified exosome containing supernatant. After centrifugation, flow through containing eppendorf was placed on a rotator for 15-30 mins in a medium speed, then spinned for 5 mins at 16000 X g to get rid of remaining exosome bound slurry reagent. Exosomes were ready for further quantification assays.

2.2.7 Protein isolation from cells and exosomes

Cells were collected from one confluent culture flask and pellet was resuspended in previously prepared or freshly prepared ice-cold RIPA buffer. The amount of RIPA to be used, was depend on the cell number or exosome amount. For cells; pellet collected from one confluent T75 flask was resuspended in ~300 µl RIPA buffer and for exosomes; 50 µg exosomes were mixed with 50 µl RIPA as 1:1 ratio. After addition of RIPA, exosomal protein isolation process requires three repeats of 5 mins sonication and 15 secs vortex between each sonication. Hereafter, the rest of the process was the same for both cellular protein isolation and exosomal protein isolation. As a continuation, samples were incubated on ice for 20 mins and vortexed every 5 mins. Following the centrifugation at 10000 X g (or at 15000 rpm) for 20 mins at 4^{o}C, the supernatant which was the cell lysate was transferred to a new eppendorf to be stored at -80^{o}C.

2.2.8 Determination of protein concentration

Protein concentration of isolated proteins and EVs/exosomes were determined by Micro BCA Protein Assay Kit (Thermo Fisher Scientific). The protocol was carried out by performing the manufacturer's instructions with minor modifications as described in the following. BSA standards dilutions were prepared between 1.96-2000 µg/ml (by diluting 10 times as 2x dilution with 1x PBS) and loaded into flat bottom 96-well plate as 25 µl/well and mixed with 200 µl of working reagent. Besides, the sample to be quantified, was added as 5 µl/well, duplicate and mixed with 200 µl of working reagent. The plate was covered with aluminum foil and incubated at 37^{o}C for 30 mins then 10 mins at RT. After incubation, the absorbance of samples was measured at 562 nm by spectrophotometer (Synergy HT, BioTek) and their concentrations were determined by BSA standard curve.

2.2.9 Exosome characterization by flow cytometry

Bead-based strategy was used to increase the size of exosomes and be able to analyze by flow cytometer (Tamer Kahraman PhD Thesis, 2016 and Gözde Güçlüler PhD Thesis, 2017). Hence, Carboxyl latex beads were used to conjugate with antibodies against exosomal markers such as CD9, CD63 or CD81. After vortexing the latex beads vigorously, 10 µl carboxyl latex beads were washed with 1x PBS at 12000 X g for 10 mins at RT. Then, the beads pellet was solved in 50 µl of 1x PBS and incubated with 10 µg LEAF purified anti-CD63 antibody for 30 mins at dark. After, volume was completed to 500 µl with 1x PBS and placed on a rotator that was adjusted to middle rotation speed. After ON incubation, latex beads/anti-CD63 complex were centrifuged at 12000 X g for 10 mins at RT and blocked with 1 ml of 5% BSA containing 1x PBS for 4 hrs at RT. Blocked beads were then washed once with 1x PBS at 12000 X g for 10 mins at RT. At final step, the coated beads were resuspended in 100 µl of storage buffer (1% BSA containing PBS solution). This was the ratio to be used for preparing bead-Ab conjugation for 100 staining (10 µl carboxy latex beads + 10 µl LEAF purified anti-CD63).

For exosome-bead conjugation, exosomes were incubated with previously prepared coated beads for total number of staining to be performed (1 µg exosome mixed with 1 µl bead for each staining). Volume was completed to 50 or 100 µl with 1x PBS and incubated half hour at RT. After incubation, volumes were raised to 500 µl and placed on a rotator ON, in a medium speed. Exosomes were now conjugated to the coated beads and were ready for staining.

For staining exosomes after conjugation, 1 µg exosome+bead conjugation was used for each staining. Similar to cell staining protocol, antibody concentration was 1 µg/ml. The incubation of exosomes with fluorochrome conjugated Abs was continued for 1 hr in dark, at RT. All washing steps carried out for exosomal staining was done by 1x PBS.

2.2.10 Surface marker staining by flow cytometry

Collected cells were centrifuged at 300 X g for 5 mins and the pellet was resuspended with 50-100 µl of fixation medium A [93, 94].

Samples were incubated for 15 mins at dark and washed once with 1 ml FACS buffer for 5 mins at 400 X g. Fixed cell pellet was resuspended in 1 ml FACS buffer and stored at 4^{o}C.

For staining of fixed cells, cell pellet was centrifuged at 400 X g for 10 mins and the pellet was resuspended in desired amount of FACS buffer and distributed into tubes as 50 µl/tube. On the other hand, antibody cocktails were prepared at 1µg/ml concentration in FACS buffer and add into cell containing tubes as 50 µl/tube. Cells with fluorochrome-conjugated antibodies were mixed and incubated for 30 mins at dark, RT. After incubation, samples were washed with FACS buffer and the pellet was resuspended in 100 µl 1x PBS for flow cytometry analysis.

2.2.11 Liposome preparation

All phospholipid and cholesterol stocks were prepared in chloroform (as 20mg/ml stocks) and were kept at -20°C. Lipids were mixed in a round bottom glass flask to prepare liposomes via dehydration-rehydration method [95, 96].

To prepare neutral liposomes, Cholesterol (Chol) and L-α-phosphatidylcholine (PC) were added as 1:1 (w/w ratio). Initially, chloroform was evaporated using rotary evaporator (Thermo Fisher Scientific) and uniform thin layer was formed. Dry lipid film was further eliminated from residual chloroform and oxygen by streaming the nitrogen gas through the round bottom flask, to prevent lipid peroxidation. Following the addition of 1 ml of PBS and glass beads, lipid films were disrupted by spinning round the flask until all lipid layer was dissolved. Obtained large multilamellar vesicles (MLVs) were transformed to small unilamellar vesicles (SUVs) by sonicating liposomes 10 cycles for 1 min ON – 30 secs OFF durations with 40% amplitude (VibraCell, SONICS, Connecticut, USA). After addition of CpG ODN and other ligands, the mixture was snap frozen in liquid nitrogen, freeze dried overnight

(Benchtop K, Virtis, Pennsylvania, USA) to form lipid/ligand powder.

Controlled rehydration method was performed to encapsulate ligands within liposomes. First, 1/10 of total initial snap-frozen volume of DNase/RNase free dH_2O was added to the liposome/ligand powder and vortexed for 15 secs every 5 mins for a total of 30 mins at RT. Then, equal volume of PBS was added to the solution and incubated for 10 mins at RT. After incubation, desired amount of PBS was added into the encapsulated molecule(s) mixture and prepared liposome formulations were kept at 4°C until further use.

2.2.12 Cargo loading into exosomes

Encapsulation of TLR ligands into exosomes was done by dehydration-rehydration loading method (modified from Gürsel et al Patent, Pat# WO03040308).

First, CpG ODN and other ligands, were mixed as 1:1 ratio (30 µg/mouse, except for αGal-Cer, that was used as 0.1 µg/mouse) and the mixture was snap frozen in liquid nitrogen, freeze dried overnight (Benchtop K, Virtis) to form exosome/ligand powder.

Controlled rehydration method was performed to encapsulate ligands within exosomes. First, 1/10 of total initial snap-frozen volume of DNase/RNase free dH_2O was added to the exosome/ligand powder and vortexed for 15 secs every 5 mins for a total of 20 mins at RT. Then, equal volume of PBS was added to the solution and incubated for 10 mins at RT. After incubation, desired amount of PBS was added into the encapsulated molecule(s) mixture and prepared exosome formulations were kept at 4°C for further use.

2.2.13 Cytokine ELISA and SEAP reporter assay

After stimulation assays, supernatants or plasmas were transferred into a new plate after centrifugation of cells in 96-well plate at 300 X g for 5 mins. All antibodies (Abs) which were used in ELISA were prepared in blocking solution (See *Appendix A*).

High binding 2 HB ELISA 96-well plates were coated with anti-cytokine coating Abs and transferred as 50 µl/well and incubated overnight (O/N) at +4^{o}C. Specificities and concentrations of all Abs used in ELISA were listed in **Table 2.2**. After ON coating, blocker solution was used to block non-specific bindings and it was loaded as 200 µl/well and incubated 2 hrs at RT. Then, plates were washed 5 times with washing buffer and 3 times rinsed with ddH_2O. After washing step, samples and serially diluted (11 series of 1/2x dilution, in duplicates) recombinant proteins were layered into ELISA plate as 50 µl/well and incubated O/N at 4^{o}C. Following the washing step as described earlier, biotin-labeled anti-cytokine Abs were added for 2 hrs incubation at RT as 50 µl/well. The next step was followed by washing and 1:1000x diluted Streptavidin–Alkaline Phosphatase (SA-ALP) addition as 50 µl/well and incubated for 1 hr at RT. Finally, plates were washed and developed by adding p-nitrophenyl phosphate substrates (PNPP) as 50 µl/well. Optical density (OD) values of samples and standard cytokines were detected by a Spectramax, microplate reader (Molecular Devices) at 405 nm. According to the standard curve, concentration of secreted cytokines was calculated in different reading time points.

For detection of murine type I IFNs, B16-Blue IFN-α/β cells were seeded into 96-well flat bottom tissue culture plates as 7x10^{4} in 180 µl/well and incubated with supernatants of stimulated cells as 20 µl/well at 37^{o}C incubator. After 24 h, supernatants were collected and transferred to a new 96-well plate and incubated with PNPP (50 µl/well). In the same way with cytokine ELISA protocol OD values were detected by microplate ELISA reader at 405 nm

2.2.14 Immunoblotting

2.2.14.1 Preparation of protein samples

Before the use of proteins in immunoblotting, micro BCA protein quantification assay was performed to determine the amount of proteins (Thermo Fisher Scientific). Then for each loading, 15 µg and 25 µg proteins were taken from cellular protein and exosomal protein respectively to prepare the mixture with β-Mercaptoethanol containing (1/3 of total volume) 4x loading dye (laemmli buffer (See *Appendix A*), diluted to be 1x at final volume) and tubes were placed in a heater which was pre-heated to 95°C where incubated for 5 mins. Since from each sample, equal volume would be loaded into SDS gel, additional RIPA buffer was added into the mixture if necessary. After heating at 95^{o}C for 5 mins, samples were spun down for 5-10 secs and loaded into SDS gel. Loading volume was depend on the comb size. In addition, the protein ladder was also loaded into SDS gel as 5 µl.

2.2.14.2 SDS-PAGE running

Since the concentration of a gel depends on the molecular weight of the proteins to be used, 10% and 12% resolving gels and 5% stacking gel were prepared throughout the study.

For the preparation and running procedures, Bio-Rad Mini PROTEAN Tetra Cell system was used. After the preparation of gels, they were transferred into mini tank, the comb was removed and the tank was filled with 1x running buffer. The samples were previously prepared and were loaded into gel. Power-supply was set to 90 volts until the samples were passed through the stacking gel, then augmented to 120 volts until the desired time. After running was completed, gels were put in transfer directly.

2.2.14.3 Transfer to the membrane

Wet transfer system was used as a transfer system by the apparatus of Bio-Rad Mini Transblot Cell. Transfer buffer was prepared freshly. A sponge, following by 2 Whatman papers, gel, PVDF membrane, 2 Whatman papers and a sponge, gel holder cassette was placed into the sandwich apparatus and placed into transfer tank filled with transferred buffer until blotting line. Transfer process was performed in an ice box at 100 volts for 90 mins.

2.2.14.4 Blotting and development

Membranes were incubated with 5% milk blocking solution at RT for 1h on a shaker. Then, incubated with primary antibodies in desired dilutions, overnight at +4°C by gently shaking.

After primary antibody incubation ON, the membranes were washed with 1x TBS-T solution 3 times for 5 mins. Following the incubation with secondary Ab in 5% milk blocking solution for 1 hr at RT, membranes were washed again 3 times for 5 mins. ECL Prime chemiluminescent detection kit was used for immunodetection and used as 1:1 reagent ratio mix (Thermo Fisher Scientific). Finally, visualization was performed by Amersham Imager 600.

2.2.15 Development of HCC xenograft in Athymic mice

HUH7 cells were subcutaneously injected to right flank of nude mice (male, 6-10-week-old) as $4x10^6$ cell/mouse, in 100 µl 1x PBS. Tumor size were measured and recorded by an electronic caliper three times a week. Tumor volumes were calcµlated as the formula below.

Tumor Volume (mm^3): height (mm) x width (mm) x length (mm)

Each group of mice were receiving different formulations of TLR ligands either in liposome and exosome encapsulated or in their free forms, every two days, intraperitoneally. Treatment groups are as follows;

1: Control - PBS only,

2: two ligands free formulation indicated as 1555-3CG+pIC,

3: exosome-loaded two ligand formulation indicated as Exo(1555-3CG+pIC),

4: liposome-loaded two ligand formulation indicated as Lipo(1555-3CG+pIC),

5: three ligands free formulation indicated as αGC+1555-3CG+pIC,

6: exosome-loaded three ligand formulation indicated as Exo(αGC+1555-3CG+pIC) and lastly,

7: liposome-loaded three ligand formulation indicated as Lipo(αGC+1555-3CG+pIC).

Total injection number was four. At the end, when volume reached to >2000 mm^3, animals were euthanized. Cardiac blood and spleens were collected from each mouse.

2.2.16 Statistical Analysis

All statistical analyses were carried out using GraphPad Prism program (version 6, USA). In order to determine the statistical significance between the groups one-way ANOVA, Tukey's test, two-way ANOVA and/or Student's t-test were performed. All Kaplan Meier Graphs' significance was calculated by Log-rank (Mantel-Cox) test. P values ≤ 0.05 were considered to be statistically significant.

CHAPTER 3

Results

3.1. Immunomodulatory Effects of Cell Line-Derived Exosomes

3.1.1. Characterization of EG7, HUH7 and RAW exosomes

Cell line supernatants were collected from i) RAW264.7 (murine macrophage-like), ii) EG7 (murine T cell lymphoma), and iii) HUH7 (human hepatocellular carcinoma) and exosomes were isolated by using ultracentrifugation method. The universal characteristics of exosomes were assessed by bead assay via flow cytometry and surface protein analyses via immunoblotting. As presented in **Figure 3.1**, cell line-derived exosomes were positively found to express TSG101 protein and exosomal surface markers such as CD9 and CD81 which identifies the vesicles as exosomes.

PD-L1 is one of the surface expressed immune checkpoint molecules frequently up-regulated on cancer cells and suppress the activation of T cells [78]. This pathway inhibition is one of the major breakthroughs in tumor immunotherapy research. Therefore, expression of immune checkpoint molecule, PD-L1 was evaluated among all three exosome species (**Figure 3.1 F and G).** Among all, RAW exosome had the highest expression level in terms of both exosome surface marker and PD-L1 co-inhibitory receptor expressions, which were assessed by bead-based flow cytometric staining.

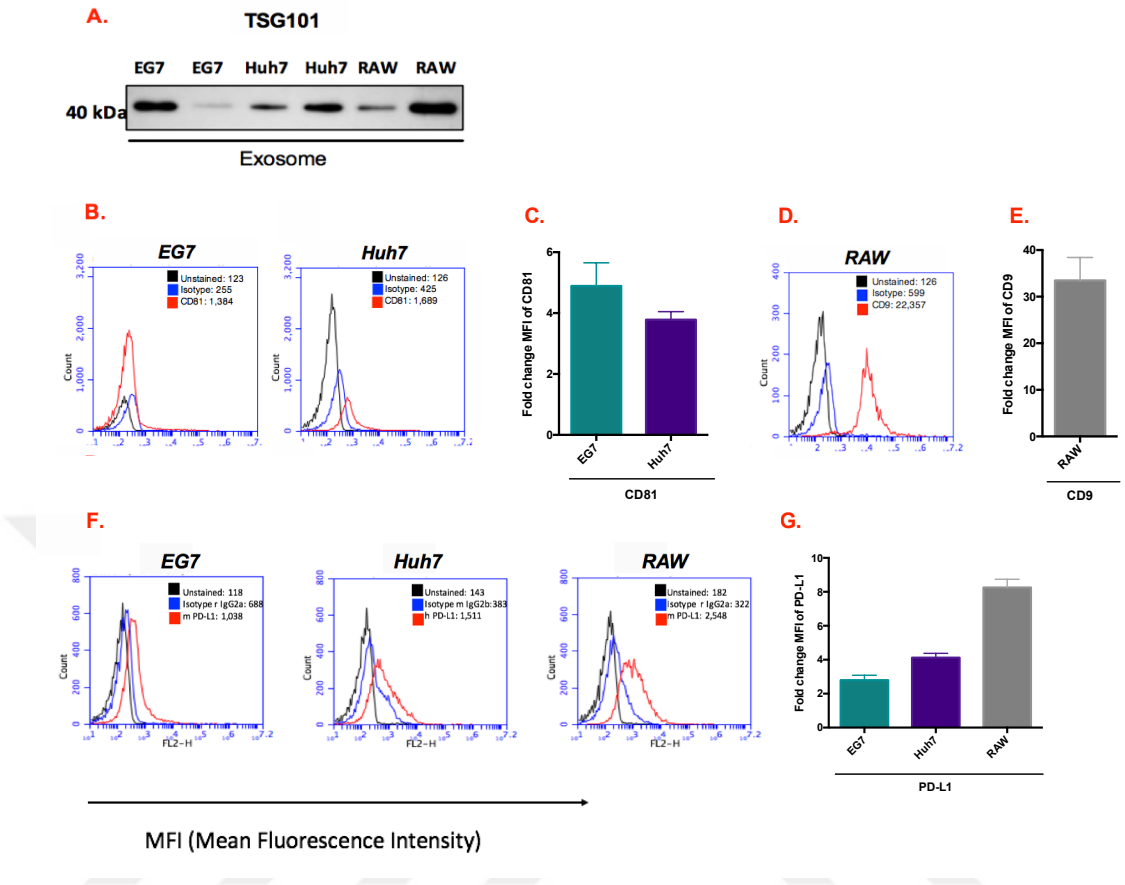
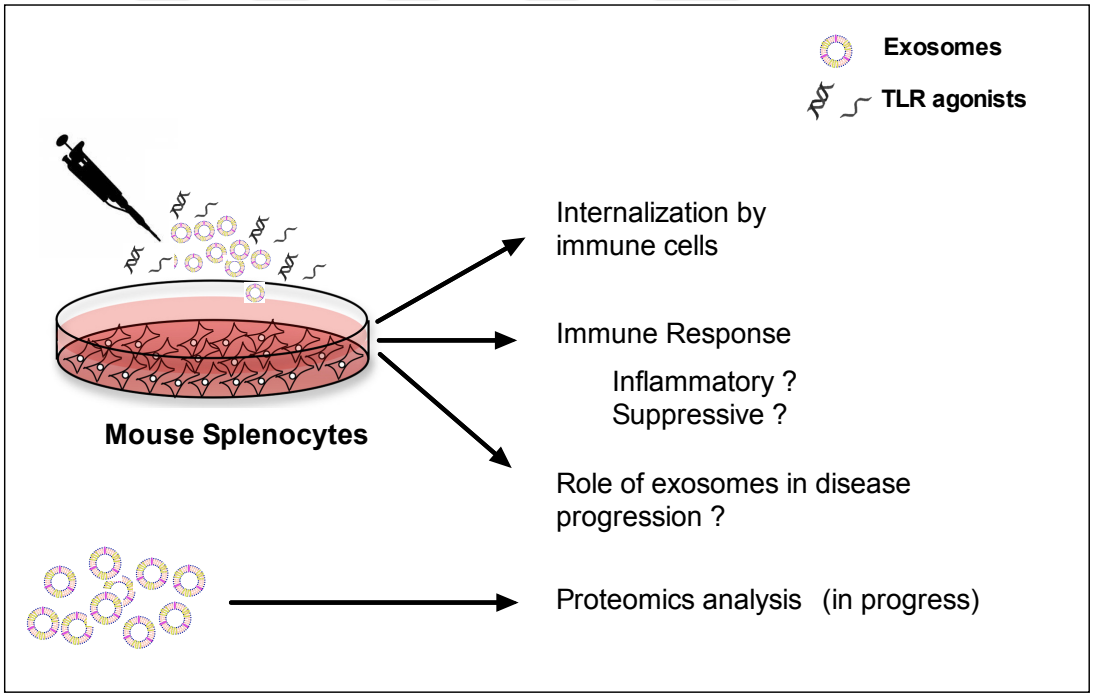


Figure 3.1. Characterization of EG7, HUH7 and RAW exosomes by immunoblotting and flow cytometric bead method.

(A) TSG101 exosomal protein validation by immunoblotting ***(B, C)*** *exosome surface tetraspanin (CD81) expression,* ***(D, E)*** *exosome surface tetraspanin (CD9) expression,* ***(F, G)*** *exosome PD-L1 expression analyzed by flow cytometry.*

3.1.2. Stimulation of mouse splenocytes with EG7, HUH7 and RAW exosomes alone or in combination with TLR agonists

As exosomes are gaining popularity for immunotherapeutic interventions [97], in this study we sought to identify the immunomodulatory role of EG7, HUH7 and RAW exosomes. To this end, murine spleen cells were incubated with exosomes (either alone or in combination with different TLR ligands) and assessed their immunomodulatory effects from culture supernatants. Cell specific time-course internalization were also sought using these exosomes on spleen cells. On the other hand, from all exosomes analyzed throughout this thesis, proteins were purified and sent for proteomic analysis, including the following sections (**Scheme 3.1**).



Scheme 3.1. Brief scheme of scientific reasoning of experimental design.

Immunomodulatory effects of the exosomes (40 µg/ml) were examined from released cytokine profiles by ELISA after stimulating mouse splenocytes alone or in combination with different doses of TLR ligands (i.e. TLR3: poly(I:C); 10 and 30

μg/ml, TLR7:R848; 1 and 5 μg/ml and TLR9: K-type 0.3 and 1.0 μM and D-type CpG ODN 1.0 and 3.0 μM).

Exosomes did not induce any appreciable effect on IL-6 and IL-12 production from splenocytes after 36 hrs incubation, regardless of their cellular origin. However, when HUH7 exosomes were administered together with K- or D-type ODNs, IL-6 and IL-12 secretions were diminished respectively. Furthermore, RAW exosomes had reduced the effect of K-ODN in terms of IL-6 secretion when co-stimulated in the presence of mixed K-ODN. Interestingly, EG7 exosomes were found to reduce not IL-6 secretion but IL-12 when given together with both K- and D-ODN (**Figure 3.2 A, B and Figure 3.3 A, B and Figure 3.4 A, B**). EG7 and RAW exosomes were found to positively contribute to type-I IFN secretion (**Figure 3.2 C and Figure 3.4 C**). While HUH7 exosome did not promote type-I IFN secretion in general, there was a synergistic augmentation when administered together with D-type ODN (**Figure 3.3 C**). Although exosomes alone (all three species) increased IFNγ levels, co-administration of TLR ligands with exosomes decreased the level of IFNγ secretion (**Figure 3.2 D and Figure 3.3 D and Figure 3.4 D**). Finally, exosomes did not promote anti-inflammatory cytokine IL10 secretion either alone or when co-administered with TLR ligands (**Figure 3.2 E and Figure 3.3 E and Figure 3.4 E**).

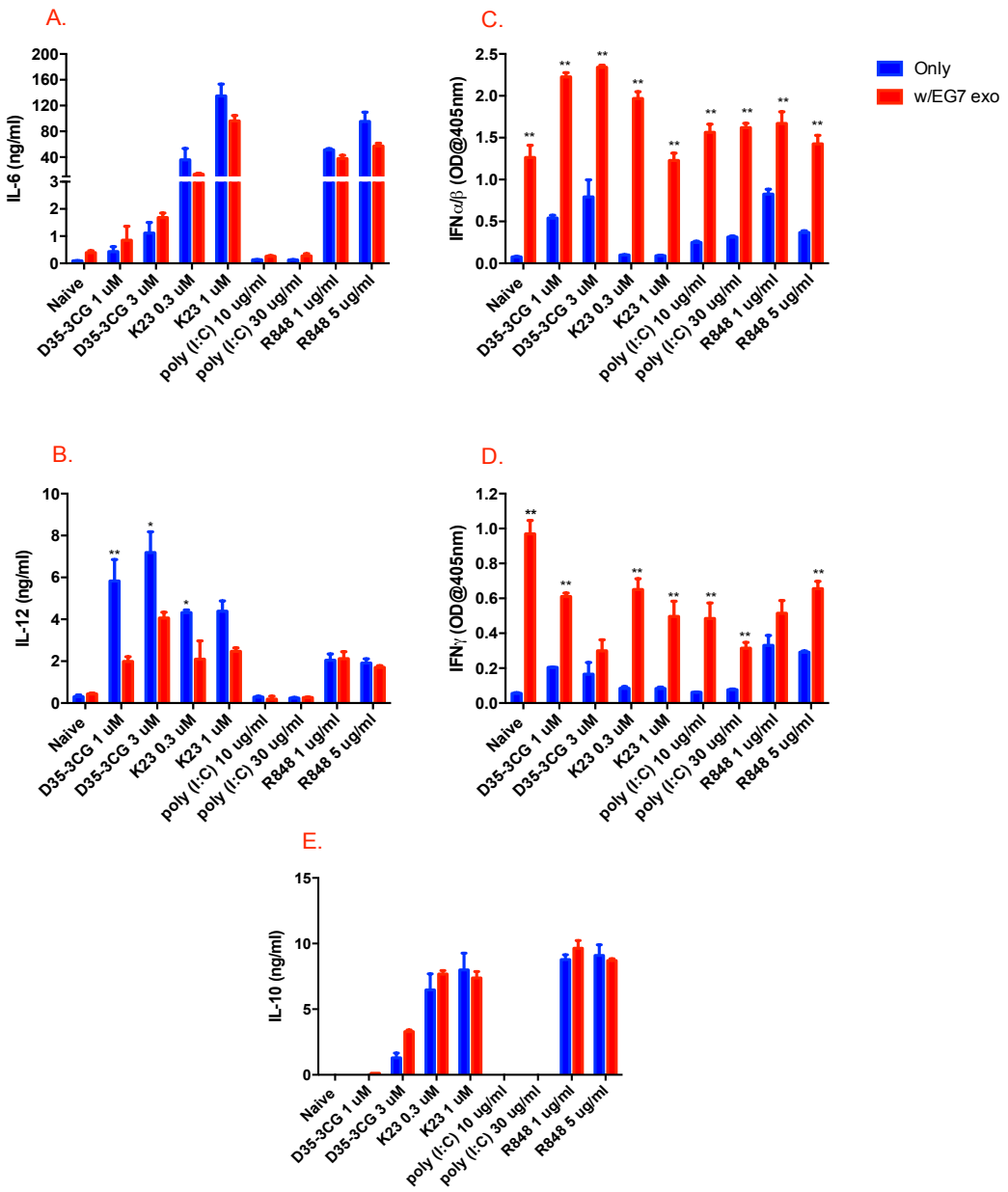


Figure 3.2. Stimulation of mouse splenocytes with EG7 exosomes either alone or in combination with TLR ligands (K- and D-type CpG ODN, p(I:C), R848).

*EG7 exosomes (40 µg/ml) were stimulated with mouse splenocytes (2x10^6/ml). Different doses of TLR ligands were examined either alone or in combination with the exosomes. TLR3: poly(I:C); 10 and 30 µg/ml, TLR7:R848; 1 and 5 µg/ml and TLR9: K-type 0.3 and 1.0 µM and D-type CpG ODN 1.0 and 3.0 µM. After 36 hrs stimulation, IL6, IL12, IFNα/β, IFNγ and IL10 cytokine levels were determined from culture supernatants by ELISA. Ligand alone vs. ligand+ EG7 exo treated groups statistical significance comparison was based on Student's t-test analysis, *p<0.05 and **p<0.01.*

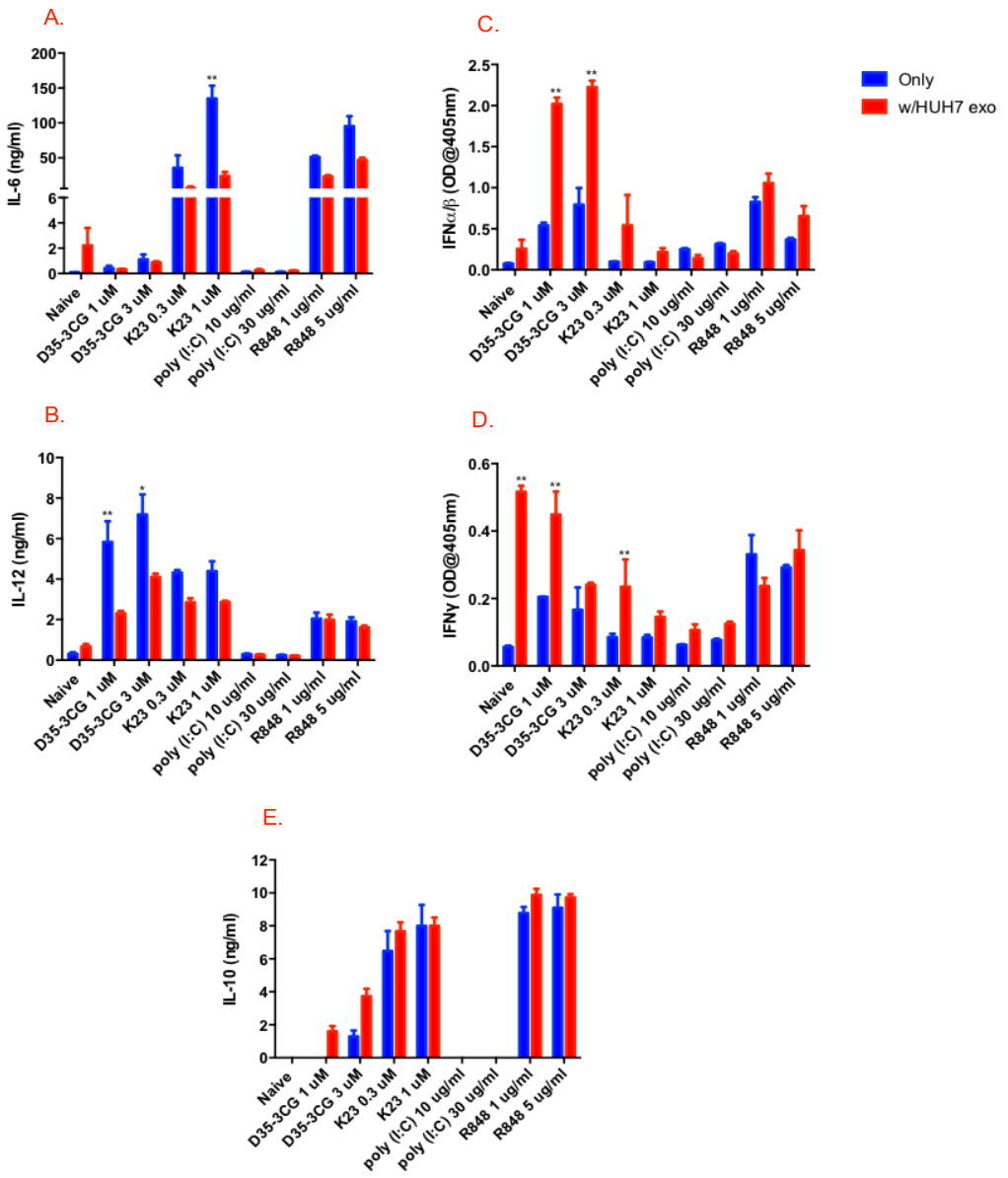


Figure 3.3. Stimulation of mouse splenocytes with HUH7 exosomes either alone or in combination with TLR ligands (K- and D-type CpG ODN, p(I:C), R848).

*HUH7 exosomes (40 µg/ml) were stimulated with mouse splenocytes (2x10^6/ml). Different doses of TLR ligands were examined either alone or in combination with the exosomes. TLR3: poly(I:C); 10 and 30 µg/ml, TLR7:R848; 1 and 5 µg/ml and TLR9: K-type 0.3 and 1.0 µM and D-type CpG ODN 1.0 and 3.0 µM. After 36 hrs stimulation, IL6, IL12, IFNα/β, IFNγ and IL10 cytokine levels were determined from culture supernatants by ELISA. Ligand alone vs. ligand+ HUH7 exo treated groups statistical significance comparison was based on Student's t-test analysis, *p<0.05 and **p<0.01.*

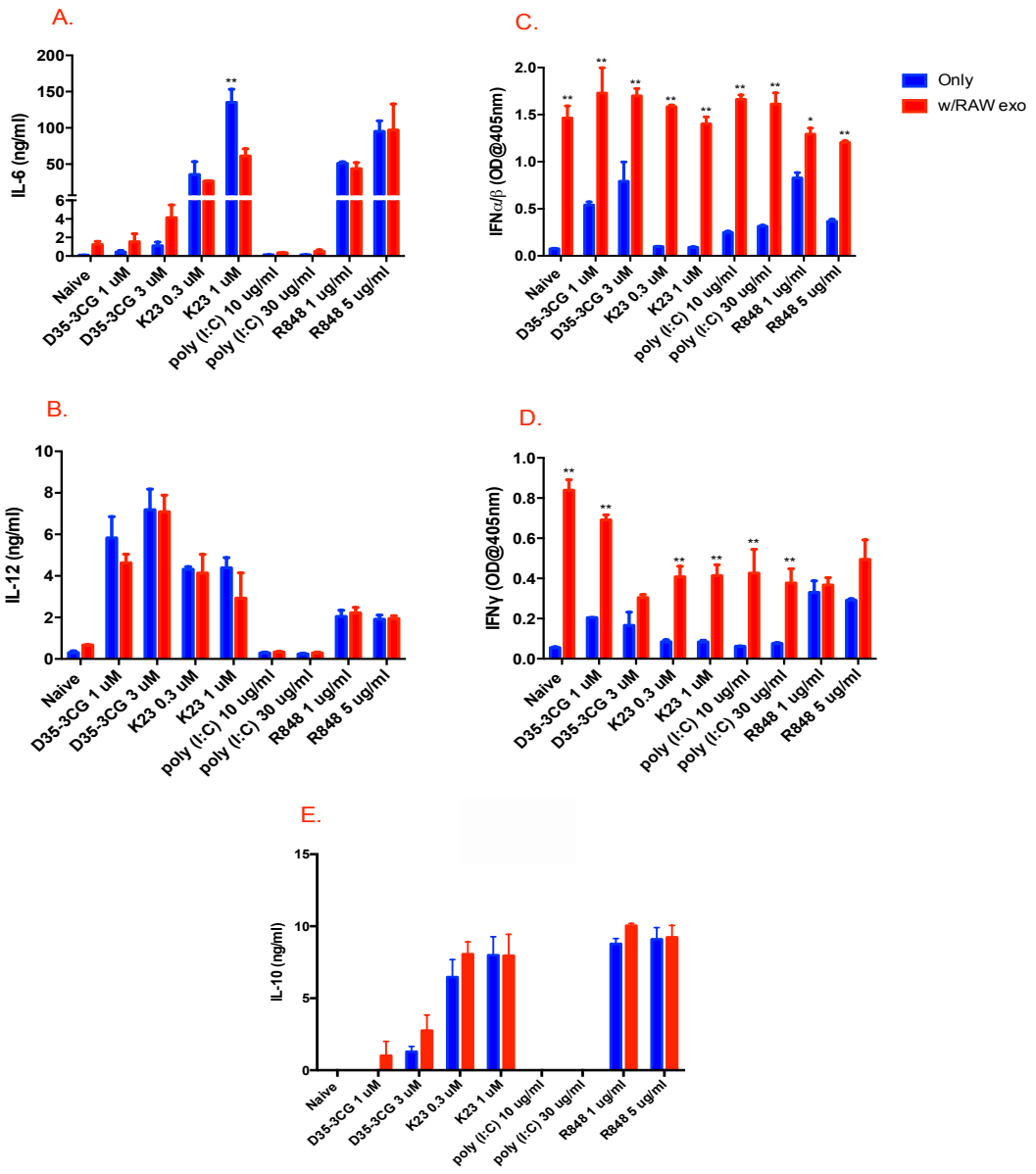


Figure 3.4. Stimulation of mouse splenocytes with RAW exosomes either alone or in combination with TLR ligands (K- and D-type CpG ODN, p(I:C), R848).

*RAW exosomes (40 µg/ml) were stimulated with mouse splenocytes (2x10^6/ml). Different doses of TLR ligands were examined either alone or in combination with the exosomes. TLR3: poly(I:C); 10 and 30 µg/ml, TLR7:R848; 1 and 5 µg/ml and TLR9: K-type 0.3 and 1.0 µM and D-type CpG ODN 1.0 and 3.0 µM. After 36 hrs stimulation, IL6, IL12, IFNα/β, IFNγ and IL10 cytokine levels were determined from culture supernatants by ELISA. Ligand alone vs. ligand+ RAW exo treated groups statistical significance comparison was based on Student's t-test analysis, *p<0.05 and **p<0.01.*

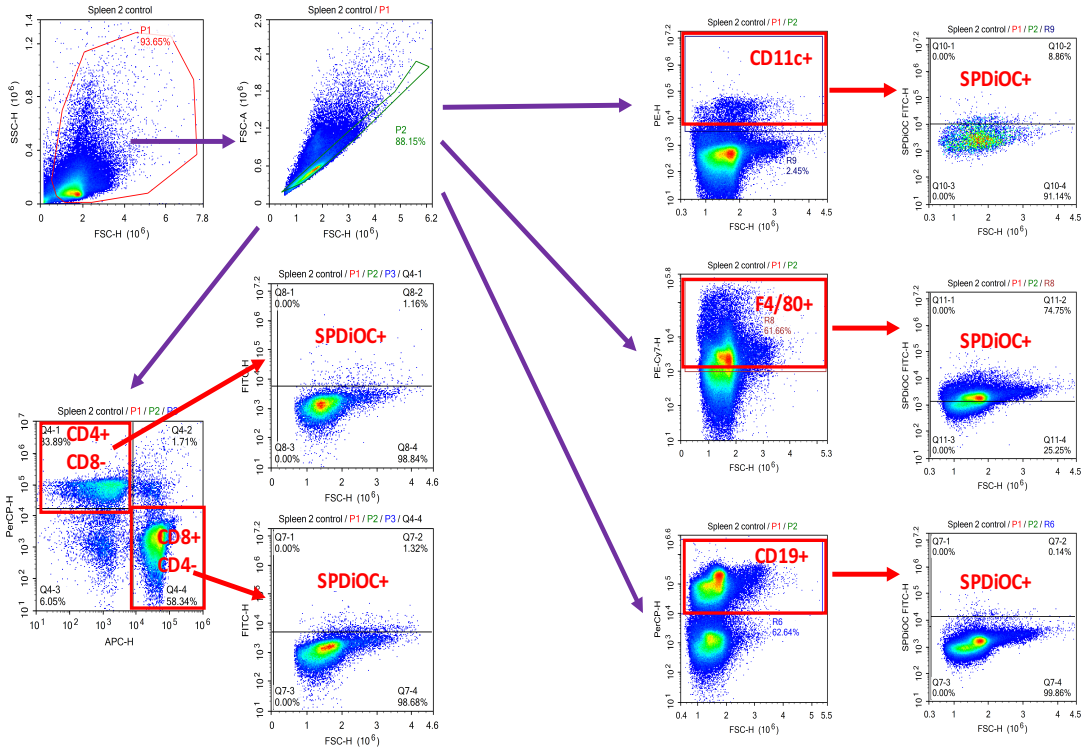
3.1.3. Internalization kinetics of cell line-derived exosomes by immune cells

For in vitro internalization assay, exosomes were first labeled with a lipidic dye SPDiOC as 1 μg dye used for a total of 50 μg exosome and then, 5 μg SPDiOC-stained exosome/well were incubated with spleen cells ($2x10^6$/ml cells) in culture for 24 hrs. At the end of incubation, cells were fixed and cell specific markers such as B-cell (a-B220-PE/Cy5), Macrophages-Mφ (a-F4/80-PE/Cy7), Dendritic cell-DC (a-CD11c-PE), and for T-cell subsets (a-CD3-PE), (a-CD4-APC), (a-CD8-Pe/Cy5) were used to analyze exosome internalization kinetics from immune cells via flow cytometry. Throughout the flow cytometric analyzes, gating strategy used to identify different immune cell subsets was shown in **Figure 3.5 A**. Also, representative dot-plots of aforementioned cell subsets that internalized specific exosomes were shown in **Figure 3.5.B**. Additional dot-plots of flow data are given in *Appendix B*.

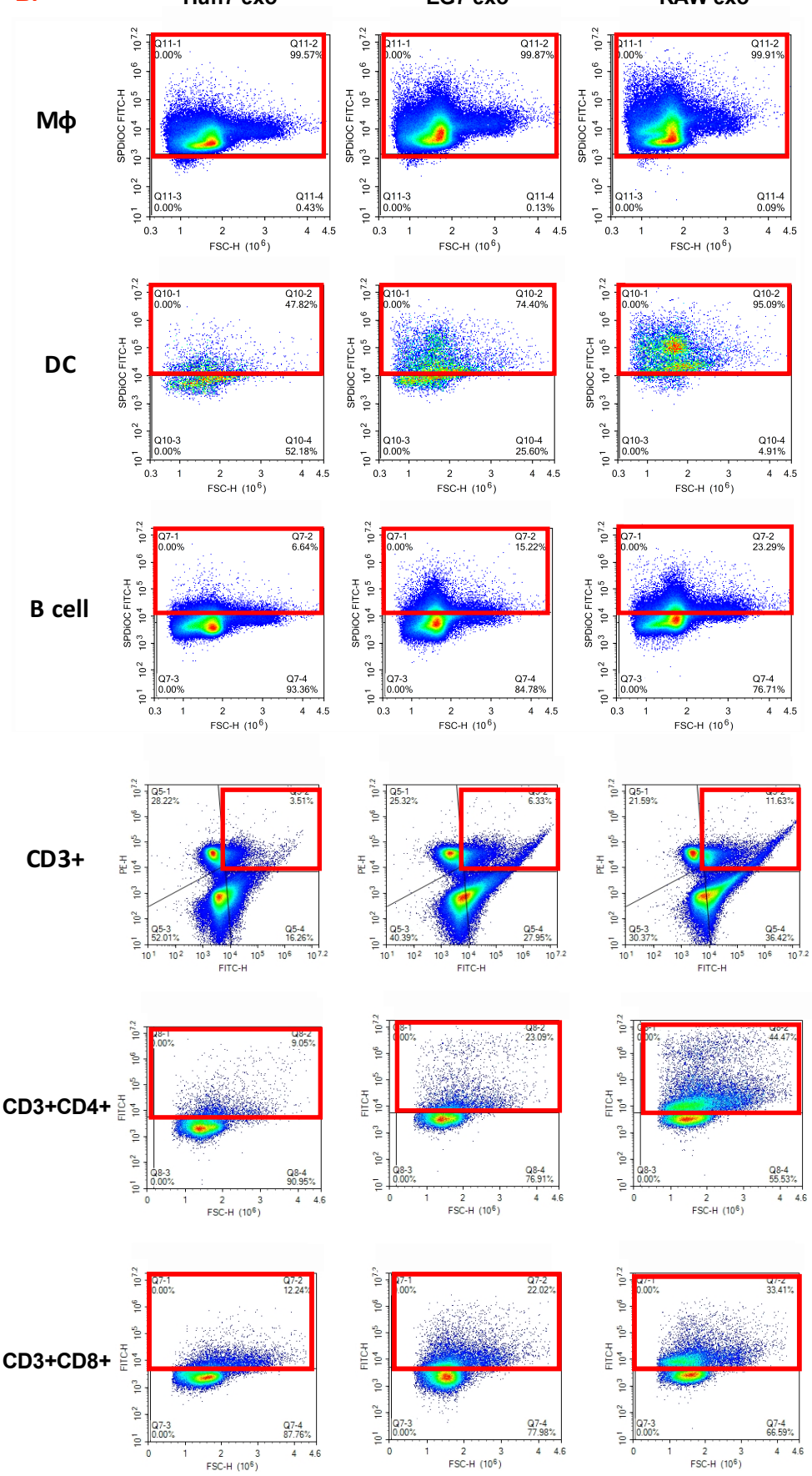
At the end of 24 hrs incubation, all macrophages took up exosomes irrespective of their cell source. DCs differentially took up different exosomes and the lowest internalization rate was seen on B-cells. Exosomes were equally internalized by CD4+CD8- and CD4-CD8+ T cells.

Even though RAW exosomes were taken up by all immune cell subsets at the highest level, and HUH7 exosome were up taken at the lowest, different immune cells internalize these exosomes at different levels.

A.


Spleen 2 control
P1
93.65%
SSC-H (10^6)
FSC-H (10^6)
Spleen 2 control / P1
FSC-A (10^6)
P2
88.15%
FSC-H (10^6)
Spleen 2 control / P1 / P2
CD11c+
PE-H
R9
2.45%
FSC-H (10^6)
Spleen 2 control / P1 / P2 / R9
SPDiOC+
Q10-1
0.00%
Q10-2
8.86%
Q10-3
0.00%
Q10-4
91.14%
SPDiOC FITC-H
FSC-H (10^6)
Spleen 2 control / P1 / P2 / P3 / Q4-1
Q8-1
0.00%
Q8-2
1.16%
SPDiOC+
Q8-3
0.00%
Q8-4
98.84%
FITC-H
FSC-H (10^6)
Spleen 2 control / P1 / P2
CD4+
CD8-
Q4-1
93.89%
Q4-2
1.71%
CD8+
CD4-
Q4-3
6.05%
Q4-4
58.34%
PerCP-H
APC-H
Spleen 2 control / P1 / P2 / P3 / Q4-4
Q7-1
0.00%
Q7-2
1.32%
SPDiOC+
Q7-3
0.00%
Q7-4
98.68%
FITC-H
FSC-H (10^6)
Spleen 2 control / P1 / P2
F4/80+
R8
61.66%
PE-Cy7-H
FSC-H (10^6)
Spleen 2 control / P1 / P2 / R8
SPDiOC+
Q11-1
0.00%
Q11-2
74.75%
Q11-3
0.00%
Q11-4
25.25%
SPDiOC FITC-H
FSC-H (10^6)
Spleen 2 control / P1 / P2
CD19+
R6
62.64%
PerCP-H
FSC-H (10^6)
Spleen 2 control / P1 / P2 / R6
SPDiOC+
Q7-1
0.00%
Q7-2
0.14%
Q7-3
0.00%
Q7-4
99.86%
SPDiOC FITC-H
FSC-H (10^6)

B.


Huh7 exo
EG7 exo
RAW exo
Mϕ
DC
B cell
CD3+
CD3+CD4+
CD3+CD8+
SPDiOC FITC-H
PE-H
FITC-H
FSC-H (10^6)
Q11-1 0.00%
Q11-2 99.57%
Q11-3 0.00%
Q11-4 0.43%
Q11-1 0.00%
Q11-2 99.87%
Q11-3 0.00%
Q11-4 0.13%
Q11-1 0.00%
Q11-2 99.91%
Q11-3 0.00%
Q11-4 0.09%
Q10-1 0.00%
Q10-2 47.82%
Q10-3 0.00%
Q10-4 52.18%
Q10-1 0.00%
Q10-2 74.40%
Q10-3 0.00%
Q10-4 25.60%
Q10-1 0.00%
Q10-2 95.09%
Q10-3 0.00%
Q10-4 4.91%
Q7-1 0.00%
Q7-2 6.64%
Q7-3 0.00%
Q7-4 93.36%
Q7-1 0.00%
Q7-2 15.22%
Q7-3 0.00%
Q7-4 84.78%
Q7-1 0.00%
Q7-2 23.29%
Q7-3 0.00%
Q7-4 76.71%
Q5-1 28.22%
Q5-3 52.01%
Q5-4 16.26%
Q5-1 25.32%
Q5-3 40.39%
Q5-4 27.95%
Q5-1 21.59%
Q5-3 30.37%
Q5-4 36.42%
Q8-1 0.00%
Q8-2 9.05%
Q8-3 0.00%
Q8-4 90.95%
Q8-2 23.09%
Q8-3 0.00%
Q8-4 76.91%
Q8-4 55.53%
Q7-1 0.00%
Q7-2 12.24%
Q7-3 0.00%
Q7-4 87.76%
Q7-2 22.02%
Q7-3 0.00%
Q7-4 77.98%
Q7-2 33.41%
Q7-3 0.00%
Q7-4 66.59%

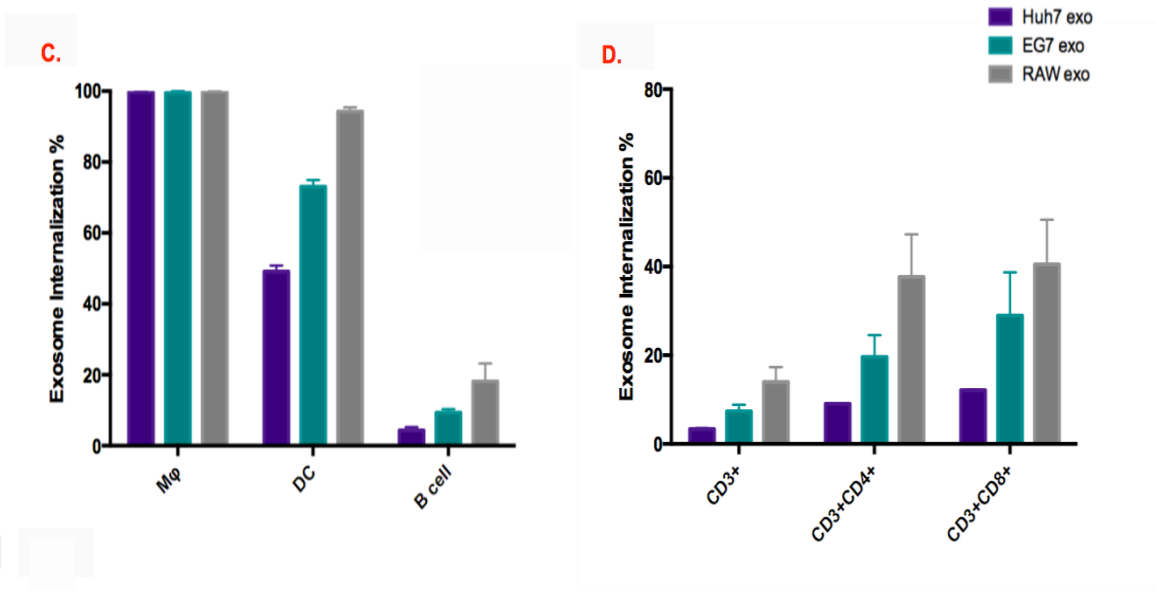


Figure 3.5. Exosome internalization by immune cell subsets in splenocytes. *Representative dot-plots displaying gating strategy* ***(A)****, representative dot-plots of internalization for a specific cell type* ***(B)*** *percentage of exosome internalization by Macrophages-Mφ, Dendritic cells-DC and B cells* ***(C)*** *percentage of exosome internalization by T cells (CD3+, CD4+CD8- and CD4-CD8+)* ***(D)****. Mouse spleen cells (2x10^6/ml cells) were incubated with 5 µg SPDiOC-stained exosome/well in culture for 24 hrs. After incubation, cells were fixed and exosome internalization kinetics were assessed via flow cytometry.*

3.1.4. Inflammatory potential of intraperitoneally administered exosomes from different cell sources

Next, previously analyzed cell line-exosomes were thought to be administrated to mice in order to assess if these exosomes would lead to any inflammatory or anti-inflammatory response in vivo. To test this, we first injected 50 μg SPDiOC-stained exosomes intraperitoneally (i.p.) to mice, and peritoneal exudate cells (PEC) and spleens were harvested and analyzed 18 hrs post injection. Data revealed that EG7 derived exosomes were internalized around 20% by total PEC population as the highest level, followed by RAW derived exosomes, around 18% and lastly HUH7 derived exosomes with almost 10% (**Figure 3.6**). As expected, distinct exosome types having different cellular origin, were differentially up taken by PEC. Furthermore, we sought to assess the contribution of these administrated exosomes on inflammation from splenocytes. To this end, spleens were removed from exosome administrated mice and were incubated either un-stimulated in culture or further stimulated with three exosome types (20 μg/ml, for each exosomes) for an additional 18 hrs. From the culture supernatants, secreted IL-6 and IL-12 profiles were identified by ELISA. Data implicated that, none of administrated exosomes had any detectable effect on IL-6, IL-12 production by spleen cells, but when further stimulated *in vitro* with the same exosome species as 5 μg/well, HUH7 cells promoted the highest IL-6 and IL-12 pro-inflammatory cytokine secretion (**Figure 3.7**).

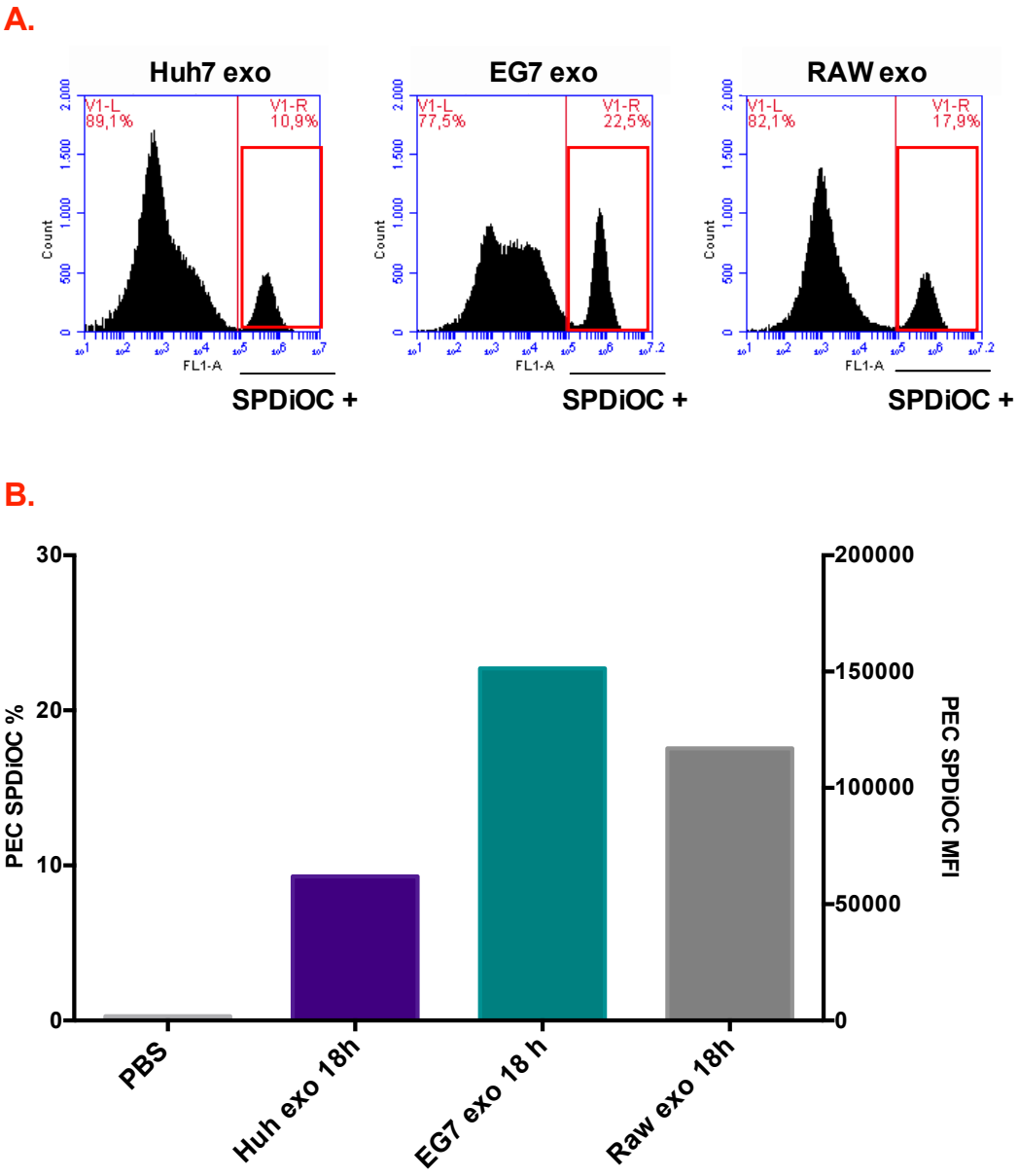


Figure 3.6. Exosome internalization in peritoneal exudate cells (PEC). *Double positive plots **(A)** graphical representation of SPDiOC percentage and MFI values of a specific exosome type in PEC **(B)**.*

SPDiOC stained exosomes (50 µg/animal) were administrated to mice. After 18 hrs, PECs were collected from the mice and analyzed by Flow Cytometry. MFI: Mean Fluorescent Intensity.

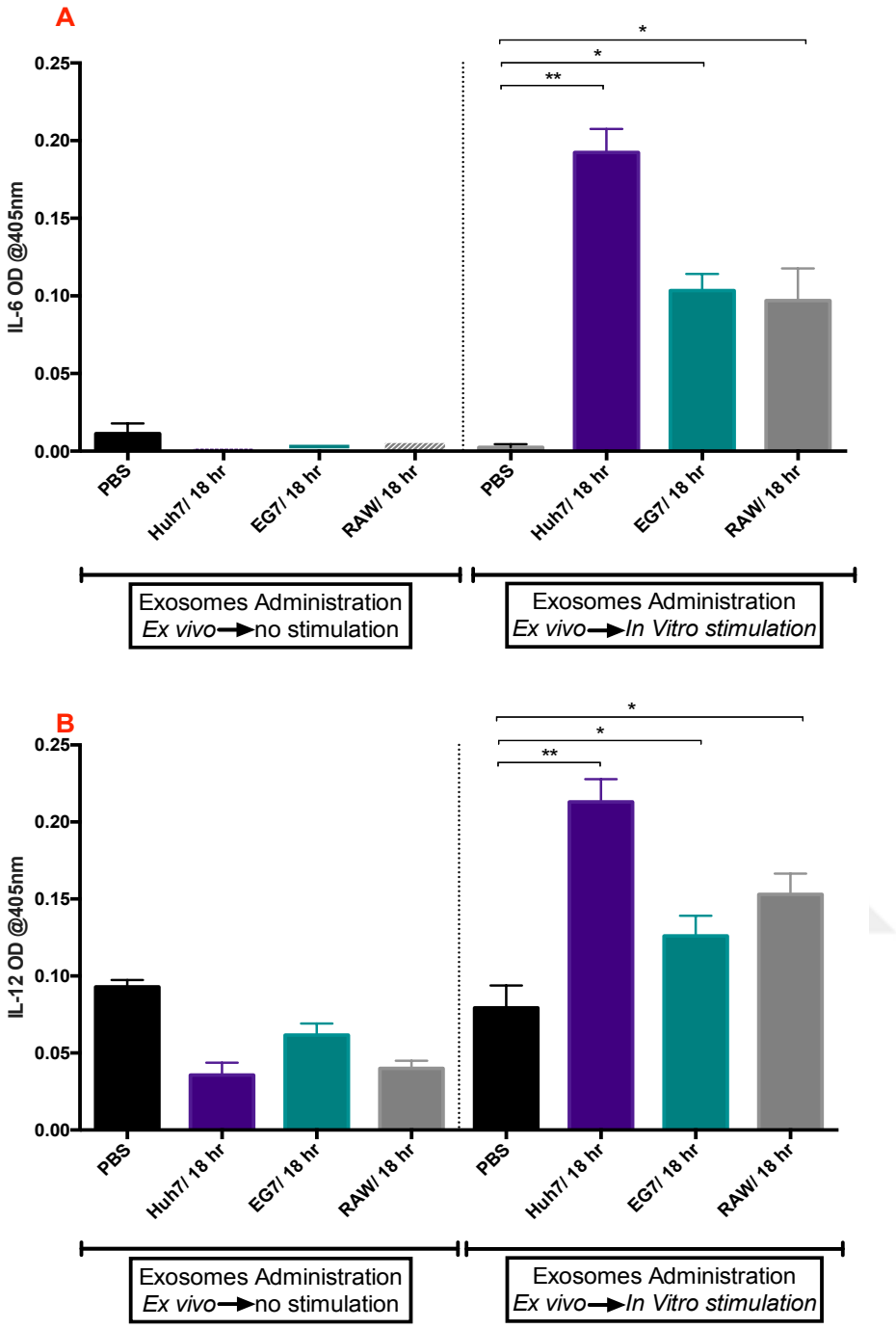
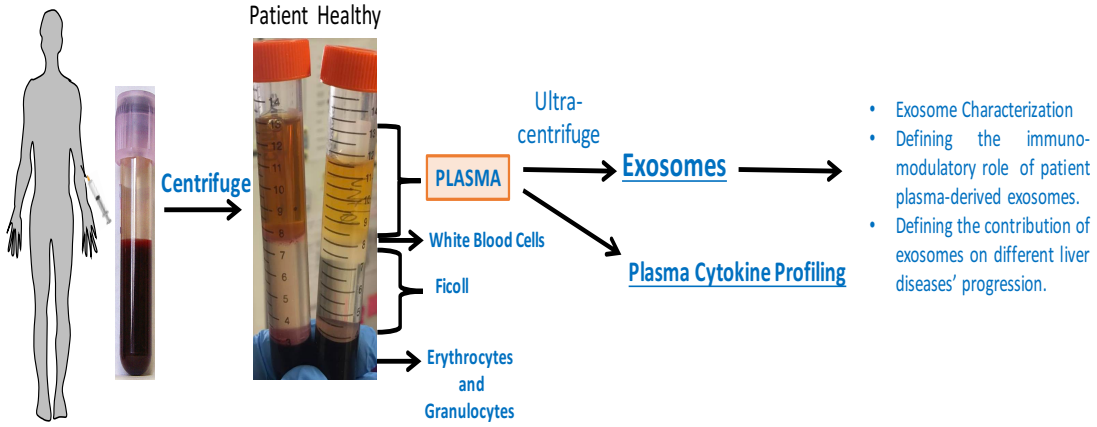


Figure 3.7. Administration of SPDiOC stained exosomes to mice. *After stimulation, culture supernatants were collected; IL-6* ***(A)*** *and IL-12* ***(B)*** *cytokine levels were determined by ELISA. 50 µg SPDiOC-stained exosomes were intraperitoneally (i.p.) administered to mice. After 18 hrs, spleens were collected. Spleen cells (5x10^5 cells/well) were seeded and* incubated either un-stimulated in culture or further stimulated with three exosome types (20 µg/ml, for each exosomes) for an additional 18 hrs. *Statistical significance comparison among groups was based on one-way ANOVA analysis, *p<0.05 and **p<0.01.*

3.2. The Role of Exosomes in HBV infection, Liver Cirrhosis and Hepatocellular Carcinoma (HCC)

3.2.1. Plasma-derived exosome characterization

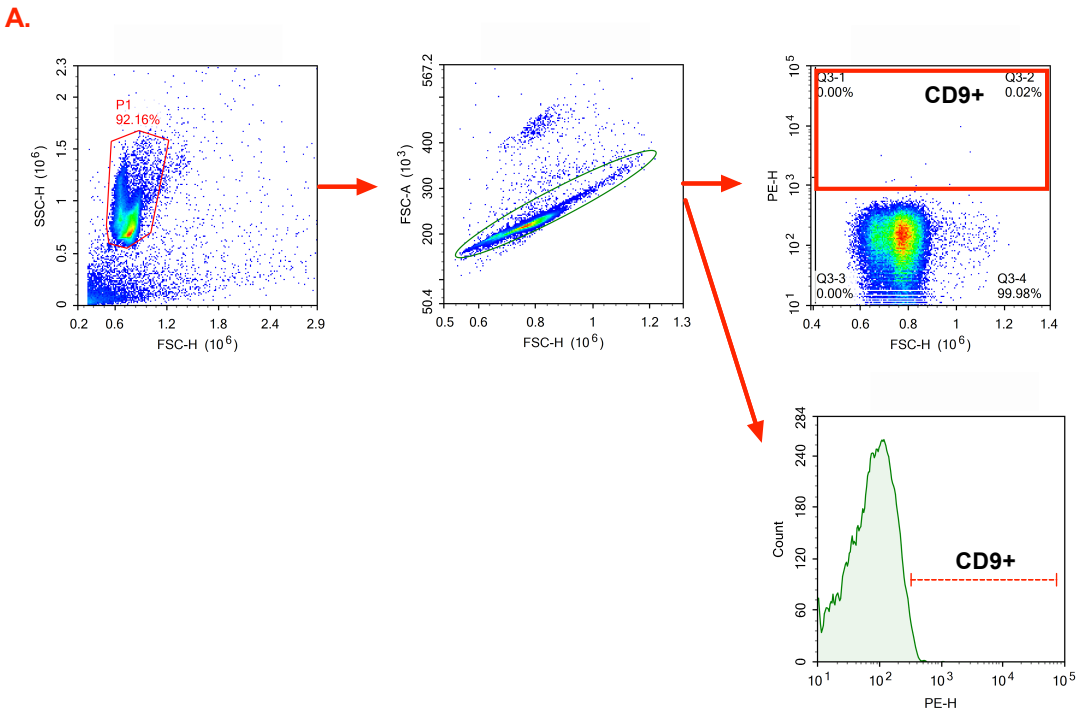
Exosomes mimic the phenotypic state of the cell of origin. Hence, under health and disease conditions, exosomes are known to act as a modifier of physiological state of the host [98, 99]. Therefore, in this part of the study, we wanted to identify the immunomodulatory roles of patient plasma-derived exosomes from three different liver conditions; HBV Carrier, Cirrhosis and HCC. These results would provide an understanding to the role of exosomes in disease progression (**Scheme 3.2**).



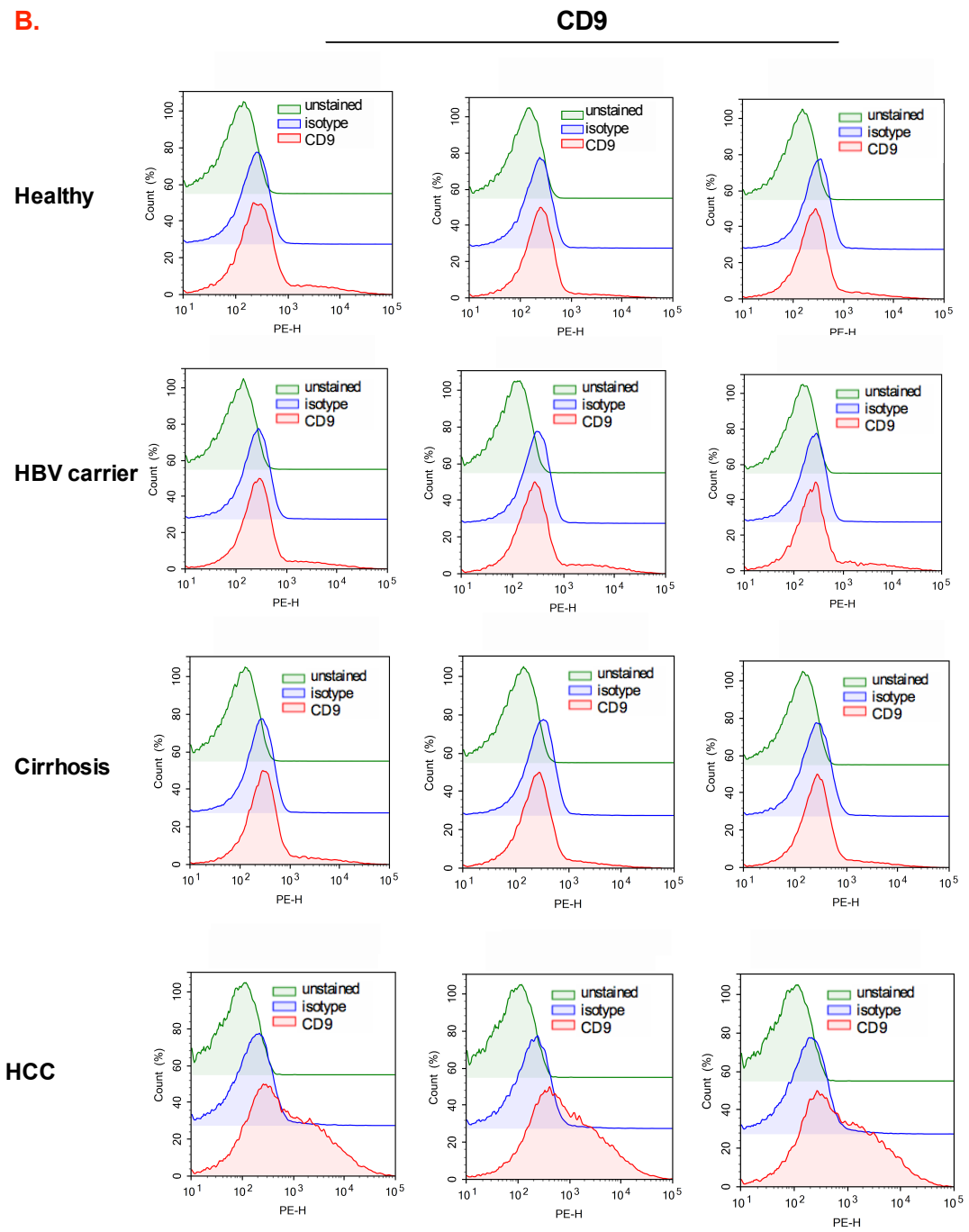
Scheme 3.2. Schematic illustration of the work-flow.

Before performing any downstream experiment, exosomes were first characterized by flow cytometry and immunoblotting. Initially exosomes were purified from healthy controls' and patients' peripheral blood plasma. Kit protocol that was used for exosome isolation, was optimized and modified from original manufacturer's instructions as indicated in Chapter 2. To assess whether isolated exosomes have the exosomal markers, they were stained via bead-based flow cytometric method and investigated for CD9 expression. In addition, proteins were isolated from the

exosomes and 25 µg of exosomal protein was analyzed by immunoblotting to determine the presence of exosome marker proteins. *ALIX* and TSG101 are important in exosome biogenesis, and commonly used protein markers for *exosomes* [97]. As expected, all exosomes were positively found to express CD9 on their surface (**Figure 3.8 C**) and they also had TSG101 (**Figure 3.8 D**) and ALIX exosomal protein (**Figure 3.9**) regardless of their cellular origin. In literature, GRP94 is highly enriched in microvesicles (MVs) [100], but is absent in exosomes, therefore, we also checked GRP94 protein expression on the exosomes as a negative marker (**Figure 3.9**). Overall, these data demonstrate that isolated exosomes from patients' and healthy donors' peripheral blood plasma have the characteristics that identify the vesicles as exosomes.



B.


CD9
Healthy
HBV carrier
Cirrhosis
HCC
unstained
isotype
CD9
Count (%)
PE-H

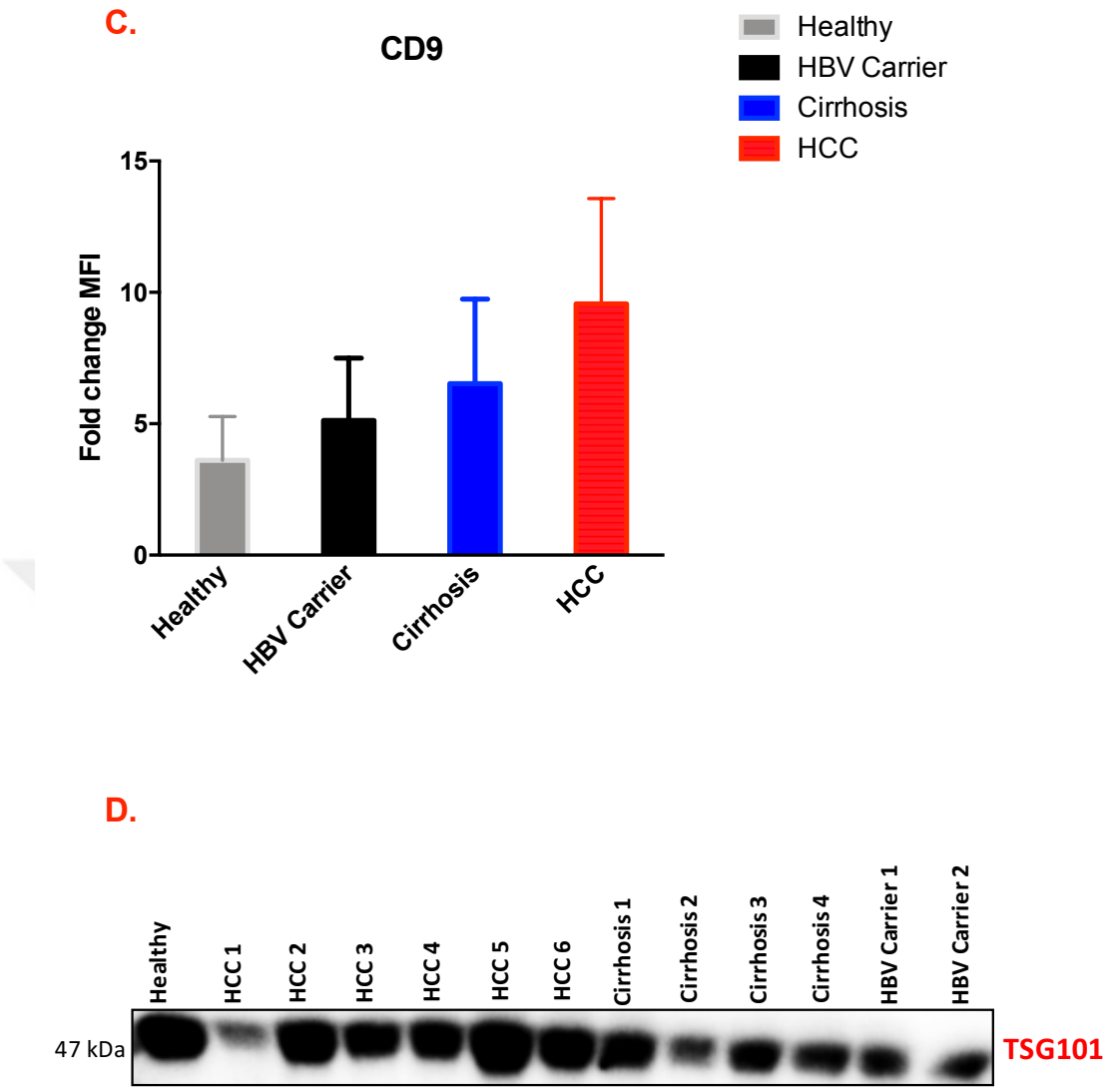


Figure 3.8. Characterization of plasma-derived exosomes by flow cytometric bead method and immunoblotting. *Representative gating strategy used to discriminate CD9+ exosome population* ***(A)*** *Representative density plots demonstrating exosomes' surface tetraspanin (CD9) expression in fluorescence intensity over isotype control* ***(B)*** *Fold change MFI of exosomes' CD9 surface expression over isotype control* ***(C)*** *TSG101 exosomal protein validation by immunoblotting* ***(D)***. *Exosomes were stained as 1 µg/ml, via bead-based flow cytometric method. Exosomal protein isolation was performed by using RIPA lysis buffer and 25 µg protein was loaded into each well for immunoblotting.*

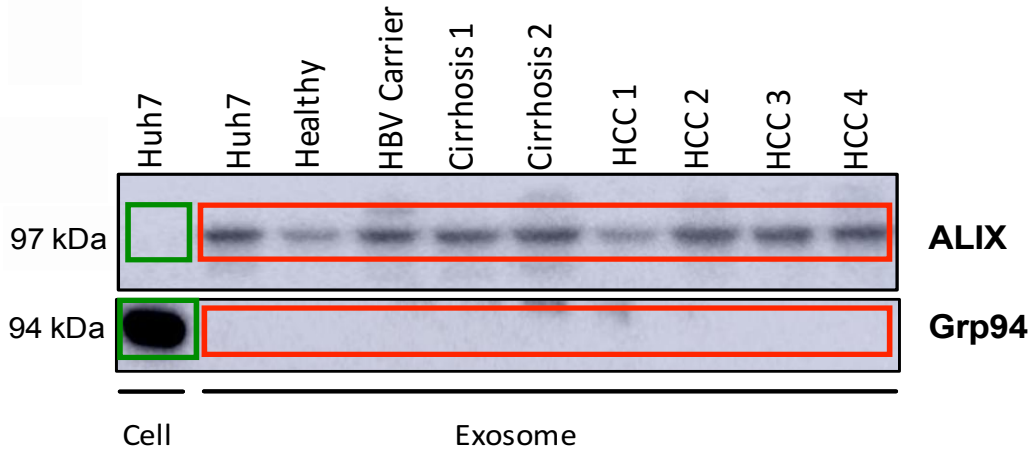


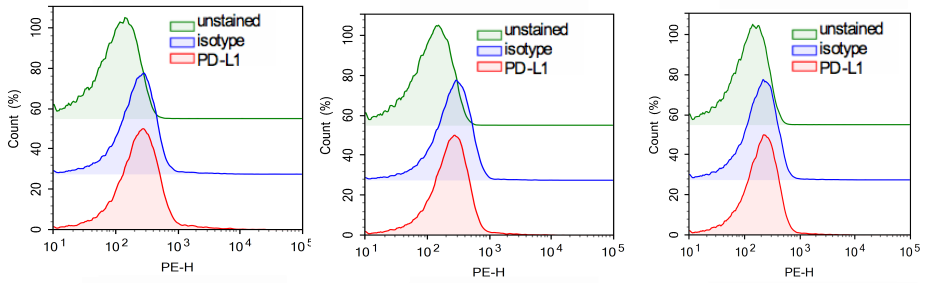
Figure 3.9. The analyses of ALIX and GRP94 protein expression via immunoblotting. *25 ug of exosomal protein was validated by immunoblotting. Huh7 cellular protein as well as exosomal protein were also investigated for cell vs. exosome comparison. Huh7: Human hepatocellular carcinoma cell line. Green boxes: cellular protein sample, Red boxes: exosomal protein samples.*

As previously mentioned in **Section 3.1.1**, Programmed death-ligand 1 (PD-L1) is a co-inhibitory molecule commonly expressed on the surface of antigen presenting cells (APCs) which afterwards can halt or limit the development of the T cell response [101]. Since many malignant tumor cells highly express PD-L1 on their surface block anti-tumor T cell response and eventually evade from the immune cells, PD-L1 pathway serves as immunotherapy target in various cancers [102, 103]. In case of liver disease, PD-L1 was suspected to play a supportive role in disease progression. Therefore, PD-L1 expression among patients' exosomes were analyzed via flow cytometry and immunoblotting. Although flow data revealed that PD-L1 expression was gradually upregulated on patients' exosomes from HBV carrier state to HCC state (**Figure 3.10 A**), there was no expression observed via immunoblotting (**Figure 3.10 B**). In addition, HUH7 hepatoma cell line was found to express PD-L1 protein but no expression was observed on HUH7 exosomal protein (**Figure 3.10 B**). This is revealing that, exosomes might not always carry the same surface marker at the same expression level, compared to the parental cancer cell line of origin. MDA-MB-231 breast cancer cell line was used as a positive control for PD-L1 [104].

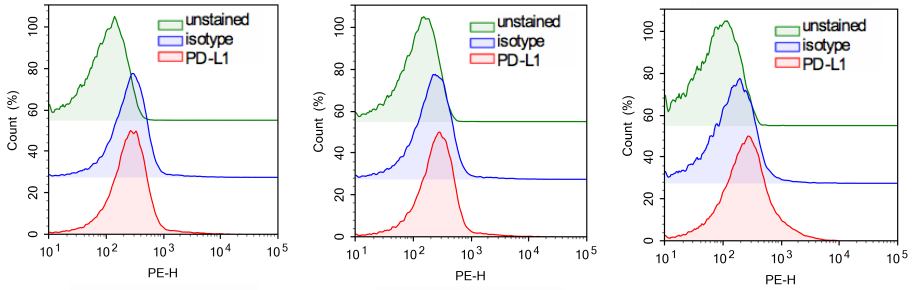
A.

PD-L1

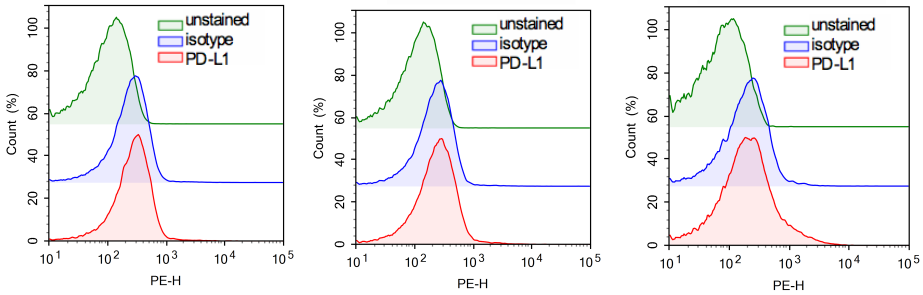
Healthy



HBV carrier



Cirrhosis



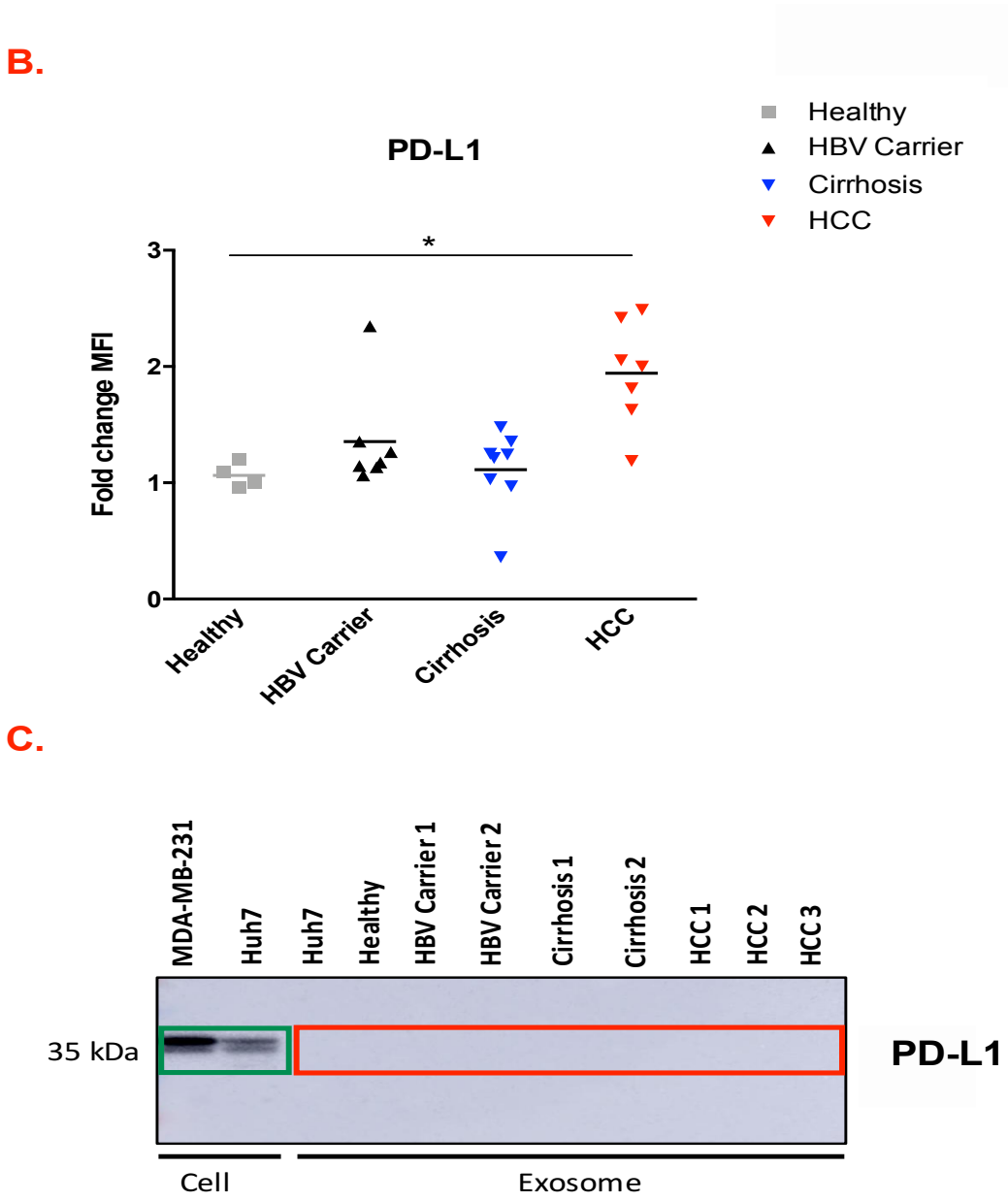


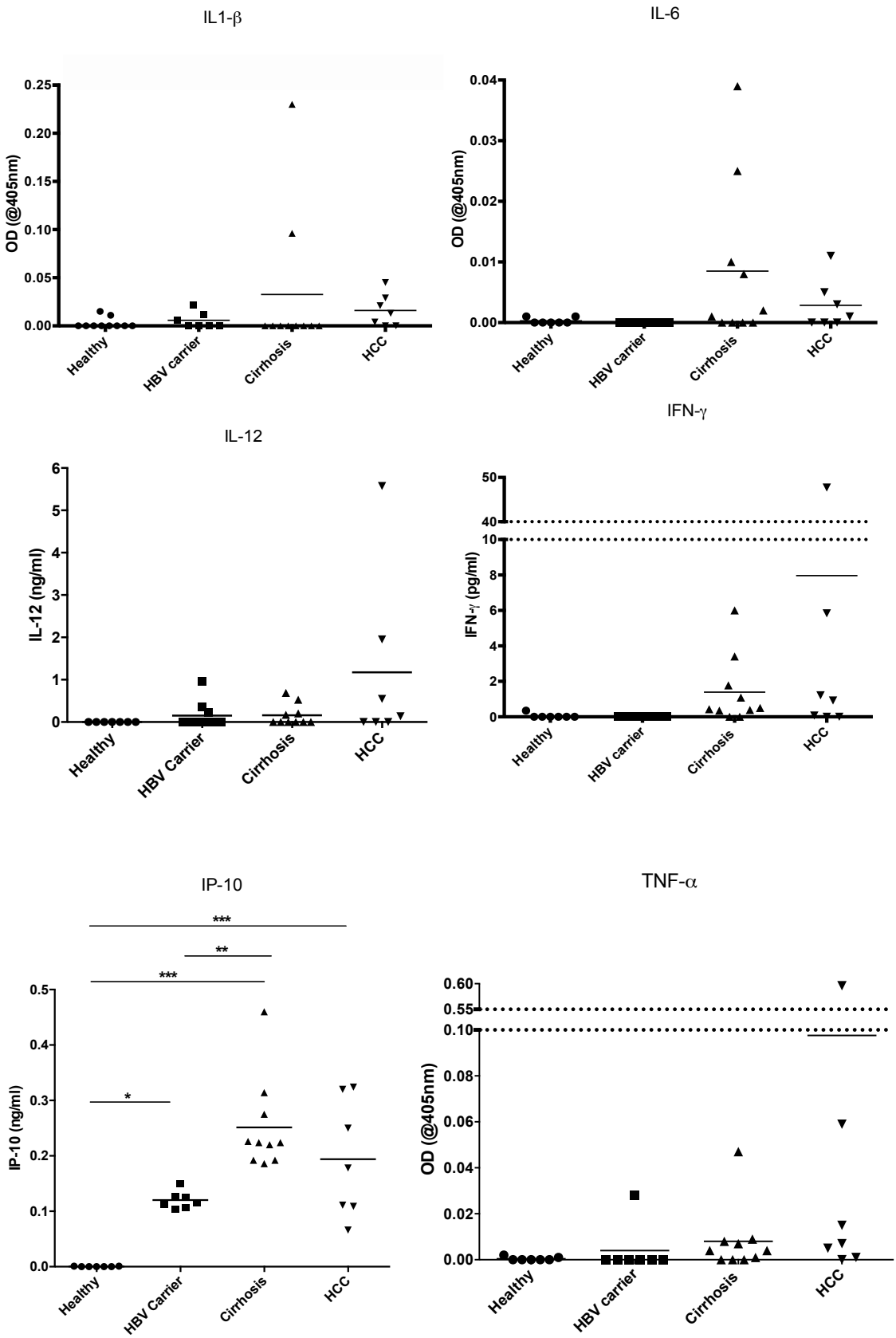
Figure 3.10. Validation of PD-L1 expression. *Representative density plots demonstrating exosomes' surface PD-L1 expression in fluorescence intensity over isotype control* ***(A)*** *Fold change MFI of PD-L1 expression over isotype control* ***(B)*** *were analyzed via flow cytometry. PD-L1 expression on exosomal proteins was validated by immunoblotting* ***(C)****. MDA-MB-231 breast cancer cell line was used as a positive control for PD-L1. Cellular protein as well as exosomal protein were also investigated for cell vs. exosome comparison. Huh7: Human hepatocellular carcinoma cell line. Green box: cellular protein samples, Red box: exosomal protein samples. Healthy vs. patient exo groups statistical significance comparison was based on Student's t-test analysis, *p<0.05.*

3.2.2. Circulating cytokine/chemokine profile of patients and healthy controls

After isolating PBMCs, plasmas were saved and used in cytokine ELISA to determine the levels of circulating pro-inflammatory and Th1 (IL1β, IL-6, TNFα, IL-12, IFNγ, IP-10, IL-8) as well as anti-inflammatory and Th2 (IL-4, IL-5, IL-10, IL-13, TGFβ) cytokines/chemokines in control and in HBV Carrier, Cirrhosis, HCC groups. Cytokines with distinguishing levels in plasma would provide an insight to disease progression and possibly are correlated with the severity of inflammation, liver fibrosis and HCC.

As it is shown in **Fig. 3.11**, there was a very little increase in IL1β level in Cirrhosis and HCC patients' plasmas. Other cytokines that play a major role in inflammation such as, IL-6, IL-8, IL-12, IFNγ and TNFα showed a slight increase specially in Cirrhosis and HCC group when compared to healthy controls. In addition, plasma IP-10 levels were comparable among the groups. Cirrhosis and HCC groups had the highest IP-10 level that is known to be associated with poorer survival in many malignancies. Cirrhosis patients' plasma IP-10 levels were significantly higher than HBV carrier and healthy donor plasmas **(Figure 3.11)**.

On the other hand, a gradual increase was observed with Th2 cytokines including IL-4, IL-5, IL-10, IL-13 from HBV carrier state to HCC state. Specially a well-known anti-inflammatory cytokine - IL-10 - level was significantly increased in HCC patients' plasmas when compared with healthy controls. Furthermore, TGF-β was significantly elevated in HBV carrier patients' plasmas when compared with other disease groups as well as healthy donors **(Figure 3.12)**.


IL1-β
OD (@405nm)
0.25
0.20
0.15
0.10
0.05
0.00
Healthy
HBV carrier
Cirrhosis
HCC
IL-6
OD (@405nm)
0.04
0.03
0.02
0.01
0.00
Healthy
HBV carrier
Cirrhosis
HCC
IL-12
IL-12 (ng/ml)
6
5
4
3
2
1
0
Healthy
HBV Carrier
Cirrhosis
HCC
IFN-γ
IFN-γ (pg/ml)
50
40
10
8
6
4
2
0
Healthy
HBV carrier
Cirrhosis
HCC
IP-10
IP-10 (ng/ml)
***
**
***
*
0.5
0.4
0.3
0.2
0.1
0.0
Healthy
HBV Carrier
Cirrhosis
HCC
TNF-α
OD (@405nm)
0.60
0.55
0.10
0.08
0.06
0.04
0.02
0.00
Healthy
HBV carrier
Cirrhosis
HCC

IL-8

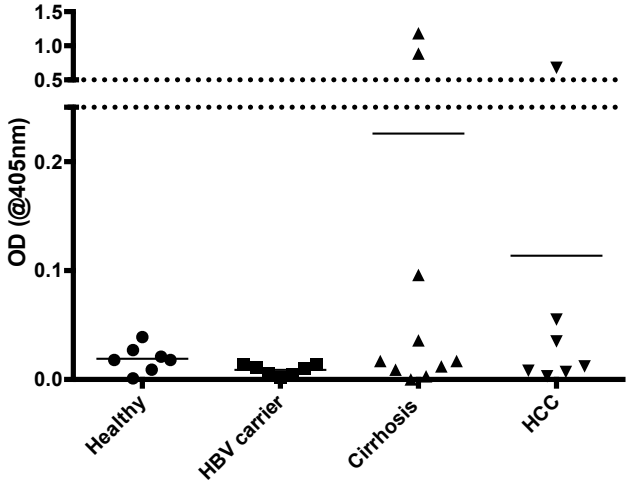
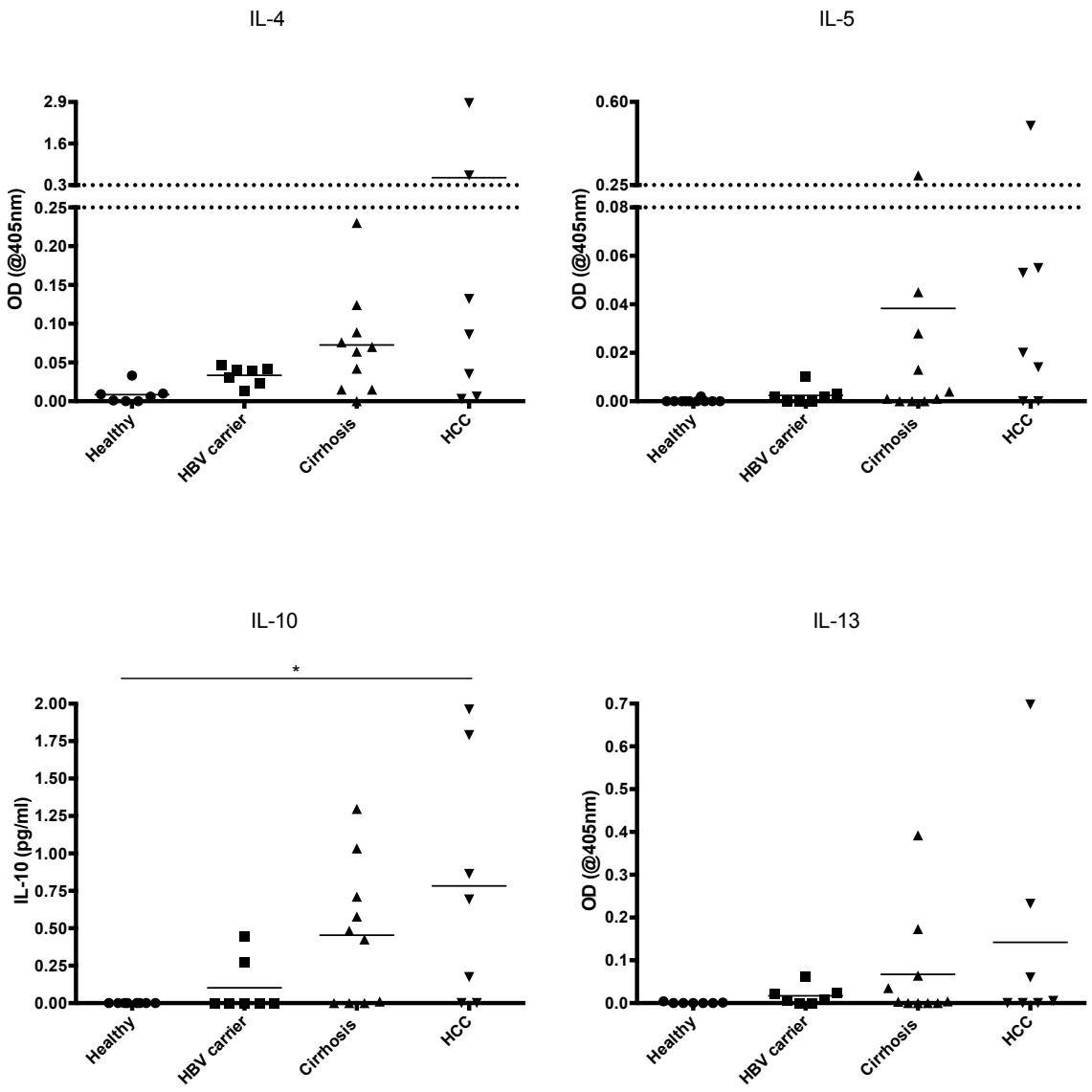


Figure 3.11. Screening of circulating Th1 and inflammatory cytokines/chemokines from patients' and healthy controls' plasmas by ELISA. *Before performing the ELISA, plasmas were centrifuged at 1500x g for 10 mins to get rid of any residual cell or debris. N=7-10 individual samples. Statistical significance among groups was based on one-way ANOVA followed by Tukey's test, *p<0.05, **p<0.01, ***p<0.001.*


IL-4
OD (@405nm)
2.9
1.6
0.3
0.25
0.20
0.15
0.10
0.05
0.00
Healthy
HBV carrier
Cirrhosis
HCC
IL-5
OD (@405nm)
0.60
0.25
0.08
0.06
0.04
0.02
0.00
Healthy
HBV carrier
Cirrhosis
HCC
IL-10
*
IL-10 (pg/ml)
2.00
1.75
1.50
1.25
1.00
0.75
0.50
0.25
0.00
Healthy
HBV carrier
Cirrhosis
HCC
IL-13
OD (@405nm)
0.7
0.6
0.5
0.4
0.3
0.2
0.1
0.0
Healthy
HBV carrier
Cirrhosis
HCC

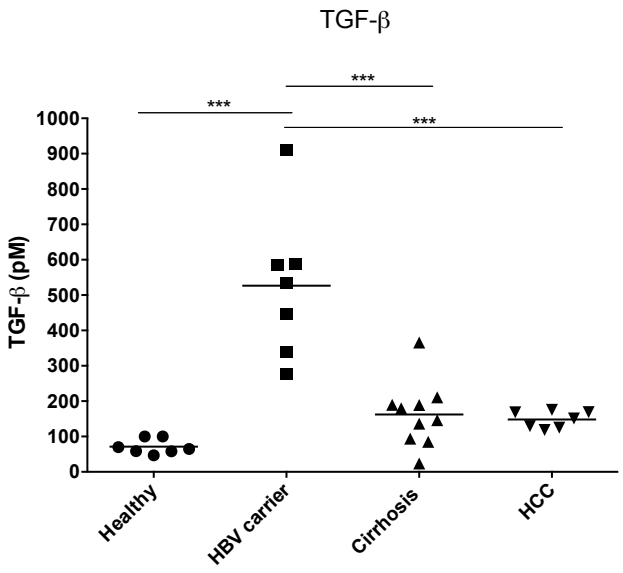


Figure 3.12. Screening of circulating Th2 and anti-inflammatory cytokines from patients' and healthy controls' plasmas by ELISA.

*Before performing the ELISA, plasmas were centrifuged at 1500x g for 10 mins to get rid of any residual cell or debris. N=7-10 individual samples. Statistical significance among groups was based on one-way ANOVA followed by Tukey's test, *p<0.05, **p<0.01, ***p<0.001.*

3.2.3. Healthy control peripheral blood mononuclear cell (PBMC) stimulation with patient exosomes

Healthy control and HBV carrier, Cirrhosis, HCC patients' exosomes were isolated from plasma by Norgen exosome purification kit as described previously. As these nano-vesicles are known to act as a modifier of physiological state of the host, we sought to identify the immunomodulatory role of patient plasma derived exosomes by stimulating healthy PBMCs ($1x10^6$/ml cells) with patient exosomes. For the stimulation assays, 3 doses of exosome; 0.5 μg, 2.5 μg and 12.5 μg were used, aiming to assess the optimal dose for an appropriate immune response. To this end, three healthy donor PBMCs were incubated with aforementioned doses of patient exosomes for 24 hrs, and then IFNγ and IP-10 levels were determined from the culture supernatants by ELISA.

Overall, IFNγ and IP-10 levels were found to be elevated in response to patient exosomes regardless of disease group. Among three healthy PBMC stimulations, the highest cytokine response was observed with the maximum dose used, 12.5 μg. As expected, healthy donors' exosomes did not induce any appreciable level of cytokine secretion. The most effective exosome dose seemed to be 12.5 μg for both cytokines. Although all patients' exosomes had an inflammatory effect on healthy PBMCs, HCC group exosomes promoted the highest IFNγ and IP-10 production, thus had the highest inflammatory effect among other disease groups (**Figure 3.13**).

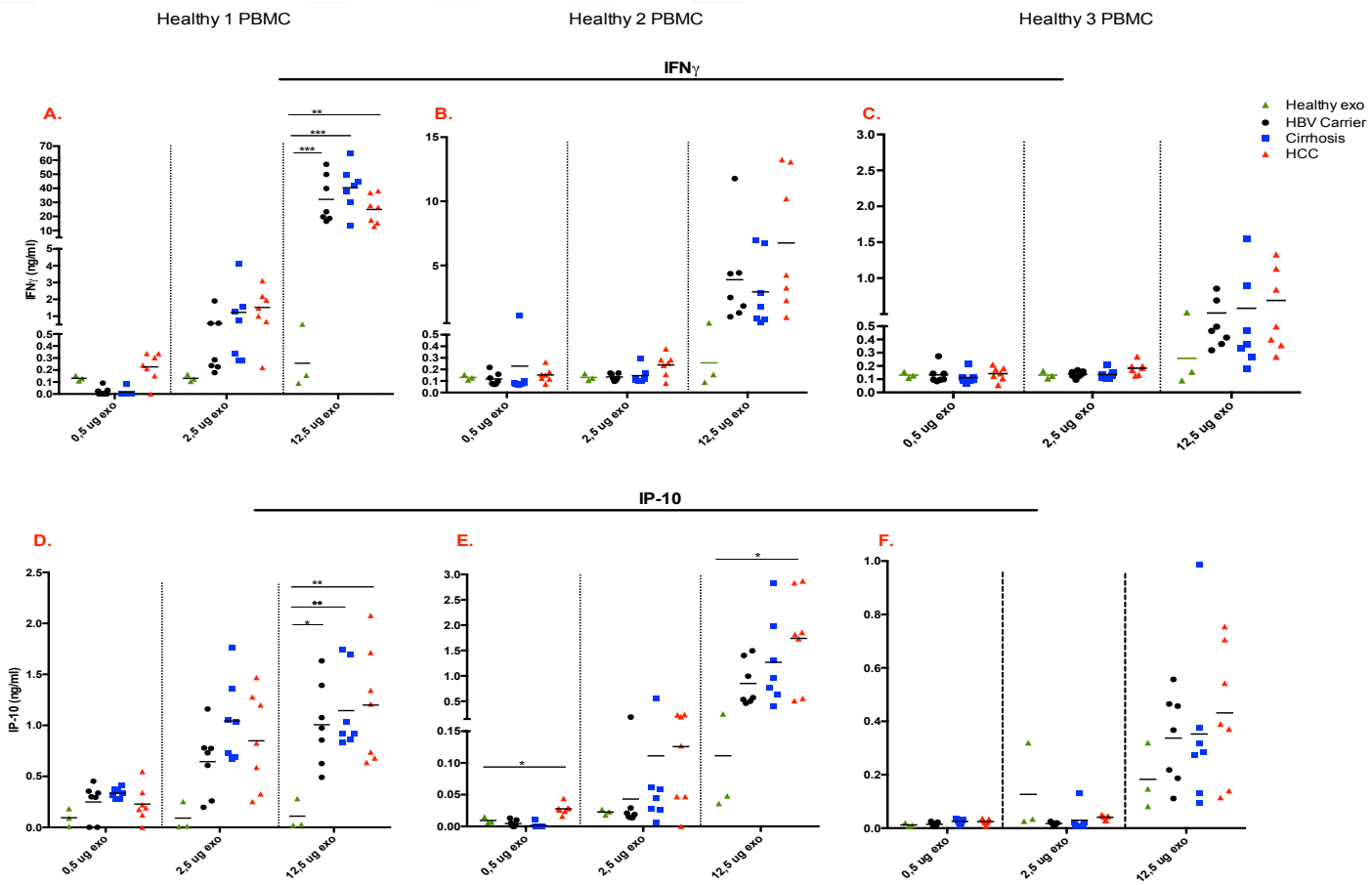


Figure 3.13. Stimulation of three different healthy controls' PBMCs with HBV carrier, Cirrhosis and HCC exosomes.

Healthy individual-1/2/3 PBMC stimulation with patients' exosome, IFNγ levels ***(A,B,C)*** *Healthy individual-1/2/3 PBMC stimulation with patients' exosome, IP-10 levels* ***(D,E,F)****. Three healthy individuals' PBMCs (*$1x10^6$/ml cells*) were stimulated with patients' exosomes. For each exosome, three doses were used as 0.5µg, 2.5 µg, 12.5 µg. After 24 hrs of incubation, supernatants were collected for cytokine ELISA. N=3-10 individual samples. Statistical significance among groups was based on two-way ANOVA *p<0.05, **p<0.01, ***p<0.001.*

3.2.4. *In vitro* stimulation of mouse strain specific immune cells with patient exosomes

As it was observed in previous section that patient exosomes had an inflammatory effect on healthy PBMCs, we hypothesized that, similar effects would be seen if we incubate naive mouse splenocytes with patient exosomes. We also aimed to assess strain specific immune response, thus Balb/c and C57BL/6 strains were used. Therefore, similar experimental design was set up, and spleens were removed from Balb/c and C57BL/6 mouse strains and prepared to be single cell suspension as explained in Section 2.2.3.

After 24 hrs incubation of mouse splenocytes ($1x10^6$/ml spleen cells) with patient and healthy controls' exosomes (12.5 μg/well), supernatants were collected and used in ELISA to determine IL-6, IL-12 and IFNγ levels. Collectively, similar results were obtained when compared with healthy PBMC stimulation assay (**Figure 3.13**). Although IL-6 and IFNγ levels were found to be elevated in both strains, higher levels were assessed in Balb/c mouse splenocytes than in C57BL/6 strain. When compared with healthy controls, patient exosomes had promoted more than two-fold induction in IL-6 and IFNγ levels of Balb/c strain over C57BL/6 strain (**Figure 3.14 A and C**). Interestingly, not detectable difference for IL-12 was seen among disease groups and healthy control exosomes except for being promoted 1.5-fold higher in Balb/c strain than C57BL/6 strain (**Figure 3.14 B**).

In summary, all patient exosomes had an inflammatory effect on splenocyte stimulation experiments regardless of having different immunologic background. However, higher cytokine production was observed in Balb/c background mouse, which is predominantly mediated by Th2 immunity than C57BL/6 mouse splenocytes which is predominantly mediated by Th1 immune cells (**Figure 3.14**) [105, 106]. This is possibly due to exosome internalization. Thus, the cells that are capable of secreting IL-6 and IFNγ internalized more exosomes in Balb/c strain than in C57BL/6 strain.

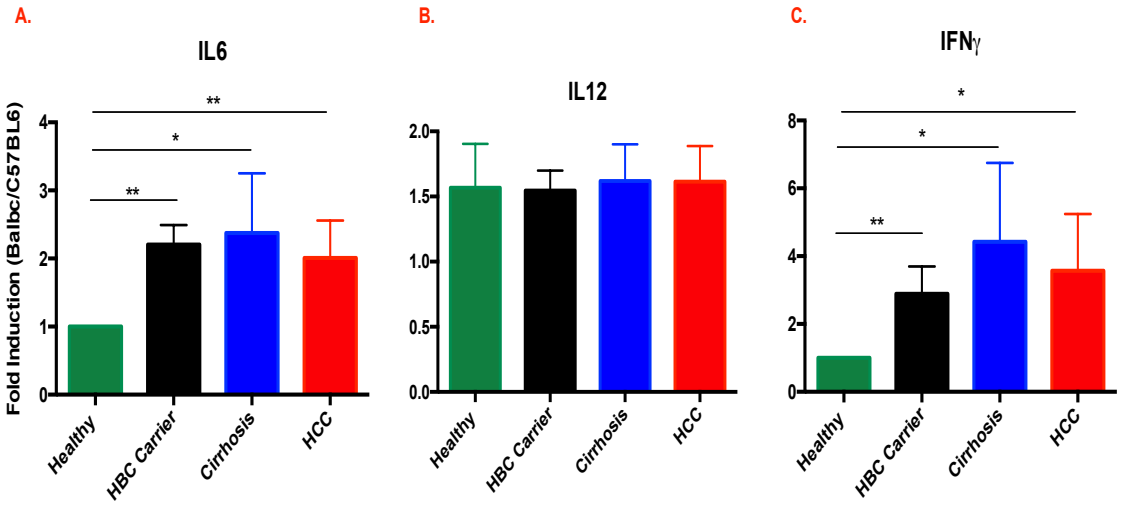


Figure 3.14. Stimulation of Balb/c and C57BL/6 splenocytes with HBV carrier, Cirrhosis and HCC exosomes. Fold induction of *IL-6* ***(A)*** *IL-12* ***(B)*** *IFNγ* ***(C)*** levels assessed in Balb/c strain over C57BL/6 strain. *12.5 µg of exosome was stimulated with Balb/c and C57BL/6 splenocytes (1x10^6/ml spleen cells). After 24 hrs of incubation, supernatants were collected for cytokine ELISA. Statistical significance among groups was based on Student's t-test analysis, *p<0.05, **p<0.01.*

3.3. Potential Therapeutic Cancer Vaccine Study: Ligand-Loaded Extracellular Vesicles (EVs) and Liposomes

3.3.1. Exosome and liposomes as therapeutic cancer vaccine delivery vehicles against established HCC model *in vivo*

3.3.1.1. Co-encapsulating CpG ODN and poly(I:C) within exosome and liposomes

In this part of the study, exosome and liposomes were utilized as potential vaccine carrier systems. While liposomes are extensively used as a conventional cargo delivery system, tumor-derived exosomes' potential against established tumors remains to be identified. In our previous unpublished data, we observed anti-tumor effect of tumor-derived exosomes in distinct established tumors *in vivo.* Therefore, we wanted to test ligand-loaded HUH7 exosomes' potential to boost antigen-specific immune response in HCC xenograft with a very challenging experimental set up. The results from this study would provide insights to develop exosome-mediated therapeutic cancer vaccine.

To establish HCC model *in vivo*, HUH7 cells were subcutaneously (s.c.) injected to right flank of athymic nude mice (male, 6-10-week-old) as $4x10^6$ cell/mouse. Since athymic mice do not have a functional T cell response, possible anti-tumor effects would be through the innate arm of the immunity. Another challenge here was that HUH7 is a human cell line and athymic mouse was the only option to establish HCC xenograft.

In summary, we sought to test the anti-tumor activity of ligand-loaded exosomes as potential exosome-mediated therapeutic cancer vaccine in HCC xenografts and compare the efficacy with liposomes that are widely used as a conventional cargo delivery systems. Thus, we externally loaded dual Toll-like receptor (TLR) ligands; TLR 3: poly(I:C), and TLR 9: K-type CpG ODN within HCC derived exosomes and neutral charged liposomes via dehydration-rehydration technique. Following the palpable tumor formation, each group of mice received different formulations of TLR ligands either in liposome and exosome encapsulated or in their free forms, for a total

of 4 injections, intraperitoneally (i.p.). There was also a control group which only received 1x PBS at each injection as the control group (n=7). Treatment groups were as follows;

(1) Control - PBS,

(2) unencapsulated two ligand mixed formulation indicated as 1555-3CG+pIC,

(3) two ligand exosome co-loaded formulation indicated as Exo(1555-3CG+pIC),

(4) two ligand liposome co-loaded formulation indicated as Lipo(1555-3CG+pIC).

As we can see in **Figure 3.15**, there was almost 70% reduction in tumor volumes of dual ligand formulated exosome (Exo(1555-3CG+pIC)) group when compared with PBS (control) or dual ligand mixed formulation (1555-3CG+pIC) groups (**Figure 3.15 C and E**). Similarly, two ligand co-loaded liposome (Lipo(1555-3CG+pIC)) administered mice showed a significant inhibition -almost 60%- in tumor size (**Figure 3.15 D**). These findings could be further supported by the representative pictures of HUH7 tumor bearing mice at day=14 after, 4^{th} injection of therapy (**Figure 3.16**). In long-term survival curve, encapsulating dual TLR ligands within exosomes Exo(1555-3CG+pIC), provided substantially improved survival among all groups (**Figure 3.17**).

Since athymic nude mice do not have a complete adaptive immunity, this significant improvement in tumor size and prolonged survival of HCC xenografts, is innate immunity dependent (NK cells, macrophages). In conclusion, exosomal and liposomal vaccine delivery system provided significantly regressed established HCC tumor development with significantly prolonged survival.

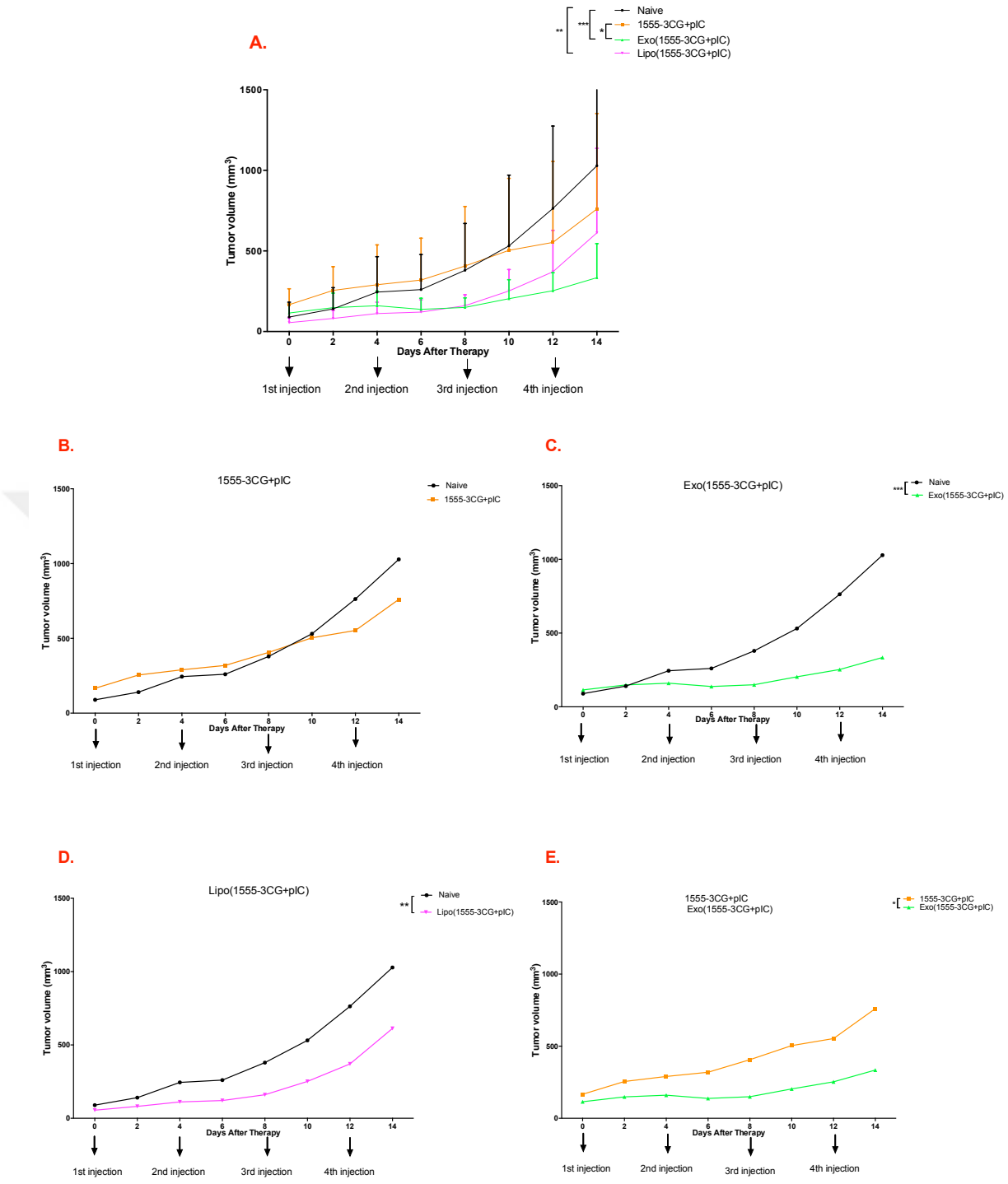


Figure 3.15. Post-treatment HUH7 tumor growth curves over time.

Average tumor volumes of each group ***(A)*** *Control vs 1555-3CG+pIC* ***(B)*** *Control vs Exo(1555-3CG+pIC)* ***(C)*** *Control vs Lipo(1555-3CG+pIC)* ***(D)*** *1555-3CG+pIC vs Exo(1555-3CG+pIC)* ***(E)****. Arrows indicate treatment days, n=7 for each group. Statistical significance among groups was based on one-way ANOVA analyses, *p<0.05, **p<0.01 and ***p<0.001.*

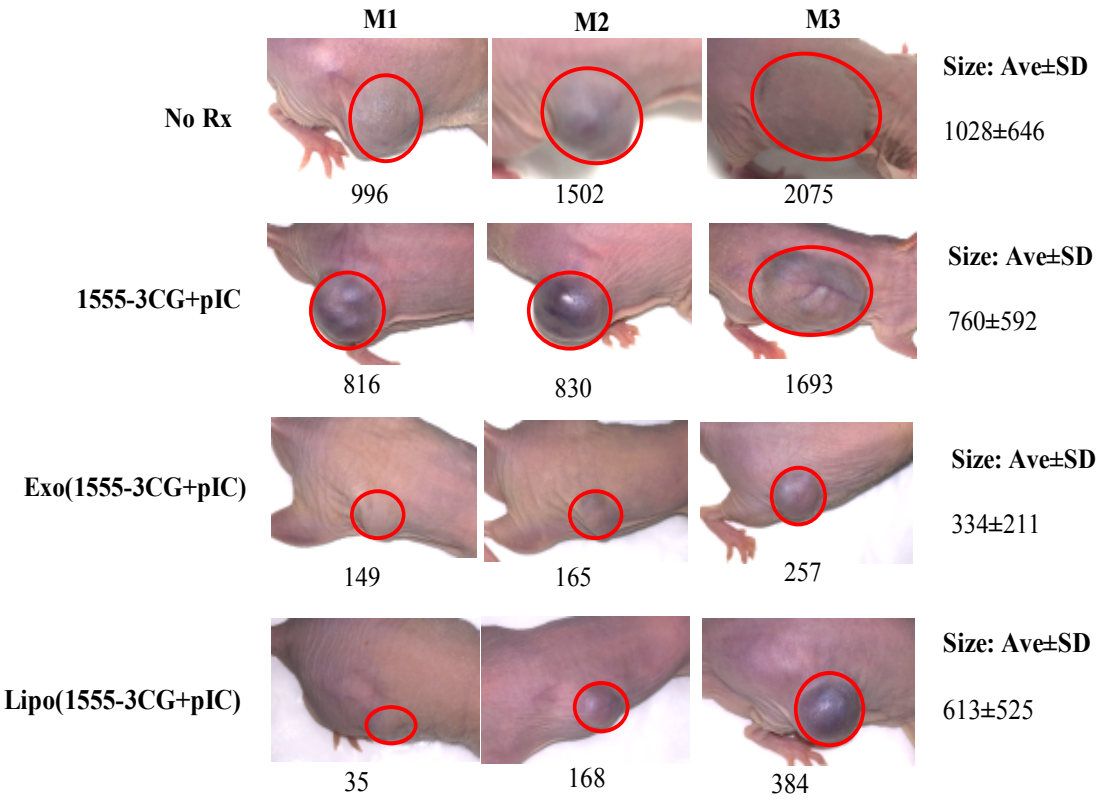


Figure 3.16. Representative pictures of HUH7 tumor bearing mice at day=14 after, 4th injection of therapy.

Mice were s.c. injected with HUH7 (4x10^{6} cells/mouse) at day=0 (n= 7 mice/group). Following the palpable tumor formation, mice were treated with different formulations; PBS, 1555-3CG+pIC, Exo(1555-3CG+pIC) and Lipo(1555-3CG+pIC) for a total of four i.p. injections. Tumor volumes were monitored.

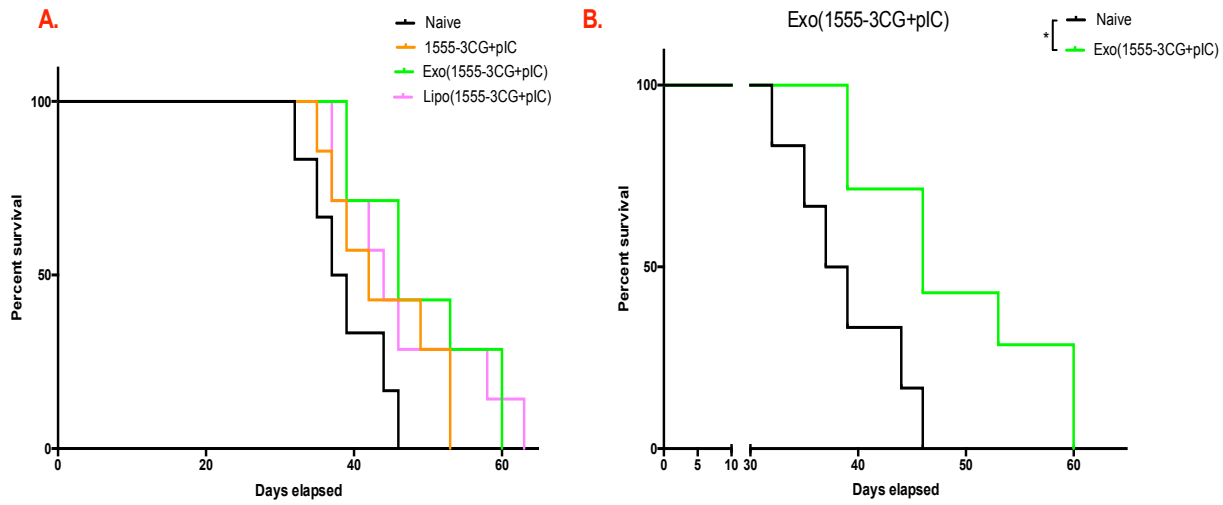


Figure 3.17. Kaplan-Meier survival graphs of HUH7 tumor bearing mice.

Collective graph displaying all groups' survival data ***(A)*** *Control versus Exo(1555-3CG+pIC)* ***(B)****. Tumor sizes were measured and recorded on alternating days, mice were euthanized when tumor volumes reached 2000 mm*^{3}*. Statistical significance among groups was based on Log-rank (Mantel-Cox) test analyses, *p<0.05, **p<0.01 and **p<0.001.*

3.3.1.2. Encapsulating triple ligands: α-Galactosylceramide, CpG ODN and poly(I:C) within exosome and liposomes

Since we developed a potent exosome-mediated vaccine carrier system in HCC xenografts in previous section, we wanted to further augment these anti-tumor effects with a parallel experimental set up *in vivo*. In this part of the study, we aimed to increase previously observed 70% reduction in tumor volume by investigating another ligand α-Galactosylceramide (αGC hereafter) which is a synthetic glycolipid, a specific ligand for Natural Killer T cells (NKT). As αGC plays a significant role in regulation of immune responses such as tumor rejection, we sought to encapsulate it with exosomes and liposomes in addition to previously used TLR ligands (poly(I:C) and K-type CpG ODN).

Following the palpable tumor formation, each group of mice received different formulations of ligands either in liposome and exosome encapsulated or in their free forms, for a total of 4 injections, intraperitoneally (i.p.). Treatment groups were as follows;
(1) Control - PBS,
(2) three ligand unencapsulated mixed formulation indicated as αGC+1555-3CG+pIC,
(3) three ligand exosome-loaded formulation indicated as Exo(αGC+1555-3CG+pIC),
(4) three ligand liposome-loaded formulation indicated as Lipo(αGC+1555-3CG+pIC).

As shown in **Figure 3.18 B,** free formulation of three ligands significantly improved tumor volume by almost 60% when compared to control group. Since our previous data showed that free formulation of two ligands had not any remarkable anti-tumor effect (**Figure 3.15 B**), this improvement was αGC dependent. However, no difference was observed in free formulation vs. exosome/liposome-loaded groups (**Figure 3.18 B, C and D**). This is indicating that, induction of tumor regression capacity by the three ligands was formulation independent.

Significant prolonged survival with anti-tumor response was observed in αGC including triple ligand free formulation (αGC+1555-3CG+pIC) and liposome encapsulated (Lipo(αGC+1555-3CG+pIC)) groups (**Figure 3.20**).

In conclusion, we developed a robust therapeutic vaccine delivery system in which injection of therapeutic vaccine to tumor burden animals enhanced anti-tumor activity and prolonged survival of HCC xenografts. In summary, this approach could broaden the immunotherapeutic utility of exosomes in clinic.

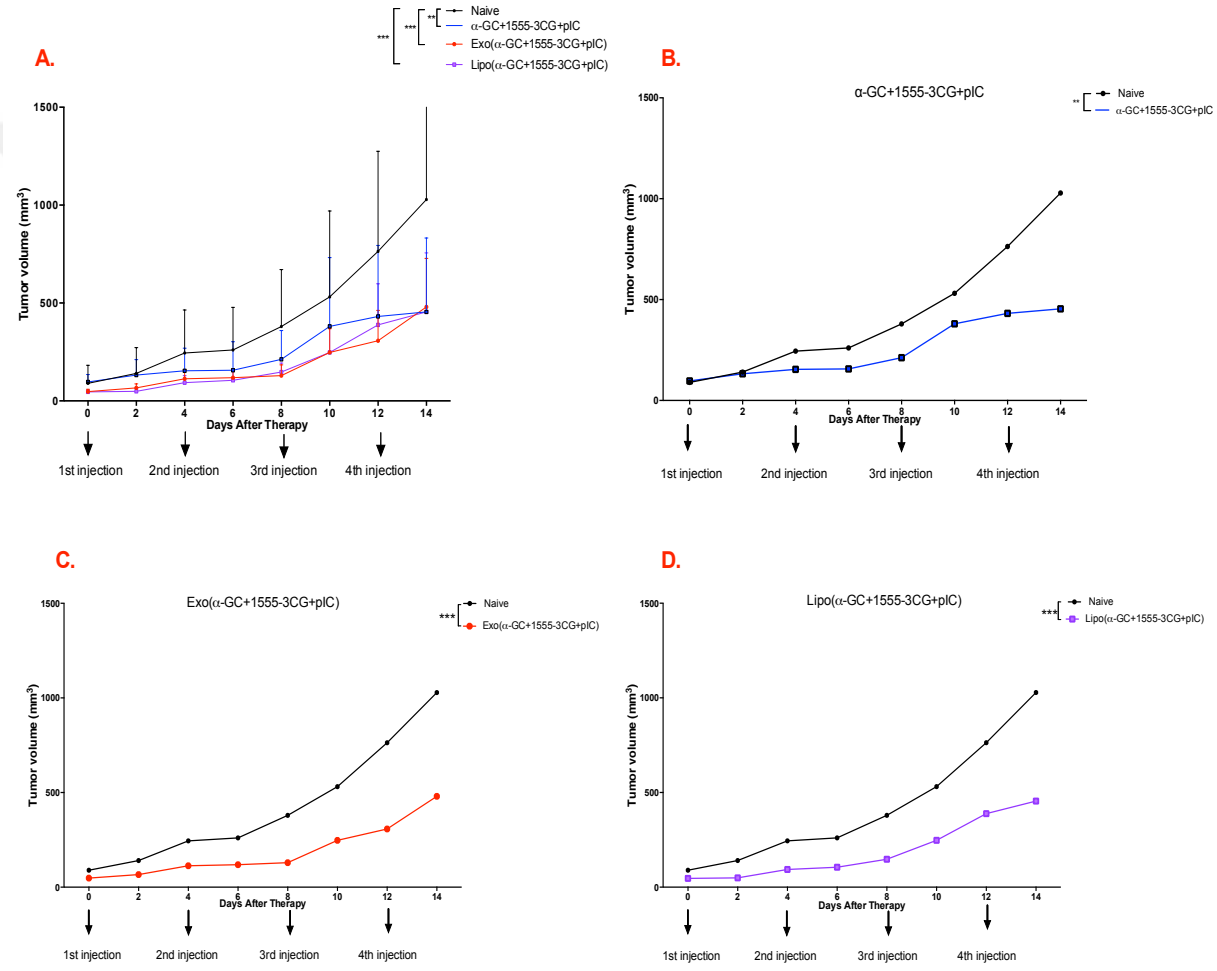


Figure 3.18. Post-treatment HUH7 tumor growth curves over time.

Average+/-SD tumor volumes of each group ***(A)*** *Control vs αGC+1555-3CG+pIC* ***(B)*** *Control vs Exo(αGC+1555-3CG+pIC)* ***(C)*** *Control vs Lipo(αGC+1555-3CG+pIC)* ***(D)***. *Arrows indicate treatment days, n=7 for each group. Statistical significance among groups was based on one-way ANOVA analyses, *p<0.05, **p<0.01 and ***p<0.001.*

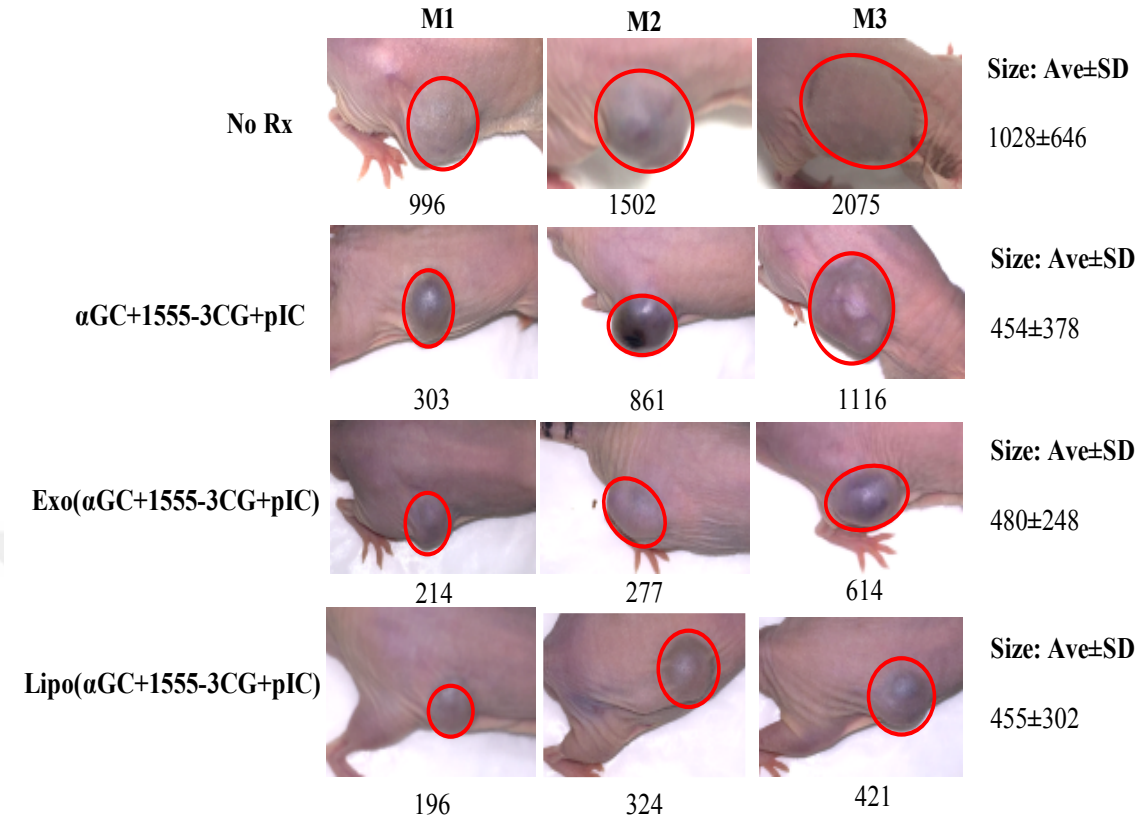


Figure 3.19. Representative pictures of HUH7 tumor bearing mice at day=14 after, 4th injection of therapy.

Mice were s.c. injected with HUH7 (4x10^6 cells/mouse) at day=0 (n= 7 mice/group). Following the palpable tumor formation, mice were treated with different formulations; PBS, αGC+1555-3CG+pIC, Exo(αGC+1555-3CG+pIC) and Lipo(αGC+1555-3CG+pIC) for a total of four i.p. injections. Tumor volumes were monitored.

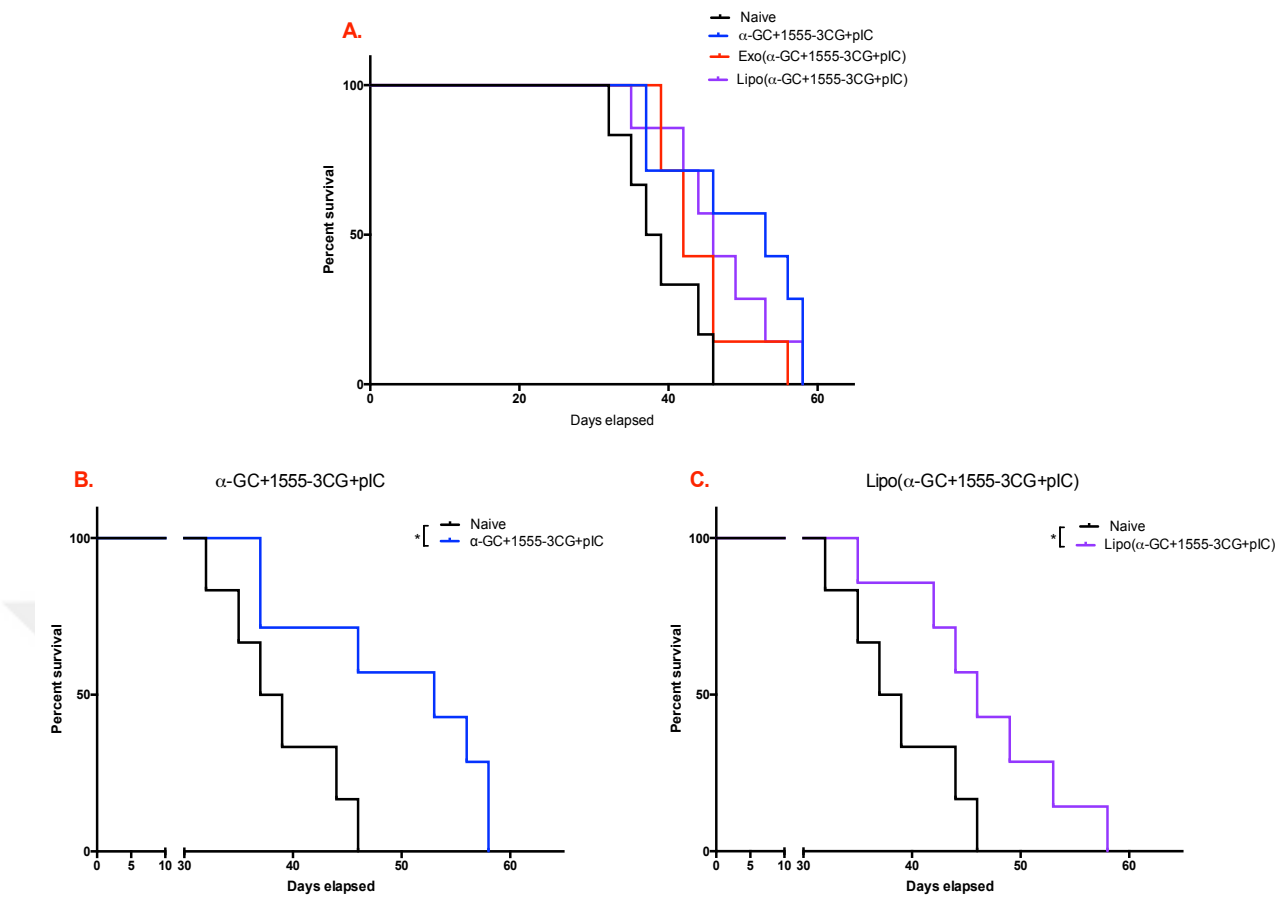


Figure 3.20. Kaplan-Meier survival graphs of HUH7 tumor bearing mice.

Collective graph displaying all four treatment groups' survival data ***(A)*** *Control vs αGC+1555-3CG+pIC* ***(B)*** *Control vs Lipo(αGC+1555-3CG+pIC)* ***(C)*** *Tumor size were measured and recorded alternating days, mice were euthanized when tumor volume reached 2000 mm^3. Statistical significance among groups was based on Log-rank (Mantel-Cox) test analyses, *p<0.05, **p<0.01 and **p<0.001.*

CHAPTER 4

Discussion

Exosomes are the subset of extracellular vesicles (EVs) that carry genomic, proteomic, and lipidic cargos within the circulation. In different physiological states, exosomes are known to act as important immune-modulators. In recent years, the roles of exosomes in distinct pathological processes have been addressed and the therapeutic potential have drawn attention but still requires thorough research [44]. Other than a wide range of putative biological functions of exosomes that mimic the phenotypic state of the cells from which they originate, they are also able to change the function of recipient cells by transferring their cargo [107]. Since exosomes play an important role in intercellular communication and molecule transfer, they have been proposed to be potent candidates for immunotherapy, and as a "natural nanocarrier" for cargo delivery against several immunological diseases and as potential therapeutic cancer vaccine [108, 109].

As distinct exosome subpopulations act differently, they also carry different cargo composition thus, are differently enriched in specific surface biomarkers and other co-stimulatory and/or co-inhibitory molecules [110]. Our study demonstrated that, different exosome subtypes that are derived from EG7, HUH7, RAW cell culture supernatants, express the same molecules at different levels including CD9, CD81, PD-L1 and TSG101 (**Figure 3.1**). Not surprisingly, these exosome species were also selectively and differentially up taken by different immune cells implicating that not all exosomes are taken up by the same cells at the same level (**Figure 3.5**). The highest PD-L1 expression that is associated with tumor aggressiveness and poor clinical outcome [111], was observed on RAW exosomes which were also taken up by all immune cell subsets at the highest level among another cell-line derived exosomes. As expected, antigen presenting cells (APCs) including macrophages and dendritic

cells (DCs) internalized all exosome types at the highest level, compared to T- and B-cells. This was most probably dependent on the phagocytic capability of these cells [112]. Exosome internalization efficiency might depend on the surface molecules located on both cells and exosomes that control exosome–cell interaction and also the exosome intercellular trafficking pathway [113]. While HUH7 exosomes were the least internalized exosome type by PEC in *in-vitro* stimulation assays, *ex-vivo* HUH7 exosome investigation following *in-vivo* administration has ended up with the highest inflammatory response (**Figure 3.7**). It is still controversial whether exosome uptake is cell type-specific, thus further elucidation for this up take mechanisms is required.
Accordingly, mouse splenocyte stimulation assays (either alone or in combination with different TLR ligands), revealed the immunostimulatory effects of EG7, HUH7, RAW exosomes (**Figure 3.2, Figure 3.3 and Figure 3.4**). Different exosomes purified from different cell source displayed various immunomodulatory properties. Of note, when injected to mice HUH7 exosomes were the most inflammatory type among others. In summary, these natural nanovesicles that act as immunostimulators are promising tools to be applied in clinical practice for immunotherapy and immunomodulation.

Exosomes are proposed to be a potent mediator of tumor initiation and disease progression due to their roles in intercellular communication. In various malignancies, tumor cells have been found to release significantly augmented levels of exosomes [114]. Recent studies have demonstrated that exosomes transfer viral components to APCs, thus activate PRRs that results with the production of pro-inflammatory, type I and type II IFN secretion. Therefore, exosomes are worth investigating as immunotherapeutic targets [115]. Chronic hepatitis B virus (HBV) infection is the main cause of liver damage and also comprises 50% hepatocellular carcinoma (HCC) cases worldwide [116]. The contribution of exosomes in disease progression from chronic HBV infection to HCC state remains poorly understood and need more investigation. To identify the role of exosomes in disease progression and on the immune system, exosomes were isolated from the peripheral blood plasma of HBV-Carrier, Cirrhosis and HCC patients. Flow cytometric analyses revealed that, exosomes express programmed death- ligand 1 (PD-L1) co-inhibitory molecule regardless of disease state, and, HCC patients' exosomes had a significantly higher

PD-L1 expression among others. This was correlated with the literature research that links PD-L1 overexpression with tumor aggressiveness and poor prognosis [117]. Since the level of exosomal PD-L1 protein may not be sufficient to be recognized via immunoblotting, the exosomal PD-L1 expression could not be validated through immunoblotting (**Figure 3.10**). Owing to its capacity to measure events at a single cell level, flow cytometry provides robust identification, even for a small proportion of specialized exosomes.

Circulating cytokine levels are important indicators in HCC pathogenesis as well as for identifying the immunologic background of the disease. Therefore, before any downstream stimulation assays, plasma cytokine levels were determined. Cirrhosis and HCC groups had the highest IP-10 secretion (**Figure 3.11**). In literature, IP-10 secretion is triggered in HCV (Hepatitis-C virus) infection caused by viral proteins and double-stranded RNA (dsRNA) from HCV [118] and also higher circulating IP-10 is correlated with poorer overall survival in patients with HCC [119]. Of note, plasma level of anti-inflammatory cytokine, IL-10 was significantly higher in HCC group that was the key cytokine which is associated aggressive clinicopathological features and support tumor immune escape [116]. Notably, patients receiving various medications might contribute to different cytokine profiles. Another key cytokine is TGF-β, that have a dual role in liver hepatocarcinogenesis; both promoting and suppressing tumor growth depending on the state of the tumor. Although in many studies, TGF-β was reported to be overexpressed in both plasma and tissue of HCC patients, we found that HBV carrier patients had significantly increased level of plasma TGF-β levels which was dramatically decreased in chronic cirrhosis and HCC patients (**Figure 3.12**). Nevertheless, Mamiya et. al., reported that reduced expression of TGF- β receptor type II was linked to intrahepatic metastasis, in concert with our data.

Eventually, to determine the immunomodulatory effects of patient-derived exosomes, healthy controls' PBMCs, as well as murine splenocytes were treated with different doses of exosomes *in vitro*. PBMC stimulation assay showed that, HCC exosomes had the highest inflammatory effect by increasing IFNγ and IP-10 levels, followed by Cirrhosis and HBV carrier groups (**Figure 3.13**). Collectively, our data elucidated that,

patients' exosomes have an inflammatory effect on healthy PBMCs [120]. Thus, severity of liver disease correlated with the inflammatory capacity of plasma exosomes of patients. Furthermore, similar results were obtained from *in vitro* murine splenocyte stimulation assays with patient exosomes. IFNγ levels were augmented after exosome administration in Balb/c strain (Th2-prone) originated splenocytes, more than that was observed in C57BL/6 strain (Th1-prone), indicating that patient exosomes might have a role in Th1 polarization possibly by promoting activated $CD4^+$ T-cells to differentiate into IFN-γ-producing Th1 cells [120] or this could be due to differential exosomal internalization. Basically, more IFN-γ-producing cells probably internalized more exosomes. More detailed study is necessary to explain this mechanism.

Exosomes as drug delivery vehicles offer fostering advantages compared to other conventional drug delivery systems including liposomes and polymeric nanoparticles. Exosomes have very similar composition as body's own cells and therefore they are non-immunogenic [121]. Recently, these nanovesicles are gaining popularity for immunotherapeutic interventions and the central interest of exosome research became the utilization of exosomes as a delivery system and in vaccine studies. Of note, tumor-derived exosomes carry tumor antigens that are capable of promoting antigen-specific immune response. Also by their internal cargo, they modulate the immune response.
In the last part of this study, we sought to investigate the possible anti-tumor activity of dual or triple-ligand-loaded tumor derived exosomes (HUH7) and liposomes against HCC xenograft as potential exosome-mediated therapeutic cancer vaccine. To this end, we efficiently loaded dual and triple TLR agonists (TLR3: pI:C, TLR9: CpG ODN K-type and NKT ligand: α-GC) into exosomes and liposomes. A method for ligand encapsulation was based on dehydration-rehydration of vesicles following the purification of exosomes (Kahraman, Ph.D. thesis, 2016). This novel method is very well established in our lab, allow multiple ligand encapsulation with high yield and without rupturing the vesicles that is the main obstacle in electroporation method. This efficient dehydration-rehydration encapsulation method can enhance the activity of different immunomodulatory molecules or drugs especially against cancer and many other incurable diseases [122-124].

Overall, encapsulation of dual ligands (CpG ODN and p(I:C)) within exosomes showed a promising therapeutic pattern, that regresses established HCC tumors more effectively than liposomes (**Figure 3.15).** Thus having 70% and 56% reduction when compared to control and free ligand formulated group respectively (**Figure 3.16)**. Exosomes harboring dual ligands also elicited prolonged survival **(Figure 3.17**).

Addition of a third ligand, 'αGC', resulted in almost 60% regression in tumor volume. Even though athymic nude mice are lack of cell-mediated immunity, they have elevated cytotoxic activity of NK cells and macrophages than their euthymic counterparts. Thus, NKT cell agonist, αGC demonstrated its anti-tumor effect most likely by triggering NK and macrophage activity through CD1d and inducing an anti-tumor response in formulation-independent manner (**Figure 3.18**) [125-127]. In addition, significant prolonged survival was observed with tumor bearing mice (**Figure 3.20**). Thus, data suggests that, suppression of tumors was dependent on αGC. . The lackluster efficacy of αGC in encapsulation within exosomes and liposomes may be attributable to its administered level. Little amount of this glycolipid (such as 20ng/mouse) might be more efficient in terms of encapsulation within exosomes and liposomes. Selecting optimal dose is important otherwise, αGC is known to induce anergy and also provide toxicity. To reveal this mechanism, we next need to find the optimal dose -maybe by performing threefold-dose titration- with appreciable efficiency.

Since athymic nude mice do not have a complete adaptive immunity, this significant improvement in tumor size and prolonged survival of HCC xenografts, is innate immunity dependent (NK cells, macrophages). Nevertheless, therapeutic exosomal tumor vaccine suppressed tumor progression and prolonged survival of tumor bearing mice.

Exosomes' long-term safety along with the ability to transport intercellular nucleic acids and molecules across locations where difficult to penetrate, such as blood-brain barrier (BBB), make these vesicles attractive candidates for clinical utility. In summary, results are of clinical importance. Moreover, it provides a new direction for disease characterization and therapy. Hence, the information obtained from this study will allow a better understanding of the development of exosome-based therapeutics and exosome-mediated therapeutic cancer vaccine [128].

Bibliography

1. Abbas, A.K., A.H. Lichtman, and S. Pillai, *Cellular and molecular immunology*. Eighth edition. ed. 2015, Philadelphia, PA: Elsevier Saunders. viii, 535 pages.
2. Stuart E. Turvey, M.B., DPhil and David H. Broide, MB ChB, *Chapter 2: Innate Immunity*, in *Journal of Allergy Clinical Immunology*. 2010. p. 24-32.
3. Hoffmann, J. and S. Akira, *Editorial overview: Innate immunity.* Current Opinion in Immunology, 2013. **25**(1): p. 1-3.
4. Webb, A.E., et al., *Adaptive Evolution as a Predictor of Species-Specific Innate Immune Response.* Mol Biol Evol, 2015. **32**(7): p. 1717-29.
5. Scully, C., E.A. Georgakopoulou, and Y. Hassona, *The Immune System: Basis of so much Health and Disease: 3. Adaptive Immunity.* Dent Update, 2017. **44**(4): p. 322-4, 327.
6. Bayersdorf, R., A. Fruscalzo, and F. Catania, *Linking autoimmunity to the origin of the adaptive immune system.* Evol Med Public Health, 2018. **2018**(1): p. 2-12.
7. Ward AE, R.B., *Evolutionary responses of innate immunity to adaptive immunity.* Infect Genet Evol., 2014. **492**(6).
8. Paul, W.E., *Bridging innate and adaptive immunity.* Cell, 2011. **147**(6): p. 1212-5.
9. Janeway CA Jr, T.P., Walport M, *Immunobiology: The Immune System in Health and Disease. 5th edition.* Garland Science, 2001.
10. Warrington, R., et al., *An introduction to immunology and immunopathology.* Allergy Asthma Clin Immunol, 2011. **7 Suppl 1**: p. S1.
11. La Gruta, N.L. and S.J. Turner, *T cell mediated immunity to influenza: mechanisms of viral control.* Trends Immunol, 2014. **35**(8): p. 396-402.
12. McNeela, E.A. and K.H.G. Mills, *Manipulating the immune system: humoral versus cell-mediated immunity.* Advanced Drug Delivery Reviews, 2001. **51**(1-3): p. 43-54.
13. Bode, C., et al., *CpG DNA as a vaccine adjuvant.* Expert Rev Vaccines, 2011. **10**(4): p. 499-511.
14. Mogensen, T.H., *Pathogen Recognition and Inflammatory Signaling in Innate Immune Defenses.* Clinical Microbiology Reviews, 2009. **22**(2): p. 240-+.
15. Odendall, C. and J.C. Kagan, *Activation and pathogenic manipulation of the sensors of the innate immune system.* Microbes Infect, 2017. **19**(4-5): p. 229-237.
16. Santoni, G., et al., *Danger- and pathogen-associated molecular patterns recognition by pattern-recognition receptors and ion channels of the transient receptor potential family triggers the inflammasome activation in immune cells and sensory neurons.* J Neuroinflammation, 2015. **12**: p. 21.
17. Baccala, R., et al., *Sensors of the innate immune system: their mode of action.* Nature Reviews Rheumatology, 2009. **5**(8): p. 448-456.
18. Satoh, T. and S. Akira, *Toll-Like Receptor Signaling and Its Inducible Proteins.* Microbiol Spectr, 2016. **4**(6).
19. Kawasaki, T. and T. Kawai, *Toll-like receptor signaling pathways.* Front Immunol, 2014. **5**: p. 461.

20. Jialal, I., H. Kaur, and S. Devaraj, *Toll-like receptor status in obesity and metabolic syndrome: a translational perspective.* J Clin Endocrinol Metab, 2014. **99**(1): p. 39-48.
21. Chamorro, S., et al., *TLR triggering on tolerogenic dendritic cells results in TLR2 up-regulation and a reduced proinflammatory immune program.* J Immunol, 2009. **183**(5): p. 2984-94.
22. Zhu, G., et al., *Targeting pattern-recognition receptors to discover new small molecule immune modulators.* Eur J Med Chem, 2018. **144**: p. 82-92.
23. Kaisho T, A.S., *Toll-like receptors as adjuvant receptors.* Biochim Biophys Acta, 2002. **1589**(1).
24. O'Neill, L.A., D. Golenbock, and A.G. Bowie, *The history of Toll-like receptors - redefining innate immunity.* Nat Rev Immunol, 2013. **13**(6): p. 453-60.
25. Kawai, T. and S. Akira, *Toll-like receptors and their crosstalk with other innate receptors in infection and immunity.* Immunity, 2011. **34**(5): p. 637-50.
26. Yu, L., L. Wang, and S. Chen, *Endogenous toll-like receptor ligands and their biological significance.* J Cell Mol Med, 2010. **14**(11): p. 2592-603.
27. Shi, Z., et al., *A novel Toll-like receptor that recognizes vesicular stomatitis virus.* J Biol Chem, 2011. **286**(6): p. 4517-24.
28. Zhao, S., et al., *Toll-like receptors and prostate cancer.* Front Immunol, 2014. **5**: p. 352.
29. Jiang, S., et al., *TLR10 Is a Negative Regulator of Both MyD88-Dependent and -Independent TLR Signaling.* J Immunol, 2016. **196**(9): p. 3834-41.
30. Shao H, I.H., Castro CM, Breakefield X, Weissleder R, Lee H., *New Technologies for Analysis of Extracellular Vesicles.* Chem Rev., 2018. **118**(4).
31. Maarten P. Bebelman, M.J.S., D. Michiel Pegtel, S. Rubina Baglio, *Biogenesis and function of extracellular vesicles in cancer.* Pharmacology and Therapeutics, 2018.
32. Elie Beit- Yannai, S.T., W. Daniel Stamer, *Physical exosome:exosome interactions.* J Cell Mol Med, 2018. **22**(3): p. 2001-2006.
33. Masamitsu Kanada, M.H.B., Christopher H. Contag, *Signaling by Extracellular Vesicles Advances Cancer Hallmarks.* Trends in Cancer, 2016. **2**(2).
34. Nina Pettersen Hessvik, A.L., *Current knowledge on exosome biogenesis and release.* Cellular and Molecular Life Sciences, 2018. **75**(2): p. 193-208.
35. Thery, C., *Exosomes: secreted vesicles and intercellular communications.* F1000 Biol Rep, 2011. **3**: p. 15.
36. Mikhail A. Livshits, E.K., Evgeniy G. Evtushenko, Vassili N. Lazarev, Nikolay A. Kulemin, Svetlana E. Semina, Edward V. Generozov & Vadim M. Govorun, *Isolation of exosomes by differential centrifugation: Theoretical analysis of a commonly used protocol.* Scientific Reports, 2015.
37. Li, P., et al., *Progress in Exosome Isolation Techniques.* Theranostics, 2017. **7**(3): p. 789-804.
38. Zha, Q.B., et al., *Extracellular vesicles: An overview of biogenesis, function, and role in breast cancer.* Tumour Biol, 2017. **39**(2): p. 1010428317691182.
39. Bebelman, M.P., et al., *Biogenesis and function of extracellular vesicles in cancer.* Pharmacol Ther, 2018.
40. Hessvik, N.P. and A. Llorente, *Current knowledge on exosome biogenesis and release.* Cell Mol Life Sci, 2018. **75**(2): p. 193-208.

41. Wu, J., et al., *Role of stem cell-derived exosomes in cancer.* Oncol Lett, 2017. **13**(5): p. 2855-2866.
42. M, H.R., et al., *Exosomes: From Garbage Bins to Promising Therapeutic Targets.* Int J Mol Sci, 2017. **18**(3).
43. Beit-Yannai, E., S. Tabak, and W.D. Stamer, *Physical exosome:exosome interactions.* J Cell Mol Med, 2018. **22**(3): p. 2001-2006.
44. Frydrychowicz, M., et al., *Exosomes - structure, biogenesis and biological role in non-small-cell lung cancer.* Scand J Immunol, 2015. **81**(1): p. 2-10.
45. Liang, X., et al., *Exosomes secreted by mesenchymal stem cells promote endothelial cell angiogenesis by transferring miR-125a.* J Cell Sci, 2016. **129**(11): p. 2182-9.
46. Chen, W., et al., *Immunomodulatory effects of mesenchymal stromal cells-derived exosome.* Immunol Res, 2016. **64**(4): p. 831-40.
47. Shigemoto-Kuroda, T., et al., *MSC-derived Extracellular Vesicles Attenuate Immune Responses in Two Autoimmune Murine Models: Type 1 Diabetes and Uveoretinitis.* Stem Cell Reports, 2017. **8**(5): p. 1214-1225.
48. Mitchell, M.D., et al., *Placental exosomes in normal and complicated pregnancy.* Am J Obstet Gynecol, 2015. **213**(4 Suppl): p. S173-81.
49. Pitt, J.M., et al., *Dendritic Cell-Derived Exosomes as Immunotherapies in the Fight against Cancer.* Journal of Immunology, 2014. **193**(3): p. 1006-1011.
50. Besse, B., et al., *Dendritic cell-derived exosomes as maintenance immunotherapy after first line chemotherapy in NSCLC.* Oncoimmunology, 2016. **5**(4): p. e1071008.
51. Tan, L., et al., *Recent advances of exosomes in immune modulation and autoimmune diseases.* Autoimmunity, 2016. **49**(6): p. 357-365.
52. Ciro Tetta, E.G., Lorenzo Silengo, Maria Chiara Deregibus, and Giovanni Camussi, *Extracellular vesicles as an emerging mechanism of cell-to-cell communication.* Endocrine, 2013. **44**(1).
53. Admyre, C., et al., *Exosomes with immune modulatory features are present in human breast milk.* J Immunol, 2007. **179**(3): p. 1969-78.
54. Qin, W., et al., *Exosomes in Human Breast Milk Promote EMT.* Clin Cancer Res, 2016. **22**(17): p. 4517-24.
55. Kim, S.H., et al., *Exosomes derived from IL-10-treated dendritic cells can suppress inflammation and collagen-induced arthritis.* J Immunol, 2005. **174**(10): p. 6440-8.
56. Ching, R.C. and P.J. Kingham, *The role of exosomes in peripheral nerve regeneration.* Neural Regen Res, 2015. **10**(5): p. 743-7.
57. Sato S, L.K., Kameyama T, Hayashi T, Ishida Y, Murakami S, Watanabe T, Iijima , S.Y. S, Watashi K, Tsutsumi S, Sato Y, Akita H, Wakita T, Rice CM,, and K.M. Harashima H, Tanaka Y, Takaoka A., *The RNA sensor RIG-I dually functions as an innate sensor and direct antiviral factor for hepatitis B virus.* Immunity, 2015.
58. Kouwaki T, F.Y., Daito T, Sanada T, Yamamoto N, Mifsud EJ, Leong CR, and K.M. Tsukiyama-Kohara K, Matsumoto M, Seya T, Oshiumi H, *Extracellular Vesciles Including Exosomes Regulate Innate Immune Responses to Hepatitis B Virus Infection.* Front Immunol, 2016. **31**(7).
59. Sanada, T., et al., *Transmission of HBV DNA Mediated by Ceramide-Triggered Extracellular Vesicles.* Cell Mol Gastroenterol Hepatol, 2017. **3**(2): p. 272-283.

60. Xi Yang, H.L., Huahui Sun, Hongxia Fan, Yaqi Hu, Min Liu, Xin Li and Hua Tang, *Hepatitis B virus-encoded miRNA controls viral replication.* Journal of Virology, 2017.
61. Xiaofang Jia, J.C., Dominik A. Megger, Xiaonan Zhang, Maya Kozlowski, Lijun Zhang, Zhong Fang, Jin Li, Qiaofang Chu, Min Wu, Yaming Li, Barbara Sitek and Zhenghong Yuan, *Label-free Proteomic Analysis of Exosomes Derived from Inducible Hepatitis B Virus-Replicating HepAD38 Cell Line.* Molecular and Cellular Proteomics, 2017.
62. Yinli Yang, Q.H., Zhaohua Hou, Cai Zhang, Zhigang Tian and Jian Zhang, *Exosomes mediate hepatitis B virus (HBV) transmission and NK-cell dysfunction.* Cellular and Molecular Immunology, 2016: p. 465-475.
63. Théry C, O.M., Segura E., *Membrane vesicles as conveyors of immune responses.* Nat Rev Immunol, 2009. **9**(8).
64. Takahisa Kouwaki, Y.F. and T.S. Takuji Daito, Naoki Yamamoto, Edin J. Mifsud, Chean Ring Leong - University of Kuala Lumpur, Kyoko Tsukiyama, Michinori Kohara, Misako Matsumoto, Tsukasa Seya, Hiroyuki Oshiumi, *Extracellular Vesicles Including Exosomes Regulate Innate Immune Responses to Hepatitis B Virus Infection.* Frontiers in Immunology, 2016.
65. Takahiro Sanada, Y.H., Yutaka Naito, Naoki Yamamoto, Yoshiaki Kikkawa, Yuji Ishida, Chihiro Yamasaki, Chise Tateno, Takahiro Ochiya, Michinori Kohara, *Transmission of HBV DNA Mediated by Ceramide-Triggered Extracellular Vesicles*. Cellular and Molecular Gastroenterology and Hepatology, 2017. **3**(2): p. 272-283.
66. LI, G., *The role for transforming growth factor-beta (TGF-beta) in human cancer.* Crit Rev Oncog, 1999. **10**(4).
67. Xu, R., et al., *Extracellular vesicles in cancer - implications for future improvements in cancer care.* Nat Rev Clin Oncol, 2018.
68. Gao, L., et al., *Tumor-derived exosomes antagonize innate antiviral immunity.* Nat Immunol, 2018. **19**(3): p. 233-245.
69. Greening, D.W., et al., *Exosomes and their roles in immune regulation and cancer.* Semin Cell Dev Biol, 2015. **40**: p. 72-81.
70. Whiteside, T.L., *Tumor-Derived Exosomes and Their Role in Cancer Progression.* Adv Clin Chem, 2016. **74**: p. 103-41.
71. Kurywchak, P., J. Tavormina, and R. Kalluri, *The emerging roles of exosomes in the modulation of immune responses in cancer.* Genome Med, 2018. **10**(1): p. 23.
72. Chow, A., et al., *Macrophage immunomodulation by breast cancer-derived exosomes requires Toll-like receptor 2-mediated activation of NF-kappaB.* Sci Rep, 2014. **4**: p. 5750.
73. Fang, T., et al., *Tumor-derived exosomal miR-1247-3p induces cancer-associated fibroblast activation to foster lung metastasis of liver cancer.* Nat Commun, 2018. **9**(1): p. 191.
74. Chaput, N., et al., *The potential of exosomes in immunotherapy.* Expert Opin Biol Ther, 2005. **5**(6): p. 737-47.
75. Syn, N.L., et al., *Exosomes in Cancer Nanomedicine and Immunotherapy: Prospects and Challenges.* Trends Biotechnol, 2017. **35**(7): p. 665-676.
76. Muller, L., et al., *Human tumor-derived exosomes (TEX) regulate Treg functions via cell surface signaling rather than uptake mechanisms.* Oncoimmunology, 2017. **6**(8): p. e1261243.

77. Liu, Y., Y. Gu, and X. Cao, *The exosomes in tumor immunity.* Oncoimmunology, 2015. **4**(9): p. e1027472.
78. Tumeh, P.C., et al., *PD-1 blockade induces responses by inhibiting adaptive immune resistance.* Nature, 2014. **515**(7528): p. 568-71.
79. Buchbinder, E.I. and A. Desai, *CTLA-4 and PD-1 Pathways: Similarities, Differences, and Implications of Their Inhibition.* Am J Clin Oncol, 2016. **39**(1): p. 98-106.
80. Quek, C., et al., *Defining the purity of exosomes required for diagnostic profiling of small RNA suitable for biomarker discovery.* RNA Biol, 2017. **14**(2): p. 245-258.
81. Li, M., et al., *Analysis of the RNA content of the exosomes derived from blood serum and urine and its potential as biomarkers.* Philos Trans R Soc Lond B Biol Sci, 2014. **369**(1652).
82. Pillay, P., et al., *Placenta-derived exosomes: potential biomarkers of preeclampsia.* Int J Nanomedicine, 2017. **12**: p. 8009-8023.
83. Li, W., et al., *Role of exosomal proteins in cancer diagnosis.* Mol Cancer, 2017. **16**(1): p. 145.
84. Skotland, T., et al., *Molecular lipid species in urinary exosomes as potential prostate cancer biomarkers.* Eur J Cancer, 2017. **70**: p. 122-132.
85. Llorente, A., et al., *Molecular lipidomics of exosomes released by PC-3 prostate cancer cells.* Biochim Biophys Acta, 2013. **1831**(7): p. 1302-9.
86. Shahabipour, F., et al., *Exosomes: Nanoparticulate tools for RNA interference and drug delivery.* J Cell Physiol, 2017. **232**(7): p. 1660-1668.
87. Luan, X., et al., *Engineering exosomes as refined biological nanoplatforms for drug delivery.* Acta Pharmacol Sin, 2017. **38**(6): p. 754-763.
88. Sarko, D.K. and C.E. McKinney, *Exosomes: Origins and Therapeutic Potential for Neurodegenerative Disease.* Front Neurosci, 2017. **11**: p. 82.
89. Liang, T.J., *Hepatitis B: the virus and disease.* Hepatology, 2009. **49**(5 Suppl): p. S13-21.
90. Mittal, S. and H.B. El-Serag, *Epidemiology of hepatocellular carcinoma: consider the population.* J Clin Gastroenterol, 2013. **47 Suppl**: p. S2-6.
91. Sanyal, A.J., S.K. Yoon, and R. Lencioni, *The etiology of hepatocellular carcinoma and consequences for treatment.* Oncologist, 2010. **15 Suppl 4**: p. 14-22.
92. Kahraman, T., et al., *Circulating LL37 targets plasma extracellular vesicles to immune cells and intensifies Behcet's disease severity.* J Extracell Vesicles, 2017. **6**(1): p. 1284449.
93. Gursel, M., et al., *Differential and competitive activation of human immune cells by distinct classes of CpG oligodeoxynucleotide.* J Leukoc Biol, 2002. **71**(5): p. 813-20.
94. Takeshita, F., et al., *Cutting edge: Role of Toll-like receptor 9 in CpG DNA-induced activation of human cells.* J Immunol, 2001. **167**(7): p. 3555-8.
95. Bayyurt, B., et al., *Encapsulation of two different TLR ligands into liposomes confer protective immunity and prevent tumor development.* J Control Release, 2017. **247**: p. 134-144.
96. Gursel, I., et al., *Sterically stabilized cationic liposomes improve the uptake and immunostimulatory activity of CpG oligonucleotides.* J Immunol, 2001. **167**(6): p. 3324-8.
97. Willms, E., et al., *Cells release subpopulations of exosomes with distinct molecular and biological properties.* Sci Rep, 2016. **6**: p. 22519.

98. Myriam Oliveira-Rodríguez, S.L.-C., Hugh T. Reyburn, Agustín Costa-García, Soraya López-Martín, María Yáñez-Mó, Eva Cernuda-Morollón, Annette Paschen, Mar Valés-Gómez, Maria Carmen Blanco-López, *Development of a rapid lateral flow immunoassay test for detection of exosomes previously enriched from cell culture medium and body fluids.* Journal of Extracellular Vesicles, 2016. **5**(1).
99. Watson DC, B.D., Srivatsan A, Bergamaschi C, Valentin A, Niu G, Bear J,, S.M. Monninger M, Morales-Kastresana A, Jones JC, Felber BK, Chen X, Gursel I, , and P. GN., *Efficient production and enhanced tumor delivery of engineered extracellular vesicles.* Biomaterials, 2016(105): p. 195-205.
100. Vito Dozio, J.-C.S., *Characterisation of extracellular vesicle-subsets derived from brain endothelial cells and analysis of their protein cargo modulation after TNF exposure.* Journal of Extracellular Vesicles, 2017. **6**(1).
101. Vikram R. Juneja, Kathleen A.M., Robert T. Manguso, Martin W. LaFleur, , W.Nicholas H. Natalie Collins, Gordon J. Freeman,7 , and a. Arlene H. Sharpe, *PD-L1 on tumor cells is sufficient for immune evasion in immunogenic tumors and inhibits CD8 T cell cytotoxicity.* The Journal of Experimental Medicine, 2017. **8**(52): p. 89903–89912.
102. Caldwell, C., Jr., et al., *Identification and Validation of a PD-L1 Binding Peptide for Determination of PDL1 Expression in Tumors.* Sci Rep, 2017. **7**(1): p. 13682.
103. Li, M., et al., *Heterogeneity of PD-L1 expression in primary tumors and paired lymph node metastases of triple negative breast cancer.* BMC Cancer, 2018. **18**(1): p. 4.
104. Mittendorf, E.A., et al., *PD-L1 expression in triple-negative breast cancer.* Cancer Immunol Res, 2014. **2**(4): p. 361-70.
105. Fukushima, A., et al., *Genetic background determines susceptibility to experimental immune-mediated blepharoconjunctivitis: comparison of Balb/c and C57BL/6 mice.* Exp Eye Res, 2006. **82**(2): p. 210-8.
106. Marques, S.M., et al., *Genetic background determines mouse strain differences in inflammatory angiogenesis.* Microvasc Res, 2011. **82**(3): p. 246-52.
107. Ciro Tetta, E.G., Lorenzo Silengo, Maria Chiara Deregibus, and Giovanni Camuss, *Extracellular vesicles as an emerging mechanism of cell-to-cell communication.* Endocrine, 2013. **44**(1): p. 11–19.
108. Yáñez-Mó M, S.P., Andreu Z, Zavec AB, Borràs FE, Buzas EI, Buzas K,, et al., *Biological properties of extracellular vesicles and their physiological functions.* Journal of Extracellular Vesicles, 2015. **14**(4).
109. Greening DW, G.S., Xu R, Simpson RJ, Chen W, *Exosomes and their roles in immune regulation and cancer.* Semin Cell Dev Biol., 2015. **40**(72).
110. Villarroya-Beltri, C., et al., *Sorting it out: regulation of exosome loading.* Semin Cancer Biol, 2014. **28**: p. 3-13.
111. Fessas, P., et al., *A molecular and preclinical comparison of the PD-1-targeted T-cell checkpoint inhibitors nivolumab and pembrolizumab.* Semin Oncol, 2017. **44**(2): p. 136-140.
112. Savina, A. and S. Amigorena, *Phagocytosis and antigen presentation in dendritic cells.* Immunol Rev, 2007. **219**: p. 143-56.
113. Feng, D., et al., *Cellular internalization of exosomes occurs through phagocytosis.* Traffic, 2010. **11**(5): p. 675-87.

114. Pan, J.H., et al., *Role of exosomes and exosomal microRNAs in hepatocellular carcinoma: Potential in diagnosis and antitumour treatments (Review).* Int J Mol Med, 2018. **41**(4): p. 1809-1816.
115. Kouwaki, T., et al., *Extracellular Vesicles Deliver Host and Virus RNA and Regulate Innate Immune Response.* Int J Mol Sci, 2017. **18**(3).
116. Kaur, R.S.a.J., *Th1/Th2 cytokines and their genotypes as predictors of hepatitis B virus related hepatocellular carcinoma.* World Journal of Hepatology, 2015. **7**(11): p. 1572–1580.
117. Kraft, S., et al., *PDL1 expression in desmoplastic melanoma is associated with tumor aggressiveness and progression.* J Am Acad Dermatol, 2017. **77**(3): p. 534-542.
118. Talal, M.Z.L.M.P.A.H., *The role of chemokines as inflammatory mediators in chronic hepatitis C virus infection.* Journal of Viral Hepatitis, 2007. **14**(10): p. 675-687.
119. Wei Geng, C.-M.L., Kevin T.P. Ng, Chang-Chun Ling, Xiang Qi, Chang-Xian Li, Yuan Zhai, Xiao-Bing Liu, Yuen-Yuen Ma, and Kwan Man, *Interferon-gamma inducible protein 10 (IP10) induced cisplatin resistance of HCC after liver transplantation through ER stress signaling pathway.* Oncotarget, 2015. **6**(29): p. 28042–28056.
120. Shen, J., et al., *The role of exosomes in hepatitis, liver cirrhosis and hepatocellular carcinoma.* J Cell Mol Med, 2017. **21**(5): p. 986-992.
121. Ha, D., N. Yang, and V. Nadithe, *Exosomes as therapeutic drug carriers and delivery vehicles across biological membranes: current perspectives and future challenges.* Acta Pharm Sin B, 2016. **6**(4): p. 287-96.
122. Erikci, E., M. Gursel, and I. Gursel, *Differential immune activation following encapsulation of immunostimulatory CpG oligodeoxynucleotide in nanoliposomes.* Biomaterials, 2011. **32**(6): p. 1715-23.
123. Ishii, K.J., et al., *Immunotherapeutic utility of stimulatory and suppressive oligodeoxynucleotides.* Curr Opin Mol Ther, 2004. **6**(2): p. 166-74.
124. Zhuang, X., et al., *Treatment of brain inflammatory diseases by delivering exosome encapsulated anti-inflammatory drugs from the nasal region to the brain.* Mol Ther, 2011. **19**(10): p. 1769-79.
125. Shin-ichiro Fujii, K.S., Caroline Smith, Laura Bonifaz, and Ralph M. Steinman, *Activation of Natural Killer T Cells by α-Galactosylceramide Rapidly Induces the Full Maturation of Dendritic Cells In Vivo and Thereby Acts as an Adjuvant for Combined CD4 and CD8 T Cell Immunity to a Coadministered Protein.* Journal of Experimental Medicine, 2003. **198**(2).
126. Kitamura, H., et al., *The natural killer T (NKT) cell ligand alpha-galactosylceramide demonstrates its immunopotentiating effect by inducing interleukin (IL)-12 production by dendritic cells and IL-12 receptor expression on NKT cells.* J Exp Med, 1999. **189**(7): p. 1121-8.
127. Bieber, K., et al., *T cells mediate autoantibody-induced cutaneous inflammation and blistering in epidermolysis bullosa acquisita.* Sci Rep, 2016. **6**: p. 38357.
128. Wang, J., et al., *Chemically Edited Exosomes with Dual Ligand Purified by Microfluidic Device for Active Targeted Drug Delivery to Tumor Cells.* ACS Appl Mater Interfaces, 2017. **9**(33): p. 27441-27452.

Appendices

Appendix A

A1. Cell Culture Media, Buffers and Solutions

A1.1 Cell Culture Media

A1.1.1 RPMI-1640 and High Glucose DMEM:

- 2.5, 5 or 10% FBS (inactivated at 55°C for 1 hour)
- 50 g/ml Penicillin/Streptomycin
- 10 mM HEPES
- 0,11 mg/ml Na Pyruvate
- 1% NEAA
- 2 mM L-Glutamine

Added into 500 ml base medium and stored at +4^{o}C.

A1.1.2 Exo-free FBS preparation:

FBS was inactivated at 55^{o}C for 1 hr. Then, transferred into ultracentrifugation tubes as 35 ml/tube. Following the centrifugation at 100000 X g for 4 hrs, supernatants were collected into new 50 ml falcons, and stored at 20^{o}C.

A1.2 Buffers and Solutions

A1.2.1 PBS-BSA-Na azide Buffer (FACS Buffer)

500 ml 1x PBS 5g BSA (1%)

125 mg Sodium Azide (0.25%)

The solution was stored at +4 °C.

A1.2.2 ELISA buffers

A1.2.2.1 Blocking buffer

500 ml 1x PBS

25 g BSA (5%)

250 µl Tween20 (0,025%)

The mixture was stored at -20°C.

A1.2.2.2 Wash buffer

500 ml 10x PBS

2.5 ml Tween20

4.5 lt ddH_2O

A1.2.2.3 10X PBS (Phosphate Buffered Saline)

80 g NaCl

2 g KCl

8,01 g Na_2HPO_4 . $2H_2O$

2 g KH_2PO_4

1 lt ddH_2O

After adjusting pH to 6.8, it was stored at RT.

A1.2.3 Immunoblotting buffers

A1.2.3.1 RIPA buffer (Radio Immuno Precipitation Assay Buffer)

150 mM Sodium chloride

1.0% NP-40 or Triton X-100

0.5% Sodium deoxycholate

0.1% SDS

50 mM Tris, pH 8.0

Buffer was prepared and stored at -20 °C.

A1.2.3.2 4x Laemmli buffer

4% SDS

10% 2-mercaptoehtanol

20% Glycerol

0.004% Bromophenol blue

0.125 M Tris-HCl

Buffer pH was adjusted to 6.8 and stored at -20 °C.

A1.2.3.3 30% Acrylamide mix

73 g Acrylamide

2 g Bisacrylamide

250ml ddH_2O

A1.2.3.4 10% SDS

10 g SDS to be dissolved in 100 ml ddH_2O

A1.2.3.5 1.5 M Tris (pH: 8.8)

18.171 g Tris base

50 ml ddH_2O, pH adjusted to 8.8 then completed to 100 ml

A1.2.3.6 10.5 M Tris (pH: 6.8)

6 g Tris-base

50 ml of ddH_2O, pH adjusted to 6.8 then, completed to 100 ml

A1.2.3.7 TBS 10X

24.23 g Trizma HCl

80.06 g NaCl

Solution was prepared with 1 lt ddH_2O. Its pH was adjusted to 7.6 with pure HCl and stored at RT. It was diluted to 1x before use.

A1.2.3.8 TBS-T

100 ml of 10x TBS

900 ml ddH_2O

2 ml Tween20

Solution was mixed well and stored at RT.

A1.2.3.9 10X Running buffer

30.285 g Tris base

144,134 g Glycine

100 ml SDS

800 ml ddH_2O

Its pH was adjusted to 8.3 and stored at RT. It was diluted to 1x before use.

A1.2.3.10 Transfer buffer

6 g Tris base

28 g Glycine

400 ml Methanol (ice-cold)

1600 ml ddH_2O (ice-cold)

A1.2.3.11 Blocking and antibody incubation buffer

50 ml TBS-T

2.5 g Milk powder or BSA

Solution was mixed well and stored at +4 °C.

A1.2.3.12 5% Stacking gel

2 ml 0.5 M Tris (pH 6.8)

80 µl 10% SDS

1.3 ml 30% Acrylamide

80 µl 10% APS

16 µl TEMED

4.5 ml ddH_2O

A1.2.3.13 10% Resolving gel

2.5 ml 1.5 M Tris (pH 8.8)

100 µl 10% SDS

3.3 ml 30% Acrylamide

100 µl 10% APS

4 µl TEMED

4 ml ddH_2O

A1.2.3.14 12% Resolving gel

2.5 ml 1.5 M Tris (pH 8.8)

100 µl 10% SDS

3.96 ml 30% Acrylamide

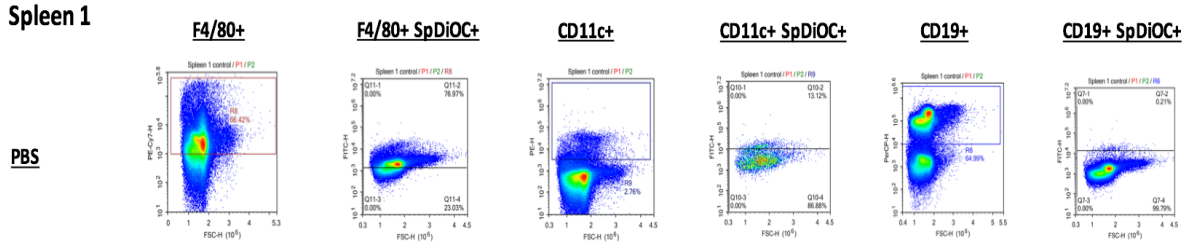
100 µl 10% APS

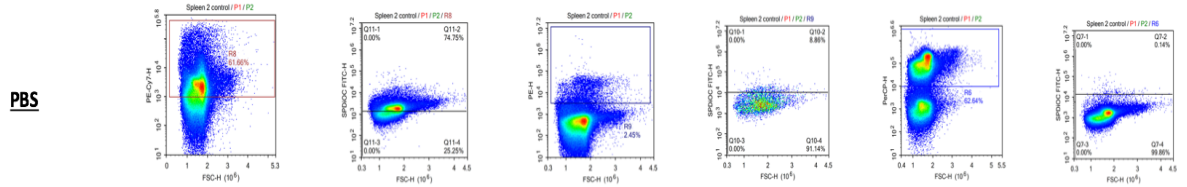
10 µl TEMED

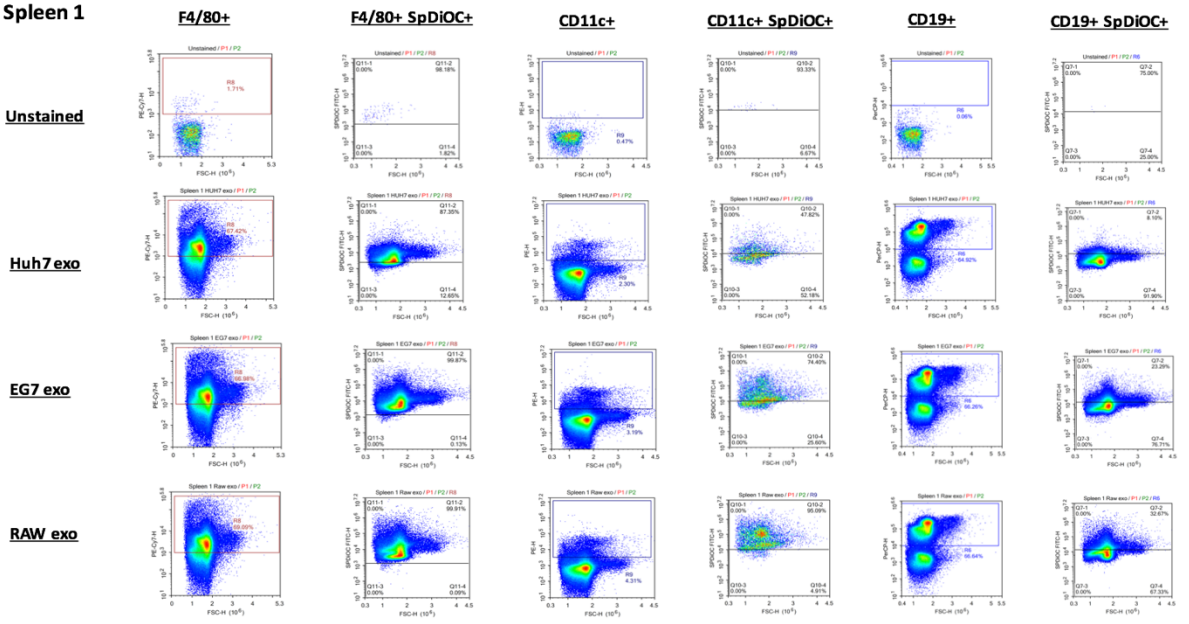
3.44 ml ddH_2O

Appendix B

Supplementary Figures







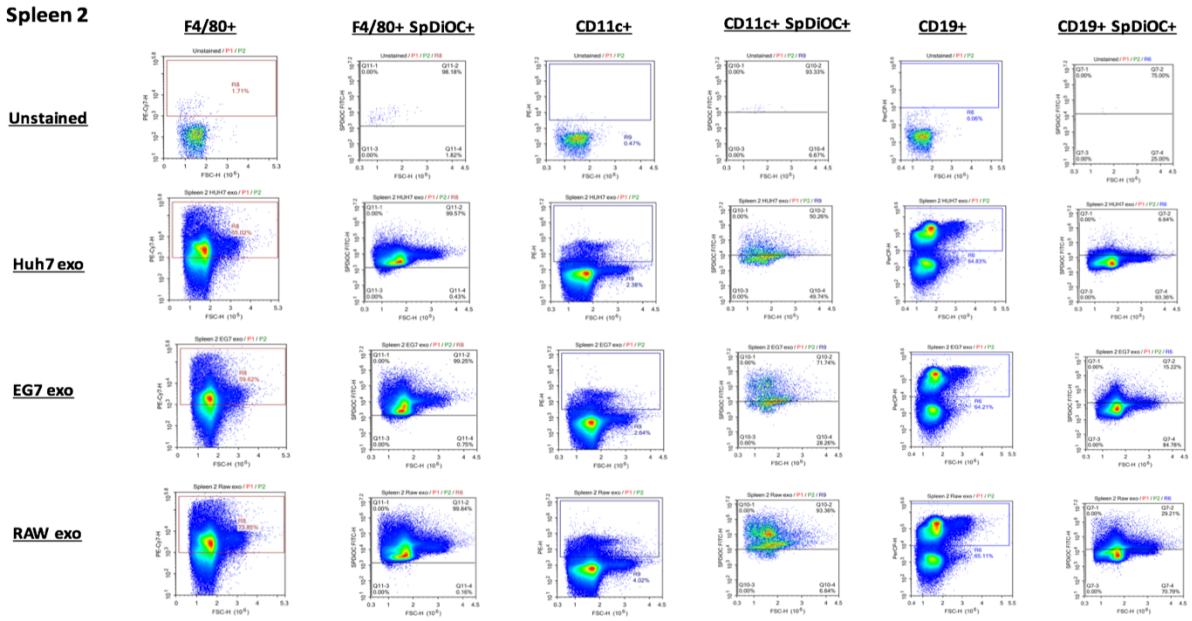


Figure S 1. Dot plots of cell-specific internalization of HUH7, EG7 and RAW exosomes by immune cell subsets in mouse splenocytes after 24 h incubation with SPDiOC labelled exosomes.

Markers for *B-cell (a-B220-PE/Cy5), Macrophages (a-F4/80-PE/Cy7) and DC (a-CD11c-PE).*

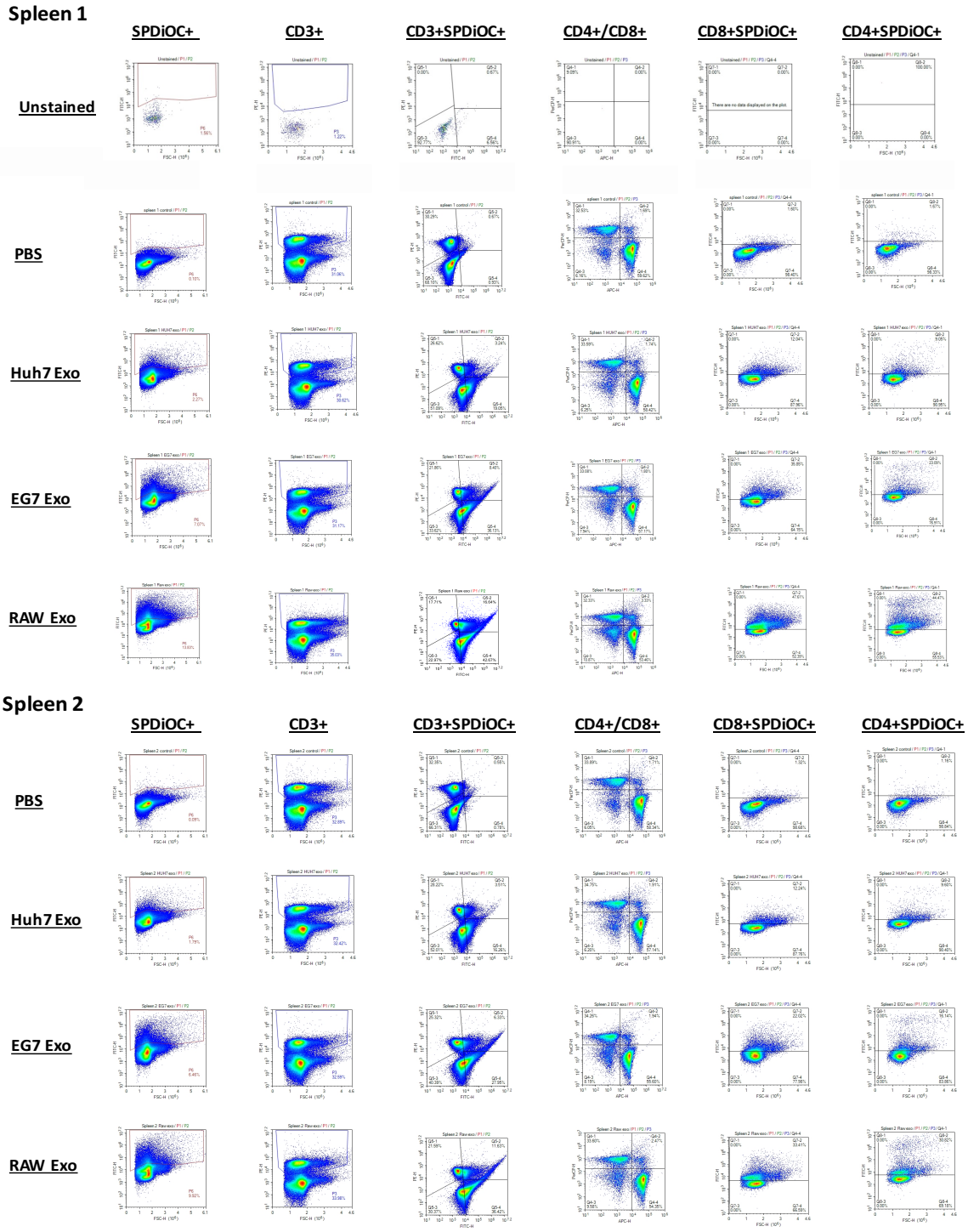


Figure S 2. Dot plots of cell-specific internalization of HUH7, EG7 and RAW exosomes by immune cell subsets in mouse splenocytes after 24 h incubation with SPDiOC labelled exosomes.

Markers for T cell subsets (a-CD3-PE), (a-CD4-APC), (a-CD8-Pe/Cy5).

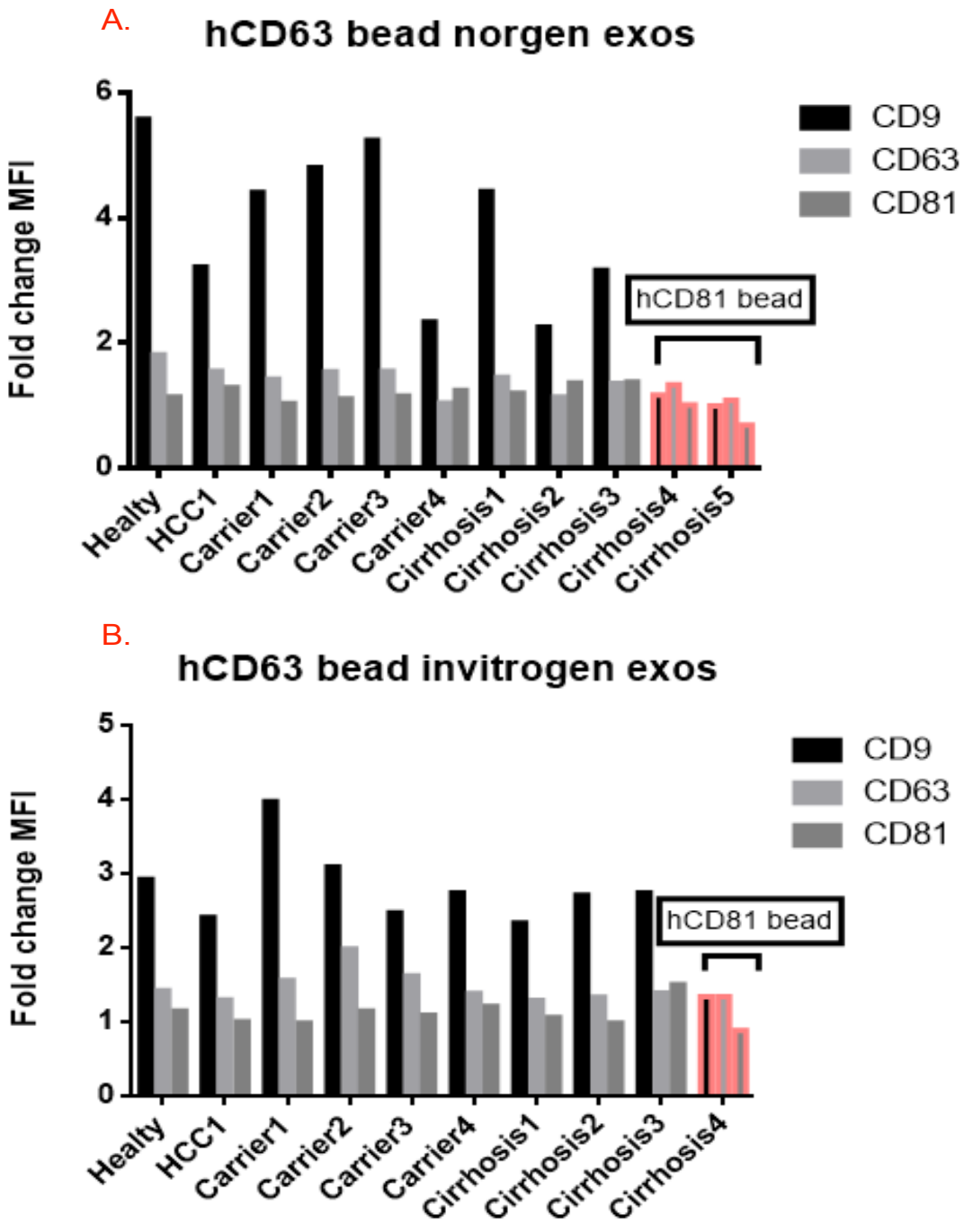


Figure S 3. Fold change MFI of exosomal markers (CD9, CD63 and CD81) on exosomes associated with anti-CD63 and anti-CD81 (last 2 patient exosomes) conjugated beads.

(A) *Norgen exosome purification kit (cat # 58300)* ***(B)*** *Invitrogen exosome purification kit (cat # 4484450).*

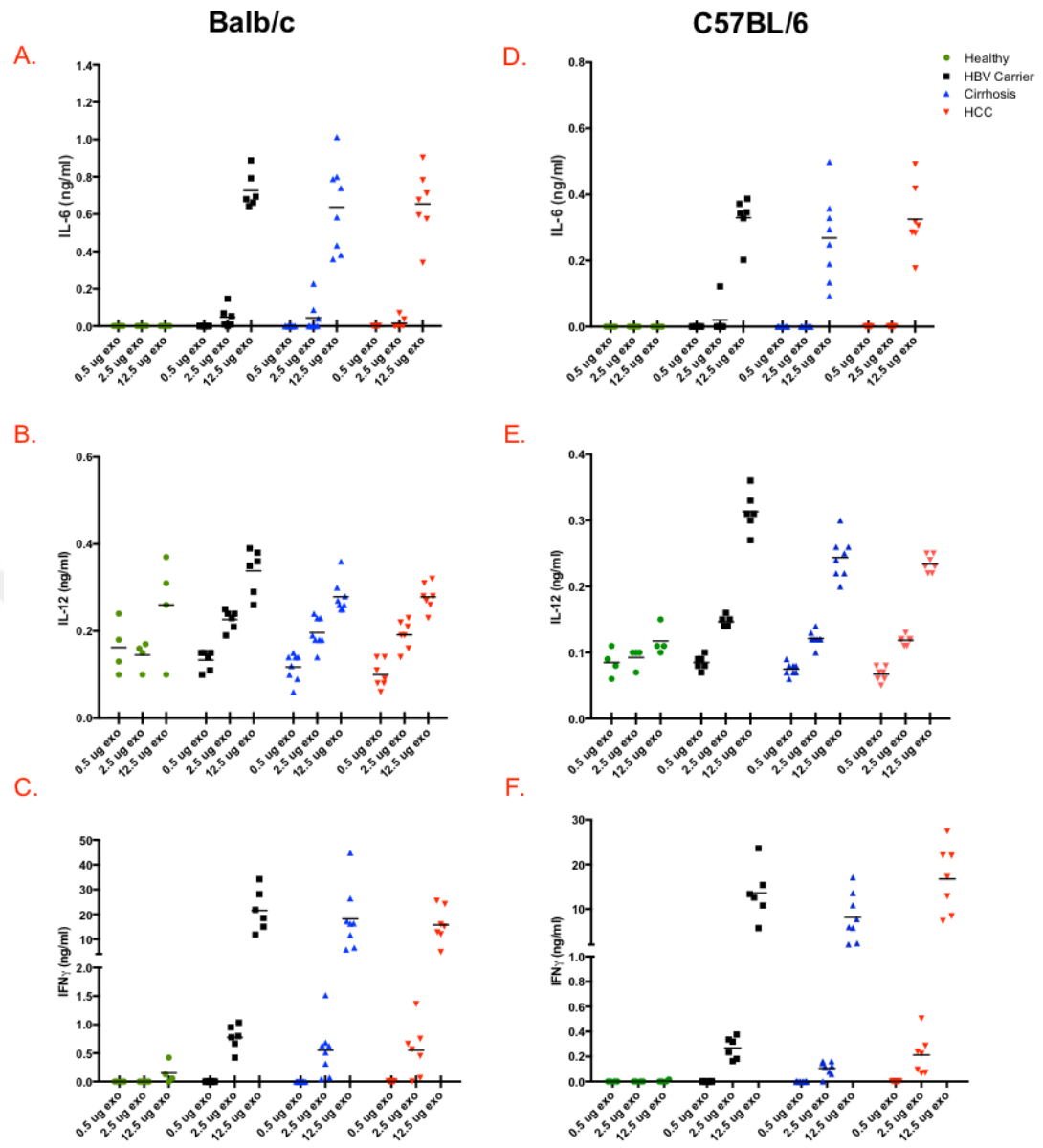


Figure S 4. Stimulation of Balb/c and C57BL/6 splenocytes with HBV carrier, Cirrhosis and HCC exosomes.

For each exosome, three doses were used as 0.5μg, 2.5 μg, 12.5 μg. After 24 hrs of incubation, supernatants were collected for cytokine ELISA. ***(A)*** *IL-6* ***(B)*** *IL-12* ***(C)*** *IFNγ levels of Balb/c splenocyte + exosome incubation* ***(D)*** *IL-6* ***(E)*** *IL-12* ***(F)*** *IFNγ levels of C57BL/6 splenocyte + exosome incubation.*

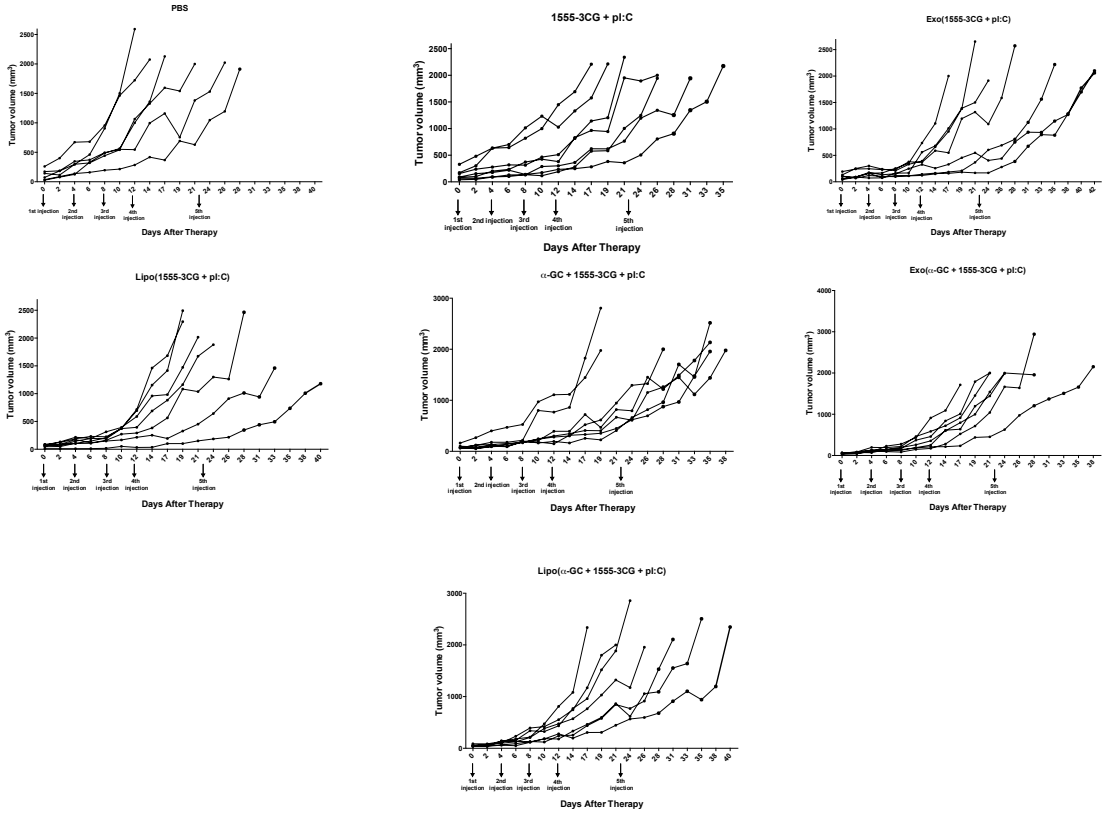


Figure S 5. Tumor volumes of each animal received different exosome/liposome formulation and control group.

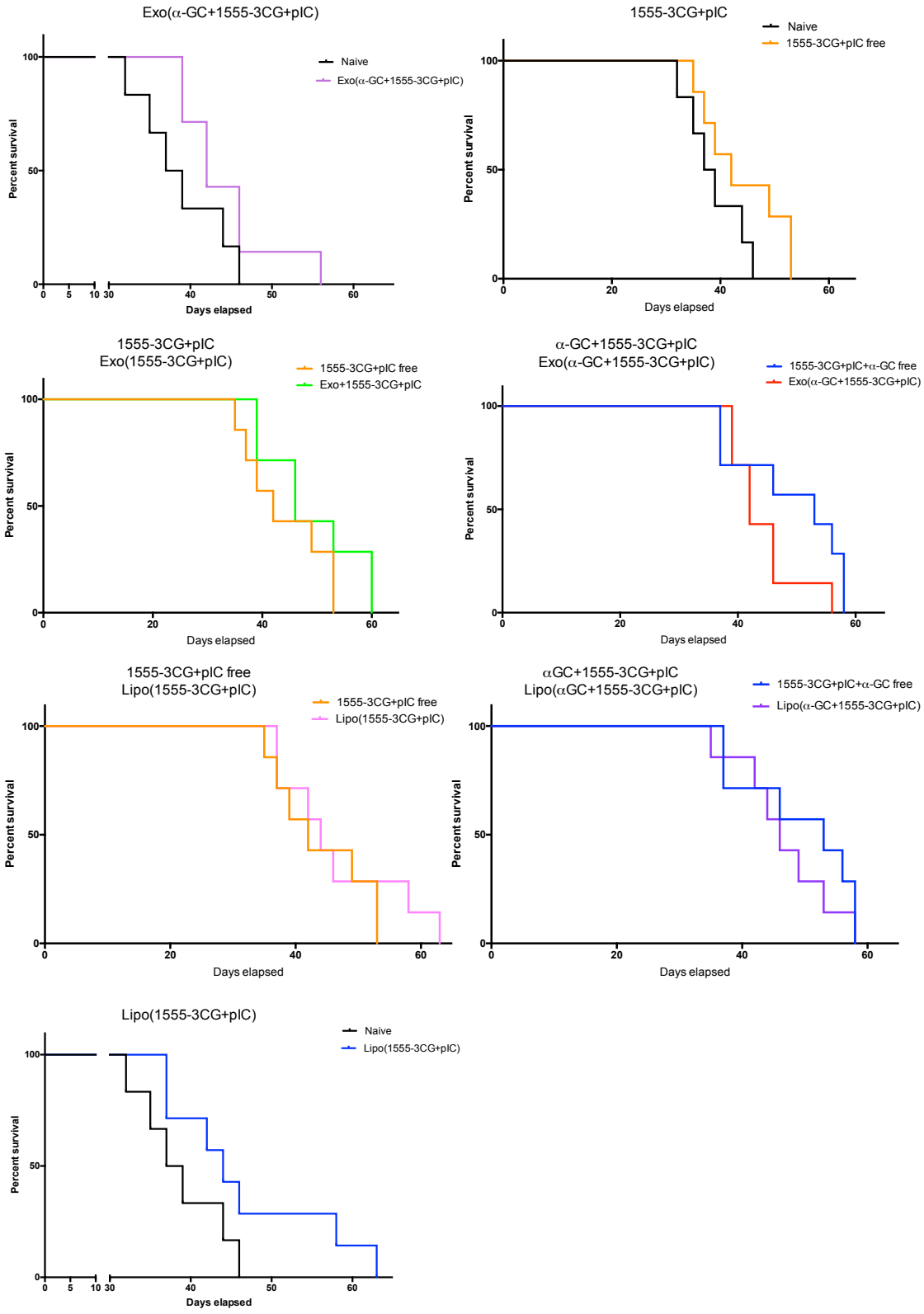


Figure S 6. Kaplan-Meier survival graphs of HUH7 tumor bearing mice.